A STUDY OF THE KINETICS AND MECHANISM OF THE THERMAL DECOMPOSITION OF SOME HYDROCARBON COPOLYMERS

A Thesis

presented for the degree of

DOCTOR OF PHILOSOPHY

in the Faculty of Science of the

University of St. Andrews

by

JOHN ATKINSON B.Sc.

United College of St. Salvator

and St. Leonard, St. Andrews.

June 1971

DECLARATION

I declare that this thesis is my own composition, that the work of which it is a record has been carried out by myself and that it has not been submitted in any previous application for a Higher Degree.

This thesis describes the results of research carried out at the Chemistry Department, United College of St. Salvator and St. Leonard, University of St. Andrews, under the supervision of Dr. J.R. MacCallum since the 1st of October 1968, the date of my admission as a research student.

JOHN ATKINSON

CERTIFICATE

I hereby certify that John Atkinson has spent eleven terms of research work under my supervision, has fulfilled the conditions of Ordinance No. 16 (St. Andrews) and is qualified to submit the accompanying thesis in application for the degree of Doctor of Philosophy.

J.R. MacCALLUM,
Director of Research

ACKNOWLEDGEMENTS

I should like to record my gratitude to Dr. James R. MacCallum for his help and encouragement in all aspects of this work.

I am indebted to the Carnegie Trust for the Universities of Scotland for the award of a Research Scholarship from 1968-1971 and to Professor The Lord Tedder for research facilities during this period.

My thanks are also due to Dr. D.H. Richards of the E.R.D.E., Waltham Abbey for some α-methyl styrene/hydrocarbon polymer samples, to Mr. James Rennie, Mr. Joseph Ward and Mr. Grenville West for their technical aid and to Miss Janette Herd who typed this thesis.

CONTENTS

		Page
Declaration		(ii)
Certificate		(iii)
Acknowledgements		(iv)
Contents		(v)
List of Figures		(vi)
Summary		(viii)

PART ONE

Chapter		Page
1	Introduction	1
2	Experimental and Results	13
3	Discussion	60
	Bibliography	84

PART TWO

1	Introduction	87
2	Calculations	90
3	Discussion	112
	Bibliography	115
	Conclusions	116

LIST OF FIGURES

PART ONE

Figure	DESCRIPTION	Immediately after Page
1, 2	Changes in Molecular Weight versus Percentage Weight	12
3	N.M.R. spectrum of head to head poly-α-methyl styrene	16
4	General N.M.R. spectrum of the copolymers	17
5	I.R. spectrum of head to head poly-α-methyl styrene	17
6	General I.R. spectrum of the copolymers	17
7	U.V. spectra of the polymers	18
8	Product Analysis apparatus	20
9	Gas Analysis apparatus	22
10	N.M.R. spectrum of residue of head to head poly-α-methyl styrene	23
11A, 11B	U.V. and I.R. spectra of residue of head to head poly-α-methyl styrene	23
12	I.R. spectrum of low M.W. fraction of copolymers	30
13	Representations of G.L.C. chromatograms of 'non-common' products	36
14	I.R. spectrum of volatile liquid fraction of copolymers	44
15	Micro-Force thermobalance	50
16	Thermobalance - Balance Head Unit and bridge circuit	50

17 - 24	Analysis of Kinetics diagrams	55, 57
25	Molecular Weight changes for the polymers	59
26	Representations of the two head to head tacticities	64
27 - 29	Mechanistic schemes for the thermal breakdown of the polymers	68, 69, 71
30	Log (time) versus n for various percentage degradation of the copolymers	81

PART TWO

Figure

1	Rate versus k_s x t for Random Scission - Evaporation Model (RS - EM) mechanism	93
2	D.P. versus Percentage Weight Loss for RS - EM mechanism	93
3	$\frac{1}{P}$ versus k_s x t for RS - EM mechanism	93
4	$\frac{W}{W_o}$ versus k_s x t for RS - EM mechanism	94
5	$\frac{P}{P_o}$ versus $\frac{W}{W_o}$ for fixed P_o for Random Scission - Unzip Model (RS - UM) mechanism	103
6	$\frac{P}{P_o}$ versus $\frac{W}{W_o}$ for fixed 'a' and 'z' values for RS - UM mechanism	103
7	Percentage degradation corresponding to maximum rate versus $\frac{a}{z}$ ratio for RS - UM mechanism	104
8	Rate versus $\frac{W}{W_o}$ for RS - UM mechanism	104
9	Comparison of $\frac{P}{P_o}$ versus $\frac{W}{W_o}$ of this work and Boyd	114
10	Comparison of Rate versus $\frac{W}{W_o}$ of this work and Boyd	114

SUMMARY

This thesis is presented as two separate yet related parts. Part one is concerned with the thermal decomposition of some α-methyl styrene/hydrocarbon copolymers. The experimental work has been primarily directed towards the investigation of the products which resulted from the thermal degradation of the polymers. However, two other analytical techniques were also utilised, firstly, the kinetics of thermal breakdown and second, the study of the molecular weight changes associated with particular percentage decompositions. From these investigations, a series of mechanistic schemes has been devised to explain the breakdown of the polymers. Conclusions concerning certain structural features of the undegraded polymers have also been drawn from these studies.

In part two of this thesis, the kinetics of decomposition have been theoretically treated for three distinct mechanistic processes. The approach involves the use of the "most probable" distribution of molecular sizes and avoids usage of the stationary state hypothesis in the derivation of the kinetic equations.

PART ONE

CHAPTER 1. INTRODUCTION

A. General

The growth in the use of polymeric materials has necessitated a great amount of research work being devoted to their study. The main objective of this research is a greater understanding of the nature of the polymers themselves so that improvements may be made wherever possible.

The development of modern instrumentation in the laboratory over the last ten years, has taken thermal analysis from being a technique used by only a few, to a sophisticated analytical method used in research and production. These studies help to solve problems of molecular structure such as the arrangement of the repeating monomer units, the existence of side groups and cross linking, the nature of chain ends and the strengths of various bonds. The investigations are also of importance in the formulation of mechanisms for thermal decomposition reactions.

Thermal degradation is of importance from a practical point of view. Many polymers are exposed to thermal stresses during their fabrication. These processes often involve heat and hence a knowledge of the effect of heat in such cases can be a useful aid in avoiding undesirable side effects.

The behaviour of polymers under various temperature conditions can also help in the selection of the most suitable material for a particular use. For instance, the requirements needed for a synthetic fibre for use in the textile industry are vastly different from those necessary for the heat shield of a space capsule.

Much of the work carried out so far on the subject of the thermal analysis of polymers, has been under conditions of reduced pressure.

This has been for three main reasons. Firstly, thermal degradation of a polymer under vacuum facilitates the collection of uncontaminated products. Secondly, any atmosphere tends to retard the diffusion of products from the sample. This gives rise to the possible occurrence of secondary reactions. The third reason applies primarily to an atmosphere containing oxygen. In this case, some of the products may be due to the combined effect of heat and oxygen. For initial investigations on the properties of a polymer, this is usually an undesirable complication.

In order that a full understanding of the mechanism of the thermal degradation of a polymer may be accomplished, three fundamental studies must be made:-

1) An analysis of the volatile and non-volatile products of the degradation (Product Analysis).

2) The kinetics of thermal breakdown.

3) The molecular weight changes occurring during the course of heating.

B. Product Analysis

Thermal degradation followed by analysis of the products is probably the oldest characterisation process still in use today. As far back as 1860, C.G. Williams[1] discovered that the basic unit of rubber was isoprene by a thermal decomposition technique. However, it was not until the 1920's that chain reactions became understood and this in turn lead to the realisation that polymers were long chains of simple molecules joined together by chemical bonds. Since that time, a great deal of work has been carried out on the products of thermal degradation

of natural and synthetic polymers. The information produced is usually used in one of two ways, either to elucidate the structure of the original polymer, or to aid the formulation of the mechanism of degradation.

Apparatus

Over the years, many forms of apparatus have been employed for the collection of the products of a thermal degradation. Most of these systems have one common feature, they are designed to separate the four product fractions that most polymers can produce. These fractions are:

1) The residue which is not volatile at the temperature of degradation.

2) The low molecular weight fractions such as dimer, trimer, etc. which are volatile at the temperature of degradation but not so at room temperature.

3) The fraction of molecules which are volatile liquids under normal atmospheric conditions, but which are gaseous at the reduced pressure of the system.

4) The fraction of molecules which are gaseous at room temperature and pressure.

Simplifications in the apparatus are made when one or more of these fractions is not produced.

Methods of Analysis

The method of analysis used varies with the fraction being investigated The residue is often closely related to the original polymer. Hence,

the most commonly used techniques of analysis are those which involve the comparison of certain properties of the residue and the original polymer. As the vast majority of polymers contain hydrogen, changes in structure may be identified by N.M.R. Spectral Analysis. Similarly, the appearance and disappearance of certain functional groups can be followed by I.R. Spectral Analysis. Information as to the nature of the reaction which has taken place may be found by investigating the changes in molecular weight. This will be discussed in greater detail later. Occasionally useful information may come from comparison of the ultra-violet spectra but this is not a very commonly used analytical technique.

These same methods of analysis may be employed in analysing the fraction which is volatile at the temperature of degradation but involatile at room temperature. However, more detailed information as to the exact nature of the constituents is obtained by the running of a Mass Spectrum.

The remaining two fractions are best identified using a combined G.L.C. - Mass Spectrometer technique. The fractions are fed into the G.L.C. and after separation, each constituent is fed into the Mass Spectrometer. The resulting mass spectra allows identification of each type of molecule present.

C. Kinetics

The effect of heat on the rate of a chemical process has emerged as one of the most important methods of investigation of a reaction mechanism. Kinetic studies may be performed in a number of ways, some of the more commonly used ones are:- Differential Scanning

Calorimetry (D.S.C.), Differential Thermal Analysis (D.T.A.), Thermal Volatilisation Analysis (T.V.A.) and Thermogravimetric Analysis (T.G.A.). It is the last of these methods (T.G.A.), that has been employed in the experimental part of this thesis.

Apparatus

T.G.A. involves the continuous measurement of the loss of weight of a sample undergoing degradation with respect to time. The apparatus used for such an operation consists of some form of automatically recording balance. The balances which are commercially available can be divided into two classes, the null-point type and the deflection type.

The Null-Point Balance

The null-point type of balance contains a sensing device which detects any deflection of the balance beam caused by a weight change. A restoring force is then automatically applied to the beam returning it to its null position. The size of this force is measured and the magnitude can be directly related to the change in weight.

The restoring forces on the early null-point balances were not automatically applied but were achieved by the manual addition of the appropriate weights. This method was eventually replaced by electronic techniques, the first electronic type of null-point balance being that of Angstrom[2] in 1885. This apparatus consisted of a beam with a sample hanging from one end and a magnet suspended into a solenoid from the other. The current through the solenoid was adjusted to maintain the balance beam at null-point. Urbain[3], in 1912, fitted a heating system

onto the above type of balance and so produced the first electronic thermobalance. Mikulinskii and Gel'd[4] in 1940 encased a similar apparatus in a glass case in which gas could be kept at a desired pressure. Alternatively the glass case could be evacuated. This type of balance, in conjunction with more sensitive ways of producing the restoring force and with better recording techniques, has lead to the development of a whole range of completely automatically recording thermobalances.

Deflection Balance

The deflection balances differ from the null-point type in that they do not contain any device which restores the balance beam to its original position. Instead, the deflection of the balance beam caused by a weight change, is directly measured, often photographically. The earliest automatic recording deflection balance was that of Kuhlman[5] in 1910. The apparatus consisted of a balance with a mirror situated at the centre of the beam. A beam of light was focussed on the mirror and any deflection on the beam was detected on a surrounding drum of photographic paper onto which the light was reflected. The drum was continually driven by a clockwork motor. The first deflection thermobalance was that of Dubois[6] who also used the photographic recording technique. Since that time, many deflection types of balance have been produced, some of the more commonly used ones are:- Strain Gauge-type, Spring-type, Cantilever-type and the Hydrostatic-type.

It is not the purpose of this introduction to describe all the thermobalances that have been produced. There are reviews by Gordon and Campbell[7], Garn[8], Lewin[9] and others, on this very subject. The

thermobalance used to give results for this thesis will be described in detail in the next chapter.

Thermogravimetric Analysis

T.G.A. is the process whereby weight loss is measured as a function of time. There are two experimental techniques, the first involves keeping the temperature constant throughout the experiment(isothermal); the second involves increasing the temperature at a constant rate until all the sample has degraded(programmed temperature). In each case, a thermogram is produced from which the results are calculated. However, because of the complex nature of their breakdown, polymers do not obey simple rate equations. Research is continually being carried out in order to produce equations which can be applied to polymer systems. A detailed description of the methods currently available will not be given, however, some of the more commonly used ones will be mentioned later.

General Theory

The list of symbols used throughout this thesis is shown below:

W - Weight of sample

W_o - Initial weight of sample

C - Degree of conversion, $1-C = \frac{W}{W_o}$

T - Temperature in degrees Kelvin

t - Time

k - Rate constant of the degradation reaction

E - Energy of activation of the degradation reaction(k.J/mole)

A - Pre-exponential factor in the Arrhenius equation

R - The gas constant

f(C) - A function of degree of conversion

n - Apparent order of reaction

It is generally accepted that for the reaction, Polymer → Products, the rate of conversion of polymer to products under isothermal conditions, is given by the equation:

$$\frac{dC}{dt} = k \cdot f(C) \qquad \text{(i)}$$

For the case of temperature varying linearly with respect to time, then:

$$\frac{dT}{dt} = \text{a constant} = \beta \qquad \text{(ii)}$$

Hence, substitution of equation (ii) in equation (i) yields:

$$\frac{dC}{dT} = \frac{k}{\beta} \cdot f(C) \qquad \text{(iii)}$$

The temperature dependence of k is given by the Arrhenius equation:

$$k = A \cdot e^{-E/RT} \qquad \text{(iv)}$$

For the temperature ranges used, the pre-exponential factor, A, is assumed to remain constant. Substitution of equation (iv) into equation (i) yields the following rate expression for <u>isothermal</u> conditions:

$$\frac{dC}{dt} = A \cdot e^{-E/RT} \cdot f(C) \qquad \text{(v)}$$

Substitution of equation (iv) in equation (iii) yields the following rate expression for <u>programmed temperature rise</u> conditions:

$$\frac{dC}{dT} = \frac{A}{\beta} \cdot e^{-E/RT} \cdot f(C) \qquad \text{(vi)}$$

Equations (v) and (vi) are used as the basis for the majority of methods of kinetic analysis.

Isothermal Methods

The usual method of solution for isothermal conditions is to first take logarithms of equation (v):

$$\ln \frac{dC}{dt} = \ln A + \ln f(C) - \frac{E}{RT}. \qquad \text{(vii)}$$

For a particular percentage conversion, taken at different temperatures, f(C) is assumed to be a constant. Hence a plot of $\ln \frac{dC}{dt}$ versus $\frac{1}{T}$ results in a straight line with a slope of $-\frac{E}{R}$.

By assuming that $f(C) = (1-C)^n$, equation (vii) becomes:

$$\ln \frac{dC}{dt} = \ln A - \frac{E}{RT} + n \ln (1-C) \qquad \text{(viii)}$$

Thus, if from the previous calculation, the energy of activation, E, is constant for all the values of percentage degradation examined, then a plot of $\ln \frac{dC}{dt}$ versus $\ln (1-C)$ at a constant temperature results in a straight line. The slope of the line is equal to the apparent order of reaction. The intercept is equal to $-\frac{E}{RT} + \ln A$, as $\frac{E}{RT}$ is known the pre-exponential factor, A, may be calculated.

If E is not constant, then this implies that more than one reaction is occurring and the above plot will not yield a straight line.

The main source of error in the above technique is the difficulty in accurately measuring $\frac{dC}{dt}$ from the thermogram. This may be overcome to a certain extent by obtaining an equation, in the form of a polynomial, for the weight versus time plot using a computer. However, small errors involved in curve fitting lead to serious errors in the differentiated equation.

The major problem in experimentally producing a thermogram under isothermal conditions is raising the temperature of the sample

to that of the degradation with minimum time delay. The only really satisfactory method of overcoming this is by having a preheated furnace inside the vacuum system which can be raised up around the sample.

Programmed Temperature Rise Methods

There are two general types of method which are used for the investigation of programmed temperature rise thermograms. They are integral methods and differential methods.

Integral Methods

The majority of the integral techniques are based on the solution of:

$$\frac{A}{\beta}\int_{T_o}^{T} e^{-E/RT}\,dT$$

where T_o is the temperature at which degradation begins to occur.

Reviews by Cameron and Fortune [10] and Flynn and Wall[11] give good accounts as to the accuracy and adaptability of these methods.

Differential Methods

These methods are based on the plot of rate of loss of weight versus inverse temperature. A number of differential equations have been produced, perhaps the most useful being the one employed by Friedman [12]:

$$\ln \frac{dC}{dt} = \ln A \,.\, f(C) - \frac{E}{RT} \qquad \text{(ix)}$$

Values of $\ln \frac{dC}{dt}$ are plotted versus $\frac{1}{T}$ at a fixed percentage conversion for various heating rates. This method, has the advantage of finding E values without any assumptions as to the nature of f(C) or to the apparent order of reaction. An account of this and other methods is

given by Tanner[13].

D. Molecular Weight Changes

When a polymer undergoes thermal degradation, there are three principal types of reaction which may occur. The first of these involves the initiation of breakdown occurring at the chain ends. This is followed by chain depolymersiation i.e. monomer units are released successively by 'unzipping' from the chain end. For a polymer which undergoes this type of reaction, each molecule present has an equal chance of being removed completely through degradation. Hence, over a period of time, the relative amounts of each size of molecule will statistically be unchanged. This means that the number average molecular weight will also be unchanged.

The second type of reaction involves the random scission of main chain bonds leading to the formation of lower molecular weight fragments. If, as is generally the case, only very low molecular weight fragments are volatile at the temperature of degradation, then, over a period of time, the number average molecular weight will rapidly decrease. However, over the same period of time, the weight of the sample will hardly have altered.

The third type of reaction involves random scission of main chain bonds followed by depolymerisation of the resulting fragments. Because a molecule with a large degree of polymerisation (D.P.) has more bonds than a molecule of small D.P., then it has more chance of being removed by this type of reaction. Hence, over a period of time, the number average molecular weight will be decreased. Over the same period of time, the weight will also have decreased.

Hence, it is possible to differentiate between the three degradation processes by a study of the molecular weight of the residue as a function of extent of reaction. A summary of the three processes is illustrated in figure 1.

However, complications can arise as there is the possibility that the above reactions may occur in modified forms. For the case of end initiation, termination of the 'unzipping' reaction may occur before the molecule has been completely removed. This would result in the molecular weight and the weight both decreasing with extent of reaction.

For the case of random scission followed by partial unzipping or, unzipping in one fragment only then again the molecular weight would decrease with respect to the extent of reaction. A summary of the different situations is shown in figure 2.

Hence, a study of molecular weight changes associated with a decomposition is only of real value if end initiation followed by complete unzipping or random scission followed by the production of smaller fragments is taking place. For the other cases, only hints as to the reaction mechanism may be concluded.

FIGURE 1

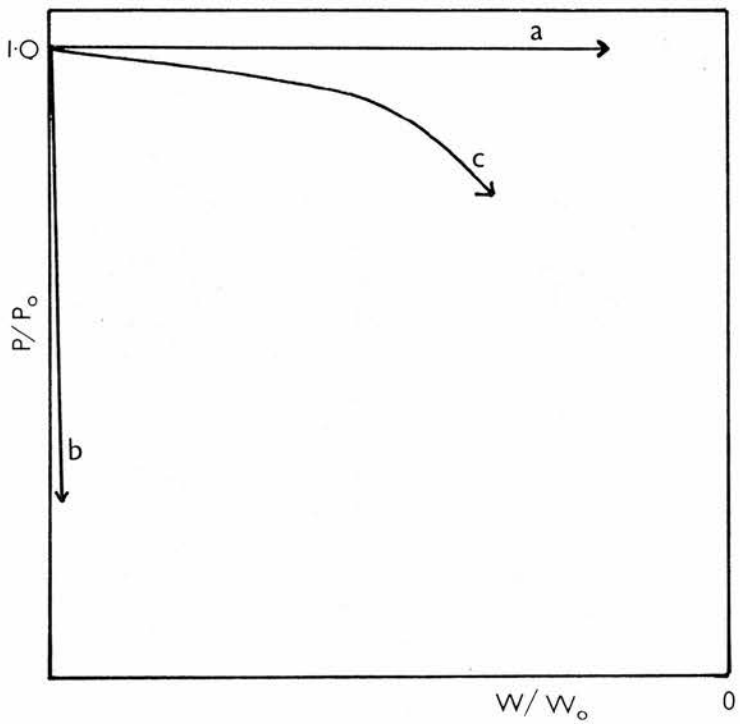

a–End Initiation
Complete Unzip

b–Random Scission
No Unzip

c–Random Scission
Complete Unzip

FIGURE 2

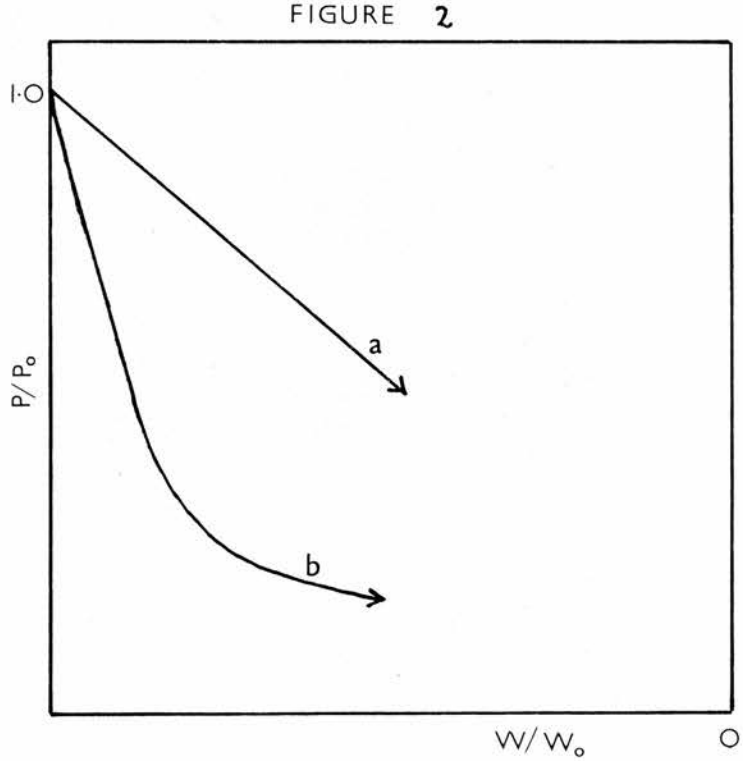

a–End Initiation

b–Random Scission
both with
Partial Unzip

The position of these curves may vary depending on the unzip length.

CHAPTER 2. EXPERIMENTAL

This chapter will be divided into four parts

A - The Polymers Investigated.

B - Product Analysis.

C - Kinetics of Degradation.

D - Molecular Weight Changes.

A. The Polymers Investigated

A series of regular copolymers of repeat unit -[M-R-M]- where M is a vinyl or diene monomer and R is a function derived from an aliphatic dihalide, has been developed by Dr. D. H. Richards and co-workers[14] at the Explosives Research and Development Establishment, Ministry of Technology, Waltham Abbey, Essex. Dr. Richards very kindly donated samples of these copolymers to this laboratory for thermoanalytical study. The copolymers which have been investigated for the purposes of this thesis are based upon α-methyl styrene as the monomer, M, and (α,ω) straight chain dihaloalkanes as the aliphatic dihalide. They have the following general formula:

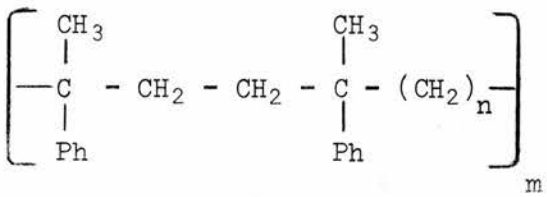

where 'n' is the number of $-CH_2-$ units in the dihaloalkane.

The series is based on an adaptation of the living polymer technique developed by Szwarc[15,16].

The preparation requires that α-methyl styrene is reacted upon by an alkali metal, usually lithium, in the presence of tetrahydrofuran (T.H.F.) as solvent. The α-methyl styrene extracts an electron from

the lithium forming a radical anion. This radical anion then dimerises to form a dianion. In the preparation of poly-α-methyl styrene by this method, only a small amount of initiator (lithium) is used and the dianion produced reacts with more α-methyl styrene until the reaction is terminated. In the preparation of the copolymers, an excess of lithium is added and the dianions produced are allowed to react with the terminal dihaloalkane. This may be summarised as follows:

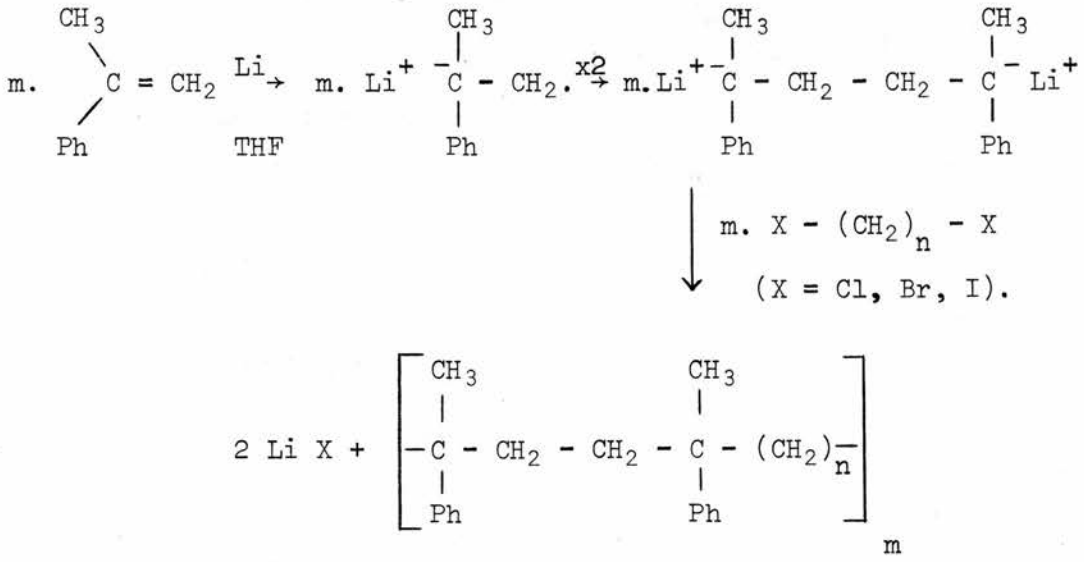

Termination of the copolymerisation is brought about by the presence of traces of proton donating impurities such as water which are attacked by the anion. Hence the end group will be of the form:

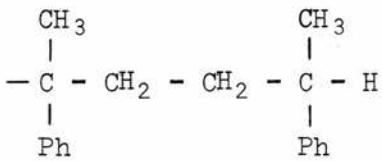

The molecular weight of these polymers is dependent upon the quantity of impurity present in the preparation. The samples investigated all had molecular weights of about 10,000.

The method of preparation has been successful for all the (α,ω) straight chain dihaloalkanes tried, with one exception, 1, 2–dihaloethane. In this case, the resulting polymer appears to be a hybrid of the n = 2 copolymer and the head to head homopolymer (n = 0). If any other vicinal dihaloalkane is used in the preparation, e.g. 1, 2–dibromocyclohexane, then pure head to head polymer is produced in good yield.

Copolymers with n = 1, 3, 4, 5, 6, 10 have been prepared and together with the head to head homopolymer will be investigated in this thesis.

The Instruments Used

It is convenient at this point to give a list of the instruments used for analytical purposes.

N.M.R. spectra were obtained using a Perkin Elmer R10 60 M.Hz N.M.R. Spectrophotometer. For the case of the head to head homopolymer, more accurate spectra were produced on a Varian HA 100 100 M.Hz N.M.R. Spectrophotometer.

Infrared spectra were obtained using a Perkin Elmer 257 Grating Infrared Spectrophotometer.

Ultraviolet spectra were produced on a Unicam SP 800 Grating Ultraviolet Spectrophotometer.

G.L.C. Two types of G.L.C. were used, the first of these was a Griffin and George D6 Gas Density Balance Chromatograph. This Chromatograph was employed for quantitative work as the peak area can be related to the quantity of product without the need for any calibrations. The second type of chromatograph was used in conjunction with the mass

spectrometer. It was a Pye 104 Chromatograph with a flame ionisation detector.

Mass Spectra were obtained from an A.E.I. MS 902 Mass Spectrometer.

When the Pye 104 was connected up to the mass spectrometer, the carrier gas was separated from the products by a Beimann All Glass Molecular Separator.

Molecular Weights were measured using a Mechrolab Vapour Pressure Osmometer.

Characterisation of the Polymers

The confirmation of the structures of the head to head homopolymer and copolymers has been carried out in detail by Richards and co-workers[17]. This was effected using data obtained from the ^{1}H N.M.R. and infrared (I.R.) spectra. However, it is necessary to mention certain characteristic features of these spectra so that comparisons may be made between the original polymers and the residues of decomposition. The ultraviolet (U.V.) spectra of the polymers were also investigated for comparison purposes.

N.M.R. Spectra

Figure 3 shows the ^{1}H N.M.R. spectrum of the head to head homopolymer. The aromatic peak occurs at 2.9τ and the aliphatic peaks between 7.7 and 10τ. The ratio of aliphatic to aromatic protons is 1:1. An important characteristic feature of the spectrum concerns the peaks at 9.0τ and 9.5τ. These have been assigned[17] to methyl groups which take up the following configurations in the polymer chain:

FIGURE 3

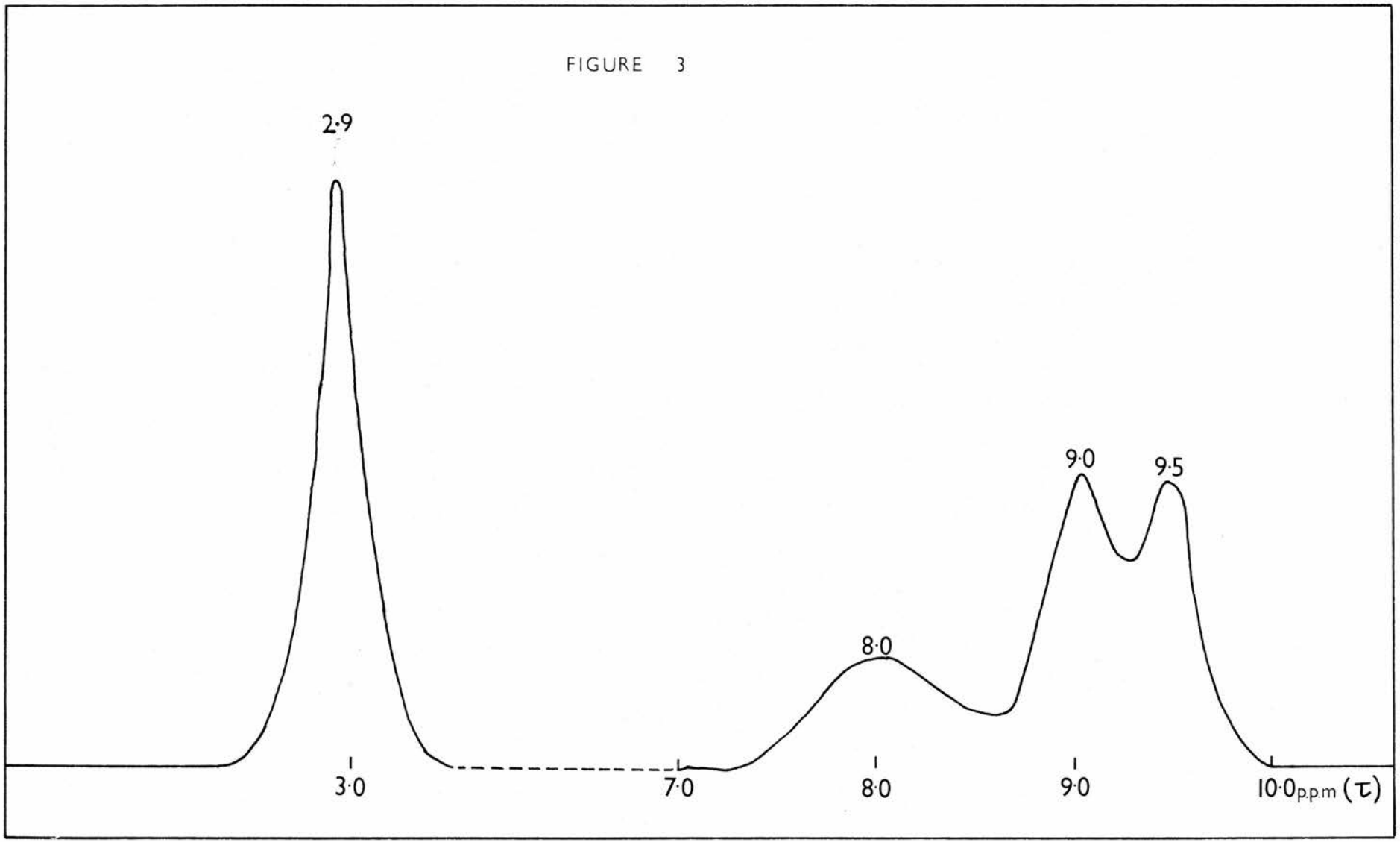

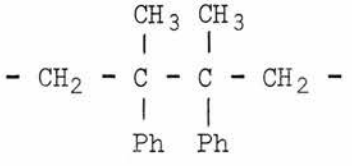

CH_3 at 9.0τ

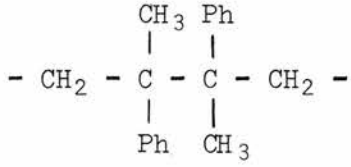

CH_3 at 9.5τ

The existence of these two methyl environments is a result of steric inhibition about the central C - C bond in the above structures. This restricts rotation about this bond.

Figure 4 shows the general form of the ^1H N.M.R. spectra obtained from the copolymers. For the case of n = 1, the spectrum is not nearly as distinct as for the other copolymers. The peak at 2.9τ is assigned to the aromatic protons, the peak at 8.9τ to the methylene groups and the shoulder at 9.05τ to the methyl groups. The spectra vary only in the relative sizes of the two aliphatic peaks and in the aliphatic/aromatic proton ratio.

I.R. Spectra

Figure 5 shows the I.R. spectrum of the head to head homopolymer in the region 1700 - 830 cm^{-1}. The peaks which distinguish this polymer from the copolymers are those at 925 cm^{-1}, 1255 cm^{-1} and 1285 cm^{-1}.

Figure 6 shows the general form of spectrum produced by the copolymers. The peak at 1290 cm^{-1} is the only peak which does not occur in the spectrum of the head to head homopolymer.

A detailed explanation of these spectra is not necessary as it is the appearance of peaks which is of interest in the spectra produced by the residues of the degradations.

U.V. Spectra

The copolymers, with n = 3, 4, 5, 6 and 10, all produced very

FIGURE 4

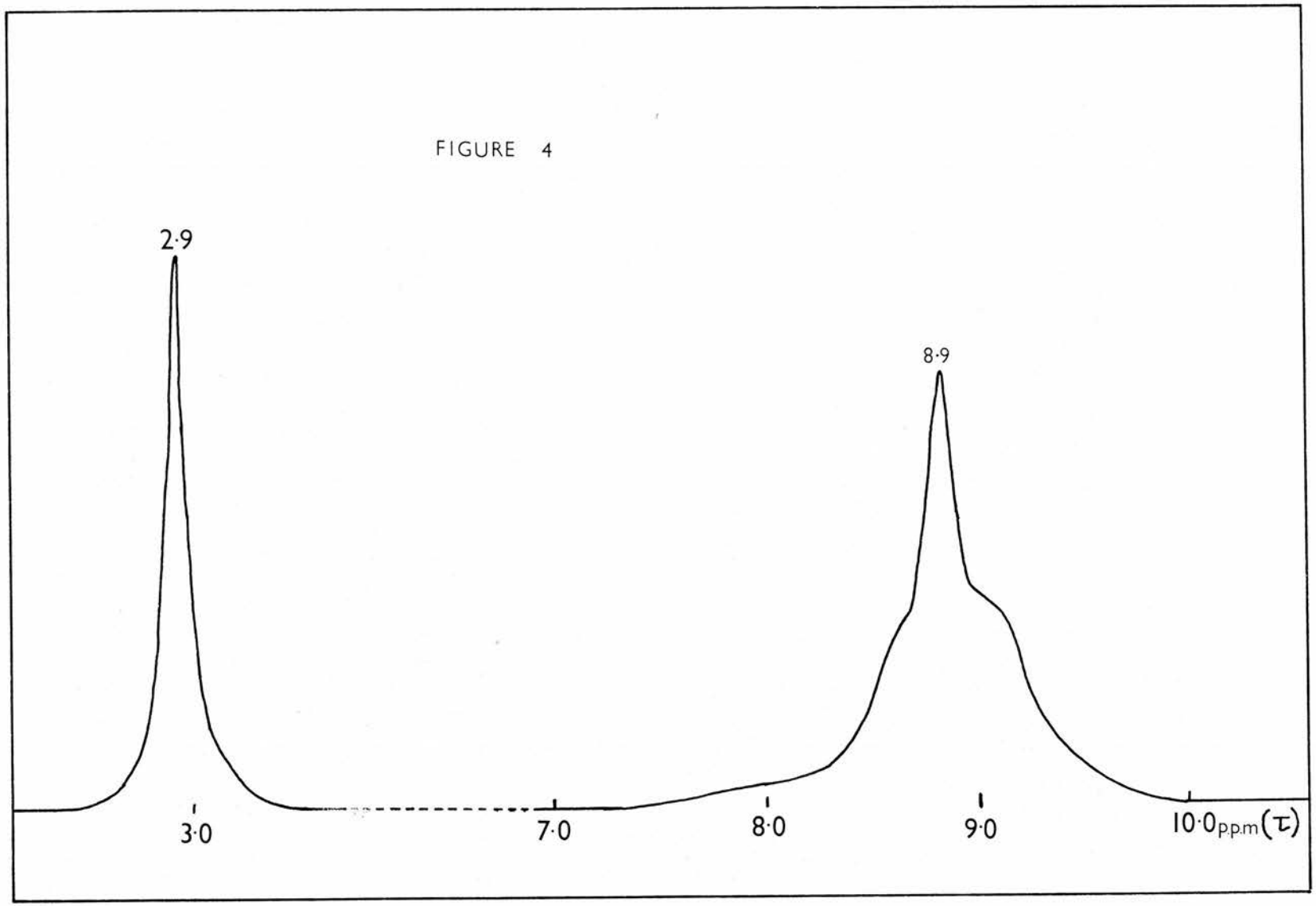

similar U.V. spectra in the region 230 - 300 nm. Such a spectrum is shown in figure 7A, the solvent used being cyclohexane. The spectra all have maximum absorbtion at a wavelength of 259 nm and they all have the same form of fine structure. The absorbtion is due to electrons in the π orbitals of the benzene ring being excited to the π^* level. The fine structure arises from the vibrational sub-levels which accompany the transitions.

For comparison of the relative absorptions of the polymers, the absorbance of a 1% solution (by weight) in a cell of length one centimeter, $E^{1\%}_{1cm}$, was evaluated in all cases. The $E^{1\%}_{1cm}$ values are very similar but decrease slightly with increasing 'n'. This is to be expected as the number of benzene rings present in a 1% solution decreases as 'n' increases. Table 1 shows the values of $E^{1\%}_{1cm}$ for the copolymers.

TABLE 1

n	$E^{1\%}_{1cm}$
3	12.0
4	11.8
5	11.7
6	11.6
10	9.0

Experimental results are usually reported in terms of the molar extinction coefficient, ε. $E^{1\%}_{1cm}$ is related to ε by the following expression:

$$10\,\varepsilon = E^{1\%}_{1cm} \times \text{Molecular Weight}$$

The above spectra are very similar to those produced from monosubstituted alkyl benzenes although not quite as distinct.

FIGURE 7

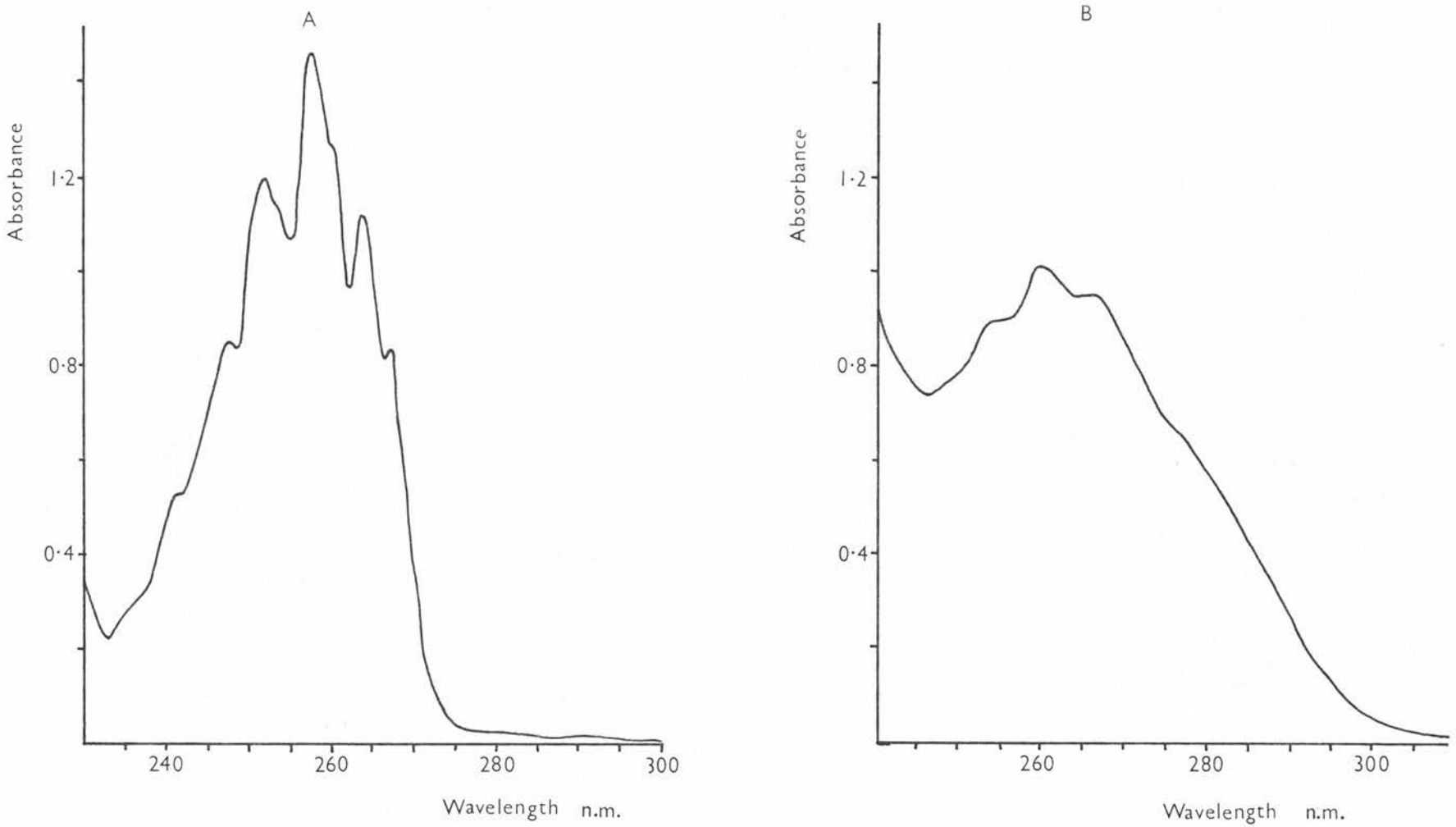
A
Absorbance
1·2
0·8
0·4
240
260
280
300
Wavelength n.m.
B
Absorbance
1·2
0·8
0·4
260
280
300
Wavelength n.m.

Hence, it would be useful if some further comparison could be made. Calculation of the molar extinction coefficient of a polymer would be totally meaningless. However, 77 grams of one gram molecular weight of any monosubstituted alkyl benzene are due to the phenyl group. As it is this group which produces the band of the spectrum which is being considered, then the weight of polymer which contains 77 grams which are due to the phenyl group, was taken for comparison purposes. For the case of n = 4, $E^{1\%}_{1cm}$ x 146 (i.e. weight of polymer which contains 77 grams attributable to the phenyl group) ÷ 10 gives a value of 175. This is in the same order as the molar extinction coefficients of monosubstituted alkyl benzenes.

Figure 7B shows the form of spectrum obtained from the head to head homopolymer and the n = 1 copolymer in the region 240 - 310 nm. The $E^{1\%}_{1cm}$ values are three times as large as was found with the other copolymers. The fine structure is also much less marked. The larger intensity of aborbtion may be explained by the fact that overlap is occurring between the band under consideration and a more intense band which exists for the main part at a shorter wavelength. For the case of the head to head homopolymer, the lack of fine structure may be attributed to the existence of two preferred configurations (see N.M.R.). Hence, the benzene rings exist in two different environments. Both types of benzene produce a spectrum which are similar in nature, but different enough to partially destroy the fine structure. Head to tail poly-α-methyl styrene has been shown by N.M.R.[48] spectral analysis to have more than one preferred configuration. In the U.V., this polymer also lacks the fine structure produced by the copolymers in the region 250 - 275 nm. It is reasonable to suppose that the n = 1 copolymer

must also exist in preferred configurations as it also lacks a well defined fine structure in the region 250 - 275 nm of the U.V. spectrum.

B. Product Analysis

This part will be divided into three sections.

1. Apparatus and Degradation Procedure
2. Methods of Analysis
3. Results of Analysis

1. Apparatus and Degradation Procedure

The polymers, when thermally degraded under vacuum, give rise to four fractions of product, the residue, a low molecular weight fraction, a volatile liquid fraction and a gaseous fraction. For the collection of these fractions, two forms of apparatus were employed. Figure 8A shows the apparatus used to obtain the residue, and in collection of the low molecular weight and the volatile liquid fractions. The diagram shows the apparatus before it has been evacuated. Figure 8B shows the apparatus which could also be used to obtain the residue and for collection of the low molecular weight fraction, but which was primarily used for the collection of gases. This figure shows the evacuated apparatus during the degradation procedure.

100 milligrams of polymer were weighed into a constricted tube, the restriction being present to minimise the loss of undegraded polymer by splashing out during the course of decomposition. The tube was placed in limb A of the degradation apparatus, the apparatus evacuated, sealed off at X and limb A placed in a thermostatically controlled furnace which had been preheated to the required temperature. Limb B was kept at room temperature and limb C placed into a Dewar of

APPARATUS

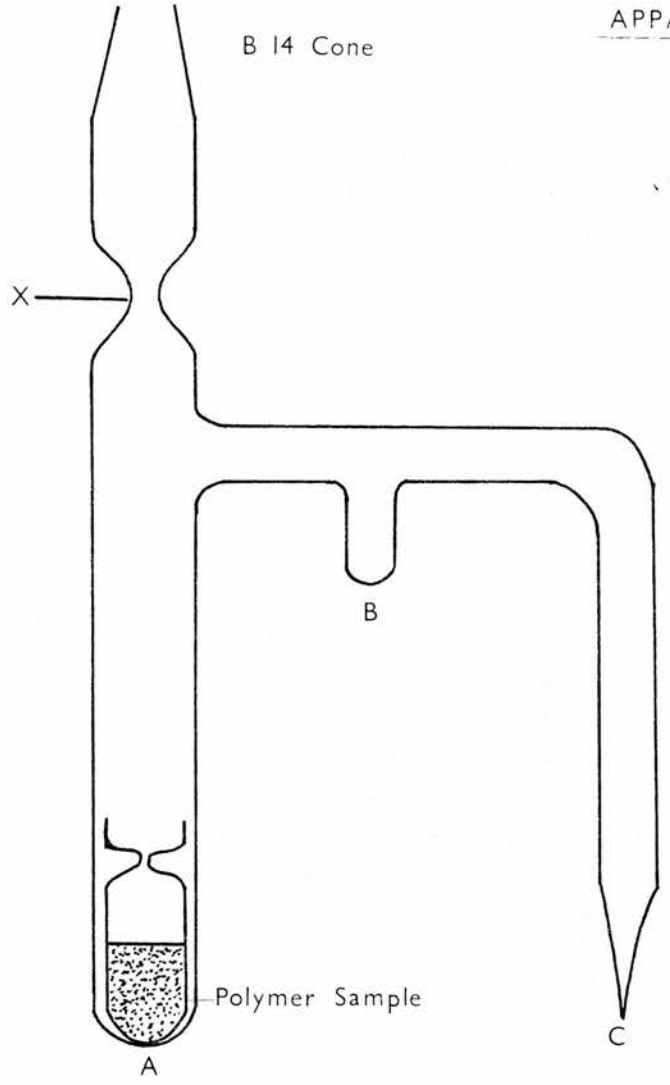

FIGURE 8A

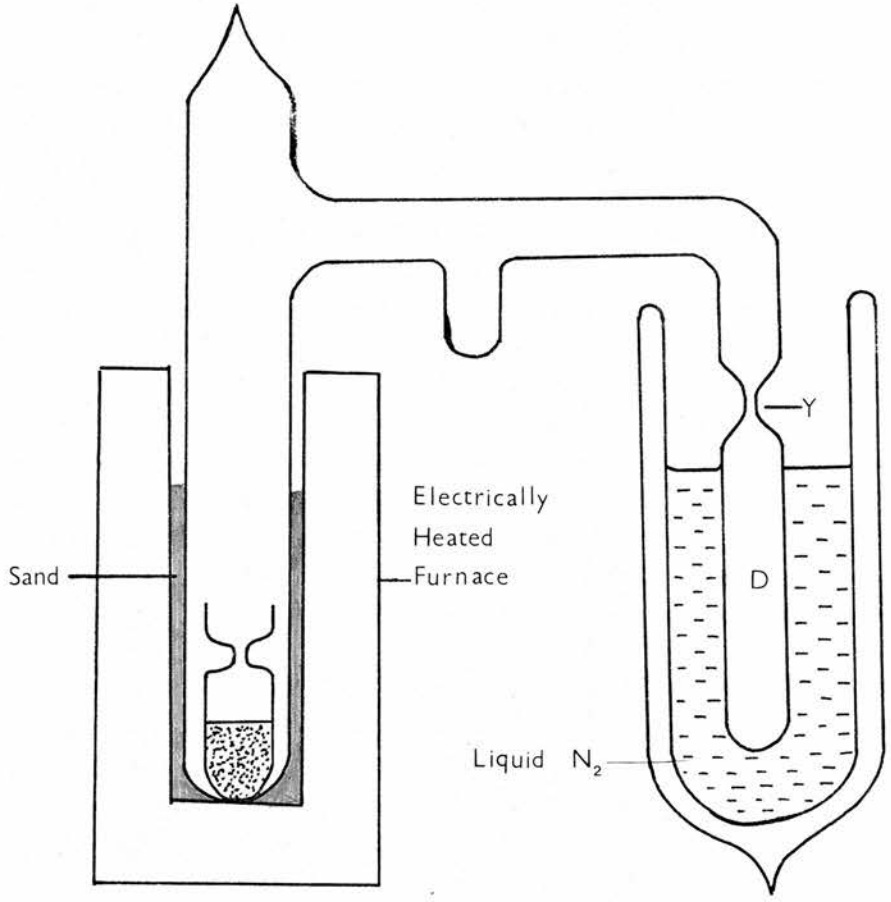

FIGURE 8B

liquid nitrogen. As the degradation proceeded, the volatile liquids and the gases were condensed in limb C by the liquid nitrogen whereas the low molecular weight fraction condensed as soon as it entered the side-arm. This viscous liquid then slowly moved along the side-arm and collected in limb B. In the form of the apparatus shown in figure 8A, the gaseous fraction was lost when the respective limbs were broken off in order that the other three fractions could be analysed.

In the modified form of the apparatus (figure 8B), the same procedure was adopted. However, the volatile liquids and the gases were trapped in limb D which was then sealed off at Y.

The degradations were conducted at a variety of times and over a range of temperatures. The head to head homopolymer was investigated at temperatures ranging from 145°C to 350°C and the copolymers from temperatures of 300°C to 400°C. The times varied from ½ hour to 4 hours.

2. Methods of Analysis

The methods employed for the analysis of the four product fractions were very similar to those described in the introduction.

The Residue was investigated by N.M.R., I.R. and U.V. spectral analysis together with molecular weight determination.

The Low Molecular Weight Fraction was also investigated by the above spectral methods. Further information was obtained using the mass spectrometer.

The Volatile Liquid Fraction was quantitatively analysed on the gas density balance. Qualitative analysis of these products was effected by the combined G.L.C. - Mass Spectrometer technique. The volatile

liquids were injected into the G.L.C. where they were separated on a 10% A.P.L. (based on celite) column. At the end of the column, 99% of the products were directed into the mass spectrometer and 1% to the flame ionisation detector. The mass spectrum of each product was hence produced. This fraction was also investigated by I.R. spectral analysis.

The Gaseous Fraction was investigated in much the same way. The injection of the gases into the G.L.C. was carried out using the piece of equipment shown in figure 9. The sealed tube containing the gases was placed in the apparatus as shown. The apparatus was then inserted into the helium flow just before the column. The tube was broken by the screw and the gases were flushed into the G.L.C. with analysis achieved as before.

3. Results of Analysis

This section will be divided into two parts. The first will deal with the products from the degradation of the head to head homopolymer. The second will deal with the more complex case of the products of the copolymer decompositions.

The Head to Head Homopolymer

The thermal degradation of head to head poly-α-methyl styrene was carried out for a variety of times at the following temperatures: 145°C, 161°C, 181°C, 197°C and 247°C. Decompositions were also conducted at 350°C in order that comparisons may be made with the copolymer degradations. In all cases, the nature of the product fractions varied only slightly, although the relative quantities of each were different. Hence, a description of the general characteristics of the products will be given followed by any variations caused by the

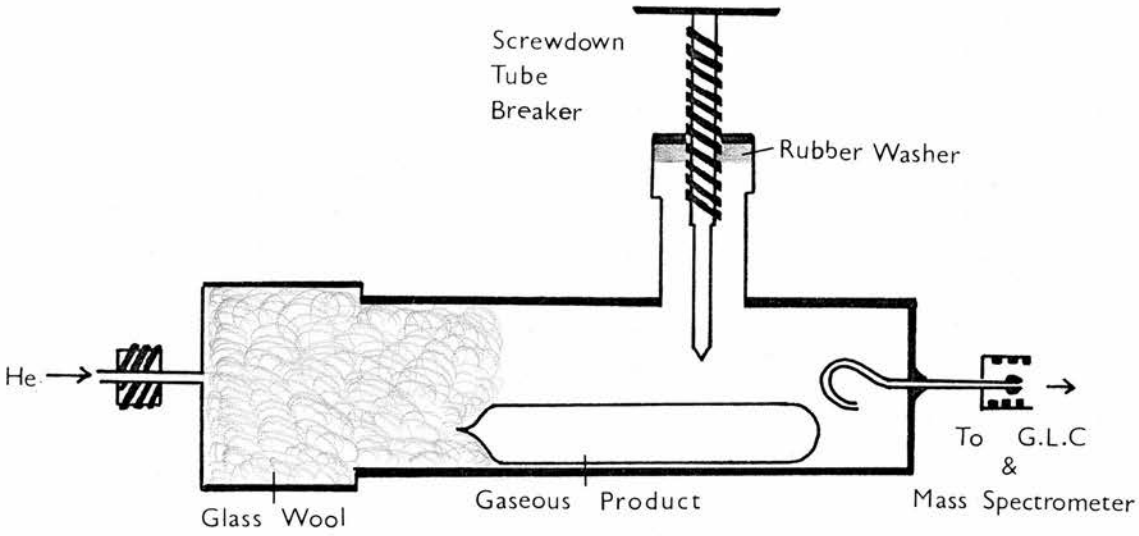
Screwdown
Tube
Breaker
Rubber Washer
He
To G.L.C
&
Mass Spectrometer
Glass Wool
Gaseous Product

FIGURE 9

changing of conditions. The investigation of this polymer was simplified by the fact that only three product fractions were obtained, the residue, a low molecular weight fraction and a volatile liquid fraction. No gases were found at any of the temperatures of decomposition.

The Residue

The residue was a brittle glassy-like solid. Figure 10 shows the ^{1}H N.M.R. spectrum obtained from the residue. There are two important features of this spectrum, both of which lead to the same conclusion. Firstly the peak due to the aromatic protons is much sharper than the equivalent peak in the spectrum of the undegraded polymer. Second, the peak which occurred at 9.5τ in the spectrum of the undegraded polymer is no longer visible in the spectrum of the residue. Both of these facts imply that one of the two configurations of the head to head poly-α- methyl styrene structure has been partially or wholly destroyed during decomposition, i.e.

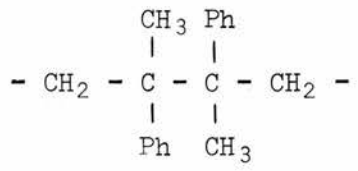

The aliphatic/aromatic proton ratio remains at 1:1 for all the values of temperature used.

The infrared spectrum of the residue, shown in figure 11B, is very similar to that of the undegraded polymer. However, the appearance of a small peak at 1630 cm^{-1} together with a shoulder at 890 cm^{-1} imply the presence of the Ph - $\overset{|}{C}$ = CH_2 group. These two are the only new peaks to appear; on the other hand, the peaks at 1285 cm^{-1} and 1255 cm^{-1} have both disappeared.

FIGURE 10

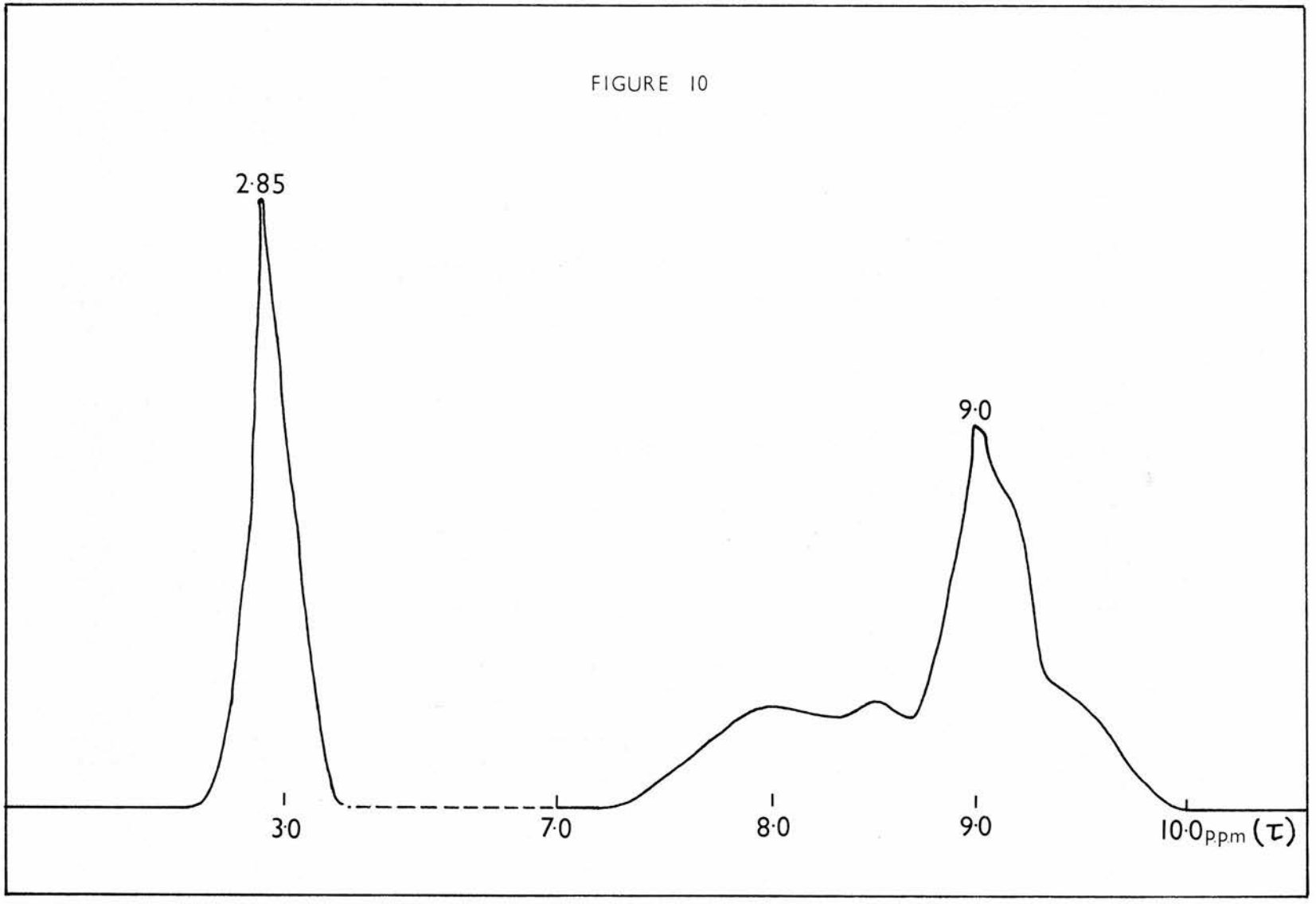

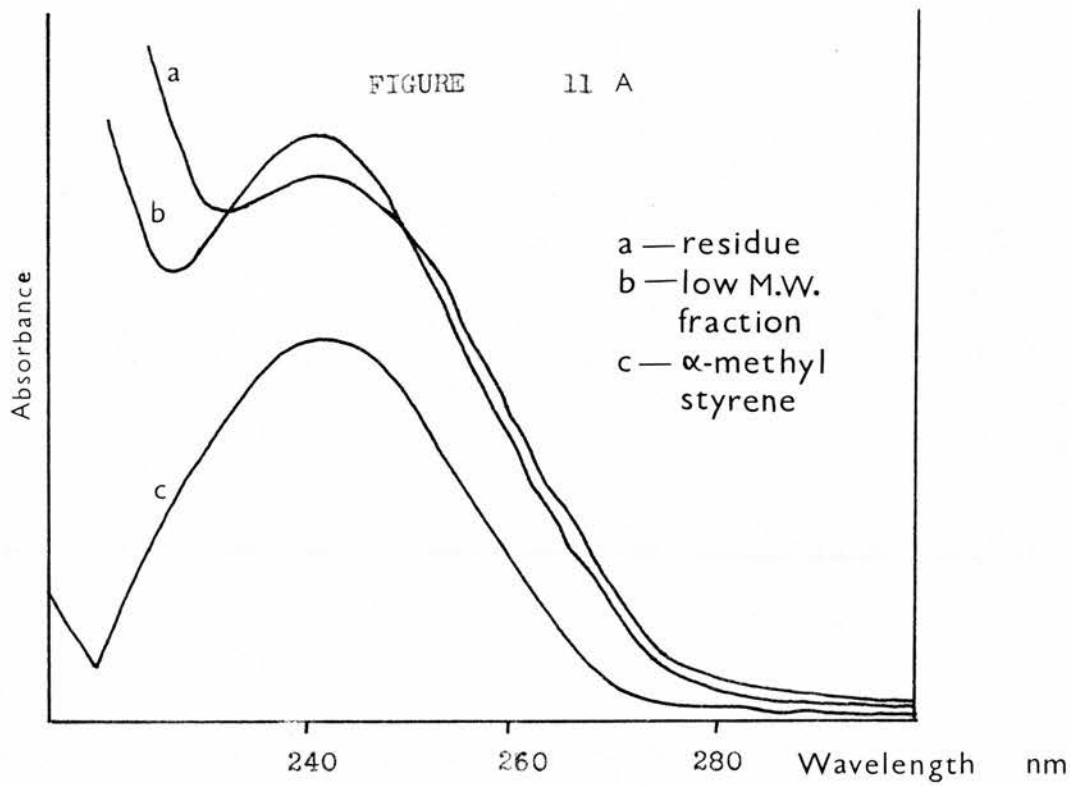
FIGURE 11 A
a
b
c
a — residue
b — low M.W. fraction
c — α-methyl styrene
Absorbance
240
260
280
Wavelength nm

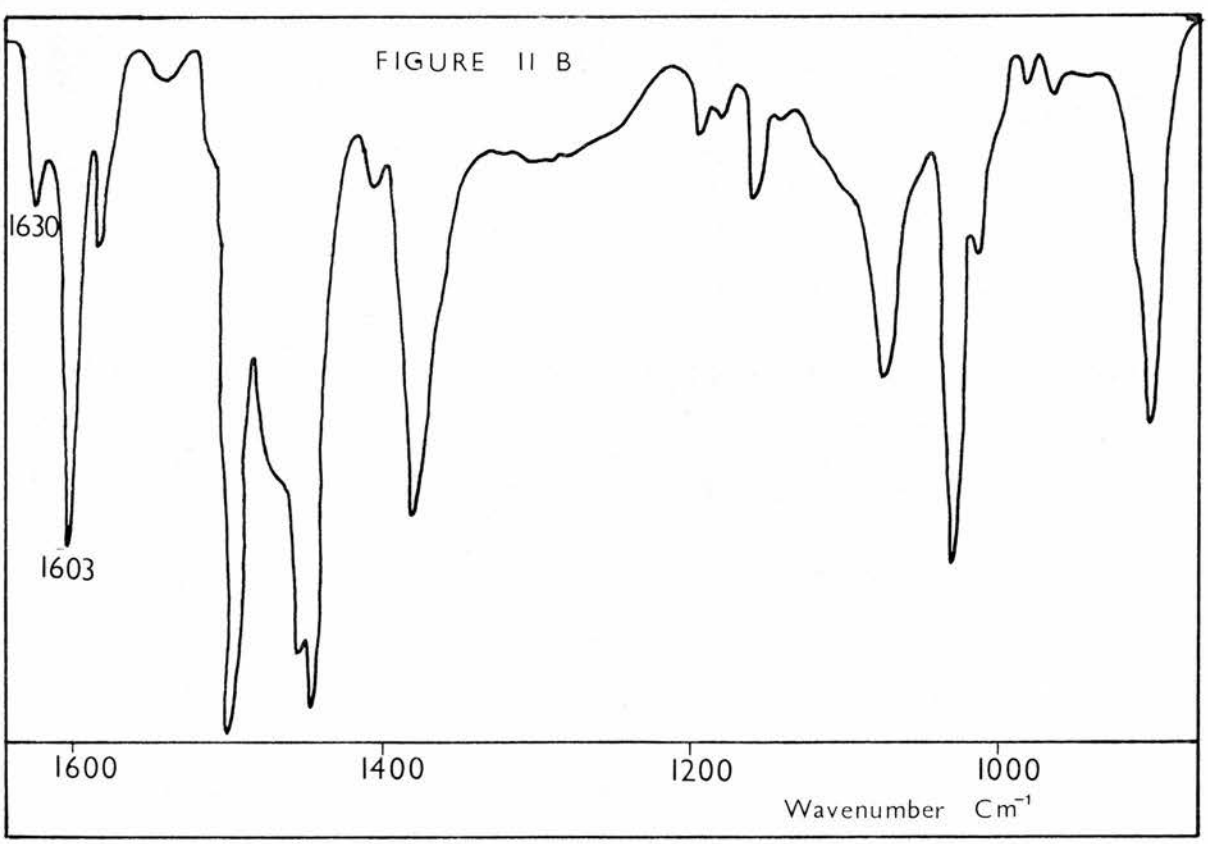
FIGURE II B
1630
1603
1600
1400
1200
1000
Wavenumber Cm⁻¹

The U.V. spectrum of the residue in cyclohexane is shown in figure 11A. It is very similar to the spectrum obtained from α-methyl styrene monomer, having a maximum at 243 nm. This could well be due to the Ph - $\overset{|}{C}$ = CH_2 group. The spectrum also shows the presence of small shoulders on the main band in the 250 - 275 nm region. These may be attributed to the undegraded polymer structure. The molar extinction coefficient, ε, of the Ph - $\overset{|}{C}$ = CH_2 band centred at 243 nm is in the region of fifty times greater than that of the undegraded polymer centred at 259 nm (see figure 7B) and hence relatively small quantities of the Ph - $\overset{|}{C}$ = CH_2 group will be sufficient to mask the band centred at 259 nm.

From these three spectra, the following conclusions may be made as to the nature of the residue. Firstly, much of the original polymer structure has been retained. Second, the residue appears to contain a number of Ph - $\overset{|}{C}$ = CH_2 groups. Third, only one of the two head to head configurations still occurs to a large extent:

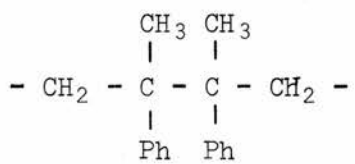

SIDE VIEW
PROJECTION

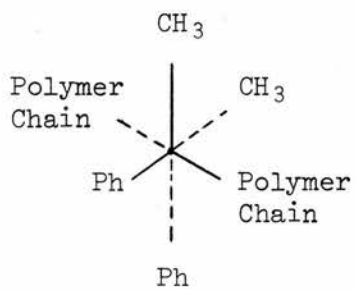

END ON VIEW

The Low Molecular Weight Fraction

This fraction was a colourless viscous liquid. The ^1H N.M.R. spectrum of the liquid was too vague to give any useful information. However, the infrared spectrum obtained was almost identical with that

produced by the residue. The only difference between the two spectra was the fact that the peaks at 1630 cm^{-1} and 890 cm^{-1} were slightly stronger in the case of the low molecular weight fraction. This spectrum still contained peaks at 2870 cm^{-1} and 1460 cm^{-1} showing that the $-CH_2-CH_2-$ function was still present.

The U.V. spectrum shown in figure 11A is similar to the spectrum of α-methyl styrene. The broad band centred at 243 nm confirms the findings of the infrared in that $Ph-\overset{'}{C}=CH_2$ is present. Small shoulders on the main band showed that some of the original polymer structure has been retained.

After diluting with carbon tetrachloride, the low molecular weight fraction was injected onto a 10% A.P.L. (based on celite) column in a Pye 104 G.L.C. The column temperature was 250°C and the carrier gas flow rate was 120 ml/minute. The resulting chromatogram showed the existence of three major products together with at least six minor ones. For comparison purposes, a standard compound of structure

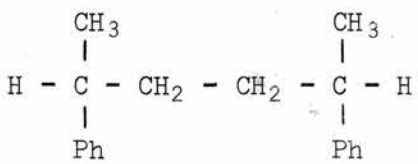

was injected into the G.L.C. The retention time of this compound was very similar to one of the major products from the low molecular weight fraction. The retention times of the other products were distributed fairly evenly on either side of that of the standard.

This fraction was too involatile to investigate on the combined G.L.C. - Mass Spectrometer system so a mass spectrum of the total liquid sample was produced. Table 2 gives a list of the major peaks.

TABLE 2

PEAKS FROM MASS SPECTROMETER	ASSIGNMENT
472	Tetramer
354	Trimer
238	Dimer
236	Dimer
234	Dimer
224	Dimer
222	Dimer
220	Dimer
208	Dimer
206	Dimer
159	
131	
105	Ph CH CH_3
91	Ph CH_2 -

There are a number of dimer-like species, some of which are saturated and some of which are unsaturated. The unsaturated ones would appear to contain the $Ph-\overset{|}{C}=CH_2$ group as there was no evidence in the infrared spectrum for any other type of non-aromatic carbon-carbon double bond.

The Volatile Liquid Fraction

This fraction was investigated on the D.6 Gas Density Balance. By using two different G.L.C. column packings, and a variety of column temperatures and carrier gas flow rates, the liquid was shown to contain only one species. U.V., N.M.R., infrared and mass spectral analysis all showed that the volatile liquid product was α-methyl styrene.

Conditional Variations

The variation of the three product fractions with temperature was studied by conducting a series of experiments over a fixed period of four hours. The relative amounts of each fraction for the different temperatures of decomposition are shown in table 3.

TABLE 3

TEMPERATURE OF DECOMPOSITION	% RESIDUE	% LOW M.W. FRACTION	% VOLATILE LIQUID
145	85	7.9	7.1
161	77	12.4	10.6
181	67	20.0	13.0
197	53	32.0	15.0
247	15	64.8	20.2

Although the relative proportions of the fractions varied with temperature, their compositions changed only slightly. The residues varied in the ratio of the concentration of the $>C = CH_2$ function to the concentration of $C = C$ of the phenyl group. Table 4 shows the ratios of the peak intensity at 1630 cm^{-1} to that at 1603 cm^{-1} in the I.R. spectrum (figure 11B), which are due to the above two functions respectively.

TABLE 4

TEMPERATURE IN ^{o}C	$\frac{\text{INTENSITY OF } C = CH_2 \text{ at } 1630\ cm^{-1}}{\text{INTENSITY OF } C = C \text{ at } 1603\ cm^{-1}}$
145	0.27
161	0.33
181	0.29
197	0.25
247	0.16

With the exception of the 145^{o} decomposition, the ratio is decreasing with increasing temperature. This implies that the relative concentration of the $>C = CH_2$ function in the residue is also decreasing.

This conclusion is substantiated by evidence obtained from the U.V. spectra. The maximum absorbtion in the spectrum of the residue

of the 197°C degradation occurs at a wavelength of 245 nm and that of the 247°C degradation occurs at 254 nm. This shows that the absorbtion due to Ph - $\overset{|}{C}$ = CH_2 is relatively decreasing.

The U.V. and infrared spectra of the low molecular weight fractions showed very little variation with changing temperature. However, the mass spectra showed a greater contribution from trimeric and tetrameric species at higher temperature decompositions. This would explain the increase in the ratio of this fraction to the volatile liquid with increasing temperature

The volatile liquid did not vary in its composition. At all temperatures of decomposition, this fraction was always 100% α-methyl styrene.

The variation of the three product fractions with time was studied at 181°C. Table 5 shows the percentage of each fraction at the various time intervals.

TABLE 5

TIME IN HOURS	% RESIDUE	% LOW M.W. FRACTION	% VOLATILE LIQUID
½	79.5	12.0	8.5
1	72.9	16.1	11.0
2	69.6	18.3	12.1
4	67.0	20.0	13.0

The table shows that most of the low molecular weight and volatile liquid fractions are produced in the first hour of degradation. The table also shows that the ratio of the amounts of these two fractions does not vary appreciably with time.

The composition of the residue is very similar for all the time intervals investigated. The ratio of the intensities of the peaks at

1630 cm^{-1} and 1603 cm^{-1} in the infrared spectra was identical in all cases.

The composition of the low molecular weight fraction also did not alter with time and the volatile liquid fraction was always 100% α-methyl styrene. Both of these facts were shown by using the D6 Gas Density Balance, the former by comparing the peak areas at the different times of the three major species, described previously, and the latter by comparison of the peak area with those of standard amounts of α-methyl styrene.

The Copolymers

The four product fractions obtained from the thermal decomposition of the copolymers had a number of common features. Hence, so that comparisons could be made, much of the work was concentrated on the analysis of the products resulting from the degradation of the copolymers at 350°C for a period of four hours. The effects of time and temperature on the decomposition products were also studied. A description of the general characteristics of the products obtained at 350°C will be given followed by the conditional variations.

The extent of degradation under the above conditions is summarised in table 6 (350°C for four hours).

TABLE 6

n	% RESIDUE	% LOW M.W. FRACTION	% VOLATILE LIQUID FRACTION	% GASEOUS FRACTION
1	9.0	76.0	13.5	1.5
3	58.0	34.0	7.0	1.0
4	72.0	23.5	3.6	0.9
5	67.0	27.8	4.3	0.9
6	64.0	32.2	2.7	1.1
10	56.0	39.3	3.4	1.3

From the table, it is evident that the n = 4 copolymer is the most thermally stable. The least quantity of volatile liquids is produced by the n = 6 copolymer. The amount of gaseous fraction does not vary appreciably for any of the copolymers.

The Residues

For all cases, the ^1H N.M.R. and U.V. spectra were alike in every respect with the equivalent spectra of the original polymers. However, the I.R. spectra, although containing all the peaks attributable to the undegraded polymers, also contained a small peak at 1642-3 cm^{-1}. This peak implies the presence of an isolated - $CH = CH_2$ group. The existence of this function is substantiated by the presence of a peak at 910 cm^{-1}. Although this peak was present in the spectra of the undegraded polymers, it is relatively stronger in the spectra of the residues. Also detectable in the I.R. spectra is a peak at 1670 cm^{-1}, this absorbtion is very weak and could well be due to the presence of a trisubstituted carbon-carbon double bond.

The Low Molecular Weight Fraction

The ^1H N.M.R. spectra of this fraction were too vague to provide any useful information.

The infrared spectra, an example of which is shown in figure 12, contained the peaks of the undegraded polymer. They also contained peaks at 1642 cm^{-1}, 1300 cm^{-1}, 990 cm^{-1}, 965 cm^{-1}, 910 cm^{-1} and 890 cm^{-1}. The peaks at 1642 cm^{-1}, 990 cm^{-1} and 910 cm^{-1} imply the presence of an isolated - $CH = CH_2$ group. The peaks at 1300 cm^{-1} and 965 cm^{-1} show the presence of a trans $\begin{matrix} R \\ \diagdown \\ H \end{matrix}\!\!>\!C = C\!<\!\begin{matrix} H \\ \diagup \\ R' \end{matrix}$ function where R and R' are alkyl or aryl groups. This is substantiated by the occurrence of a very small peak at 1670 cm^{-1}. The peak at 890 cm^{-1} implies the presence of

FIGURE 12

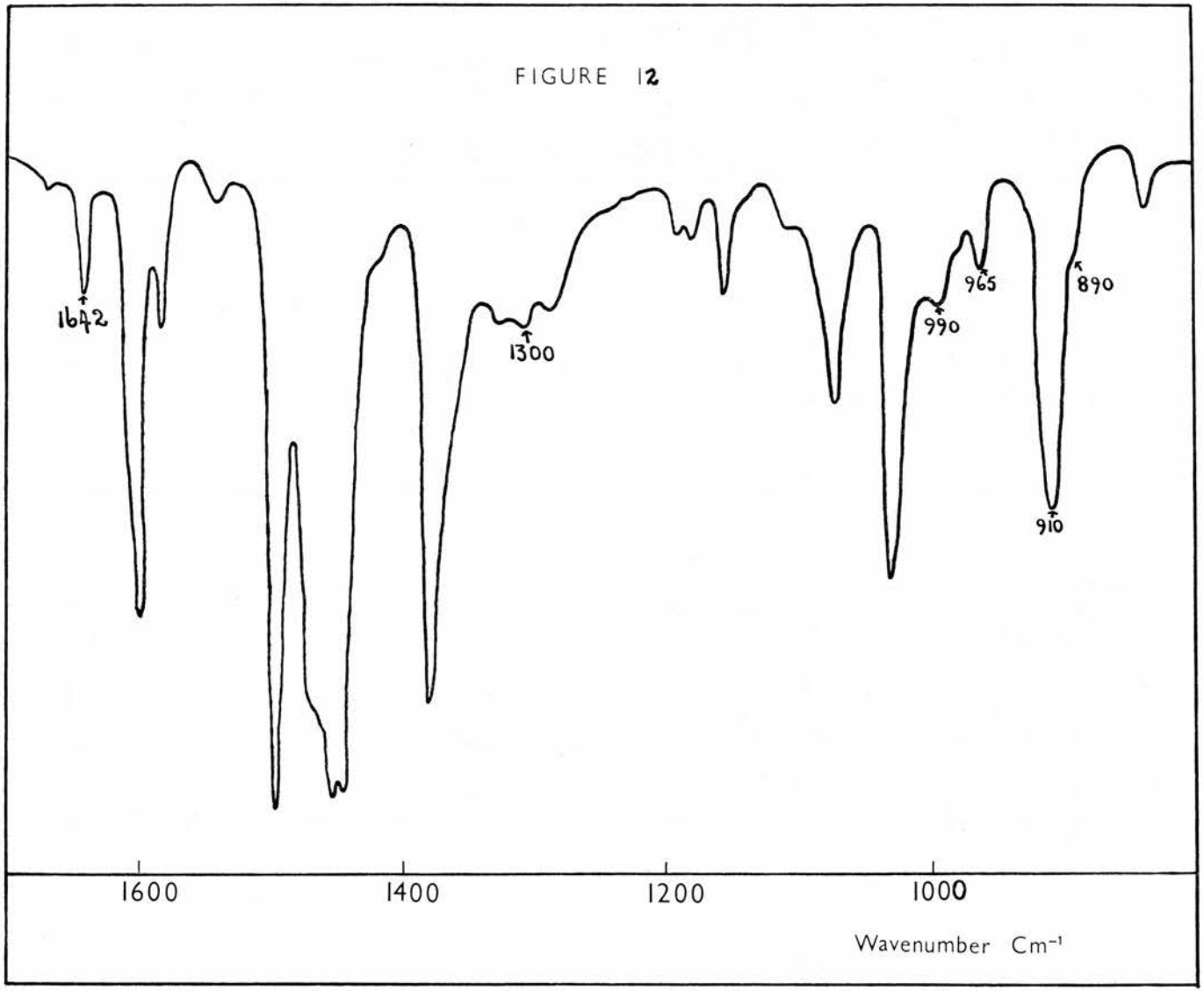

TABLE 7

n = 1	3	4	5	6	10
278	278	278	280		376*
264	264	264*	264	264	361
252	252*	252*	252*		348
250	250*	250*	250*	250*	347
239	239	239	239	239	298
238**	238**	238**	238**	238**	258
237	237		237		245*
224	224	224	224	224	244*
220		215	210	222	243*
208	208	210	208	216	238**
194	194	208	194	208	235
182		194	182	194	206
181	181	181	181	181	195
180	180	180	180	180	194*
179	179	179	179	179	181*
178	178	178	178	178	180
167	167	167		167	179
165	165	165		165	178
159	159	159	155	159	167
145	145	145	145	145	165
132	132	132	132	132	159
131	131	131	131	131*	157
119	119	119	119	119	145
118*	118*	118*	118*	118*	133
117*	117*	117*	117*	117*	132
115	115	115	115	115	131*
106	106	106	106	106	119
105**	105**	105**	105**	105**	118**
104	104	104	104	104	117
103	103	103	103	103	106
91*	91*	91*	91*	91*	105
					104
					91

* signifies a large peak
** signifies an extra large peak.

the largest of the peaks above mass number 190. This peak together with peaks at 239, 220, 191, 145, 133, 132, 131, 119, 118, 117, 106, 105 (major) 104, 103 and 91 shows the presence of

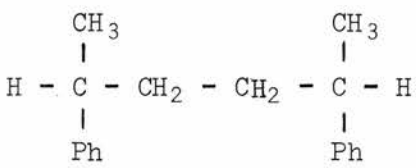

This species, as will be shown later, is unlikely to be a product of decomposition. It is more likely to have been formed in the preparation of the copolymer by termination of the dianion before any reaction with dihaloalkane had taken place. The other dimeric-like species, however, are likely to have been produced as a direct result of the decomposition.

For the case of the n = 10 copolymer, the resulting significant fragment-ion peaks below 170 are very similar in nature to those of the other copolymers. Hence, the low molecular weight species of this polymer must contain some structural similarities to the equivalent fraction of the other copolymers.

The mass spectra also showed that trimeric, tetrameric and sometimes pentameric species are present in this fraction.

From the infrared, U.V. and mass spectral evidence, the following conclusions may be made as to the nature of the low molecular weight fraction. Firstly, the structures present were similar to the structure of the undegraded polymer. Second, some of the species contained carbon-carbon double bonds. Third, there were various dimeric species together with higher molecular weight analogues present in this fraction.

The Volatile Liquids

The study of this product fraction will be divided into two parts. Firstly, a quantitative investigation of the very volatile liquids, which are produced from each copolymer, will be made. Second, the less volatile products, which in many cases are unique to one particular polymer, will be qualitatively examined.

Identification of the volatile products was effected by the combined G.L.C. - Mass Spectrometer system described previously.

From this, a mass spectrum of each component in this fraction was produced. Complete identification of every individual component was not possible as the mass spectra obtained could often be attributed to a number of isomers. Wherever possible, checks were made to ascertain that the retention times of an identified product component and the standard compound coincided.

The Common Products were toluene, ethyl benzene, styrene, isopropyl benzene, n-propyl benzene, α-methyl styrene and α-ethyl styrene. All were identified on the G.L.C. - Mass Spectrometer system and checked against the standard compounds with the exception of α-ethyl styrene which was not commercially available. However, the parent ion was 132 and the major ion peak was at 117. The retention time was between those of α- and trans β-methyl styrenes. The possible products were thought to be:

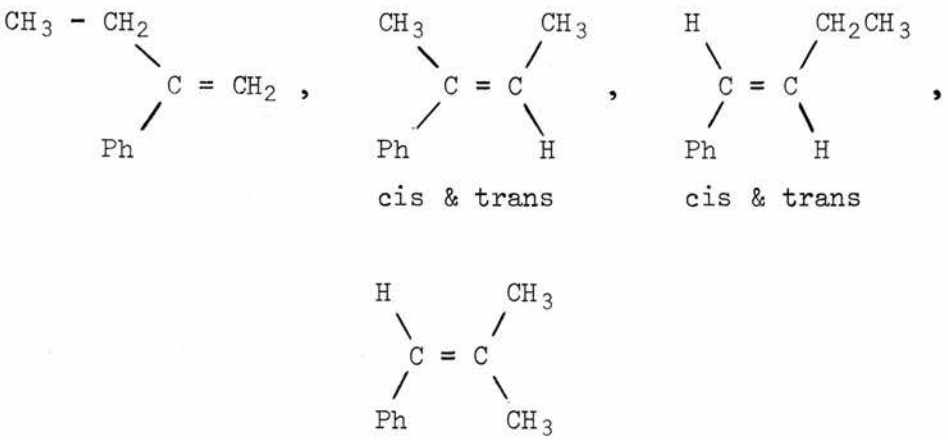

All the compounds except α-ethyl styrene were ruled out as their retention times would be expected to be greater than that of trans β-methyl styrene. This is because all the other compounds are equivalent to β-methyl styrene together with an added group.

Quantitative analysis of these products was accomplished using

the D6 Gas Density Balance. The liquid was injected onto a 10% A.P.L. column and the areas of the resulting peaks were measured using a Honeywell Precision Integrator. Under the same conditions, a known weight of a standard compound, α-methyl styrene, was passed through the column and the resulting peak integrated. The quantity by weight of each of the 'common' products was calculated using the following expression[18]:

$$\frac{W_1}{W_2} = \frac{A_1}{A_2} \cdot \frac{M_1(M_2-m)}{M_2(M_1-m)}$$

where W_1 is the weight of the product under investigation, W_2 is the weight of α-methyl styrene used as a standard, A_1 and A_2 are the corresponding integrated areas, M_1 and M_2 are the corresponding molecular weights and m is the molecular weight of the carrier gas, in this case, nitrogen.

Table 8 shows the percentages by weight of the common volatile components produced by each copolymer with respect to the total volatile liquid fraction.

TABLE 8

n	1	3	4	5	6	10
PRODUCT						
Toluene	1.2	4.0	7.0	9.0	9.0	9.5
Ethyl Benzene	4.9	4.2	5.8	9.0	8.5	6.1
Styrene	1.5	2.1	7.0	3.2	3.5	5.6
Isopropyl Benzene	3.3	1.6	2.0	5.5	3.9	2.2
n-Propyl Benzene	1.1	1.4	5.4	3.9	3.0	3.2
α-Methyl Styrene	72.0	38.0	32.5	26.7	38.3	60.0
α-Ethyl Styrene	8.1	9.8	10.8	13.3	9.5	5.6

The table shows that α-methyl styrene is always the major component of this fraction. Also, the concentration of the α-methyl styrene reaches a minimum value with the n = 5 copolymer. The total concentration due to these components is always greater than 70% of the total volatile liquid fraction.

Table 9 shows the percentages by weight of the 'common' components in the combined volatile liquid and low molecular weight fractions.

TABLE 9

n	1	3	4	5	6	10
PRODUCTS						
Toluene	0.2	0.6	0.6	0.8	0.5	0.6
Ethyl Benzene	0.8	0.6	0.5	0.8	0.5	0.4
Styrene	0.2	0.3	0.7	0.3	0.2	0.4
Isopropyl Benzene	0.5	0.2	0.2	0.5	0.2	0.1
n-Propyl Benzene	0.2	0.2	0.5	0.4	0.2	0.2
α-Methyl Styrene	11.1	5.7	3.0	2.6	2.4	3.7
α-Ethyl Styrene	1.0	1.6	1.0	1.3	0.6	0.4
Low M.W. Fraction	85.0	83.0	87.0	87.0	90.0	93.5

This table shows the quantities of the volatile liquids are very small compared to the amount of the low molecular weight fraction.

The Non-Common Products will be considered separately for each copolymer. Each volatile liquid fraction was separated into its components on the G.L.C. of the G.L.C. - Mass Spectrometer system using the same column, temperature and carrier gas flow rate. Representations of the chromatograms produced for each copolymer are shown in figure 13. With

FIGURE 13

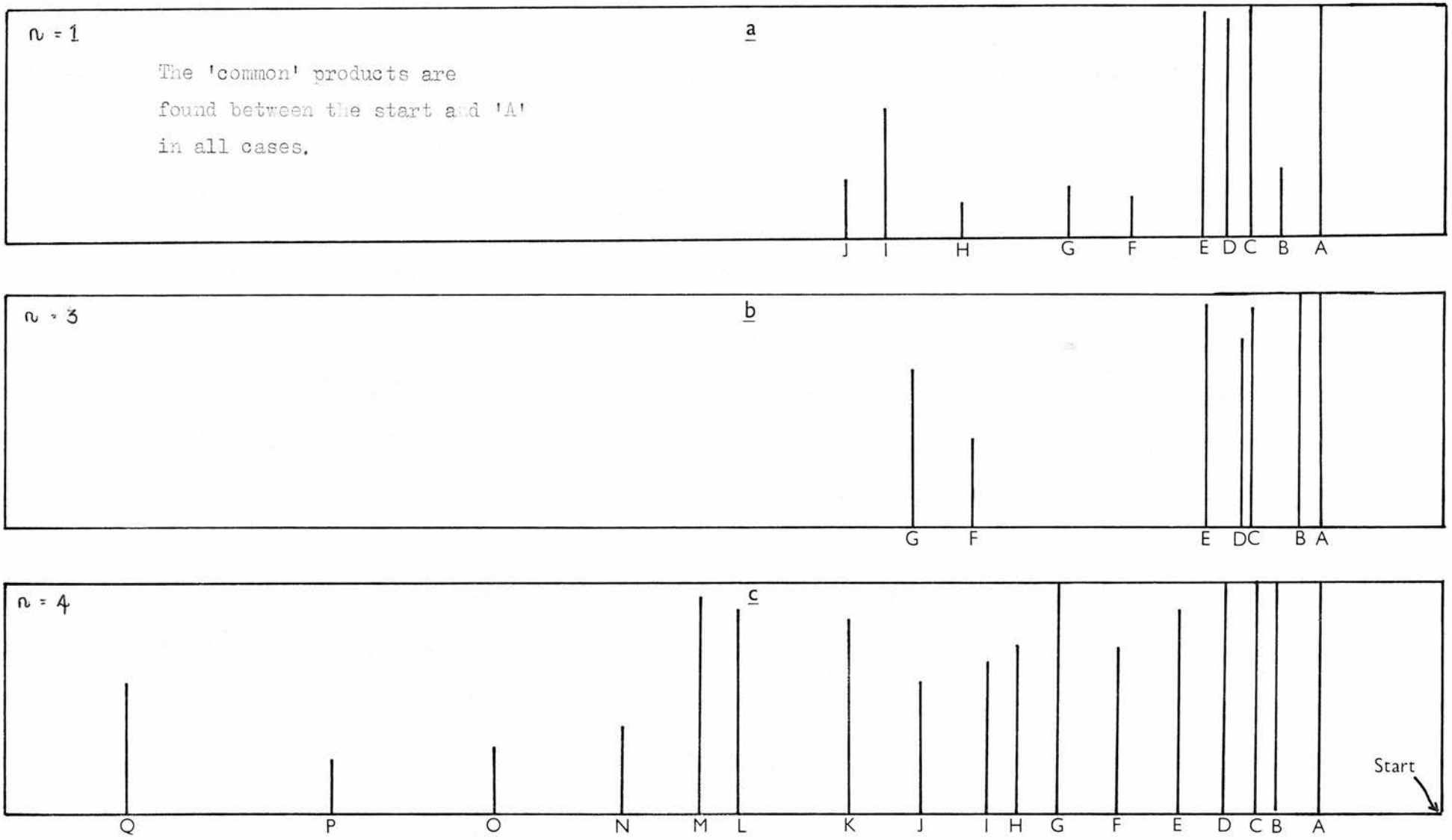
n = 1
a
The 'common' products are
found between the start and 'A'
in all cases.
J I H G F E D C B A
n = 3
b
G F E DC B A
n = 4
c
Start
Q P O N M L K J I H G F E D C B A

the Pye 104 G.L.C., the resulting peak areas are not directly proportional to the weight or the volume of the respective components. Hence, the peak heights shown in the diagrams only give an approximate indication of the relative quantities of each component.

A mass spectrum was obtained for each of the 'non-common' products and using comparisons with spectra of standard compounds[19], possible explanations as to the nature of the components were worked out. For many of the products, isomers were possible and in these cases only general characteristics have been put forward.

n = 1 Copolymer

Table 10 shows the parent molecular and prominent fragment ion peaks of the product components A - J shown in figure 13a.

TABLE 10

PRODUCT	PARENT PEAK	PROMINENT ION PEAKS IN DECREASING ORDER OF MAGNITUDE						
A	118	118	117	103	78	51	77	
B	132, 134	91	117	105	115	103	132	
C	132	117	91	115	132	131	105	
D	132	117	91	115	132	131	105	
E	132	117	91	115	132	131		
F	146	105	91	104	103	131	117	115
G	146	91	131	105	117	115	146	
H	144	91	104	105	129	128	117	115
I		118	105	91	117			
J	174	105	91	118	117	131		

Product A is α-methyl styrene.

The peaks at 91, 105, 117 together with the parent peaks at 134 and 132 show that the product B, is a mixture of a compound of molecular weight, 132, isobutyl benzene and secondary butyl benzene.

The three components, C, D and E must be very similar to each

other. On investigating the mass spectra of the known compounds with a molecular weight of 132, no molecule could be found with the order of peaks as given by C, D and E. This ruled out the possibility that C, D and E were any of the methyl indans or any of the styrenes which contained further ring substitution. Every component which has been identified so far has been a monosubstituted alkyl or alkenyl benzene. Hence, it is not unlikely that these three products with a molecular weight of 132, are alkenyl benzenes. The peak at 115 is typical, amongst other compounds, of styrene-like molecules. On the other hand, a peak at 91 usually implies the presence of the Ph - CH_2 - group which appears to be contradictory to the presence of a styrene-like structure. However, in the mass spectrum of β-methyl styrene, a peak occurs at 91. This is the third largest peak of the spectrum and is about half the intensity of the major peak at 117. The peak at 91 must be due to some rearrangement within the spectrometer. Therefore it is reasonable to suggest that components C, D and E may be related to β-methyl styrene. Possible structures for C, D and E are:

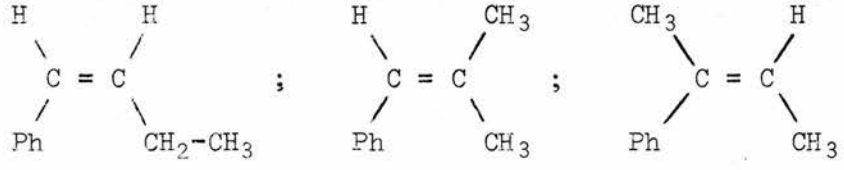

cis & trans cis & trans

No compounds with a molecular weight of 146 could be found with the order of peaks given by F and G. Both are probably alkenyl benzenes but because of the possibility of the randomisation of the double bond as is found with β-methyl styrene, it would be very difficult to relate the mass spectra to probable formulae.

Compounds H and J are also difficult to relate to formulae for

the same reason, however, H would appear to contain two double bonds and J, one.

Compound I could not be related to any structure as no parent peak was visible.

Randomisation of the double bond of an olefin within the spectrometer is not an uncommon occurrence. This has been explored in greater detail by Benyon, Saunders and Williams[20].

n = 3 Copolymer

Table 11 shows the parent molecular and fragment-ion peaks of the mass spectra of the product components A - G shown in figure 13b.

TABLE 11

PRODUCT	PARENT PEAK	PROMINENT ION PEAKS IN DECREASING ORDER OF MAGNITUDE						
A	118	118	117	103	78	51	77	115
B	118	117	118	91	115	105		
C	146	105	91	131				
D	132	117	91	115				
E	132	117	91	115	132	131		
F		91	105	104	115	117		
G		91	105	131	115	133	118	117

Compound A is α-methyl styrene.

Compound B is β-methyl styrene. This spectrum also contained a very small peak at 134. A peak at 105 showed that isobutyl benzene was probably present.

It is likely that all the compounds with a molecular weight of $104 + n \times 14$, where n is an integer, are monoalkenyl benzenes. Similarly, it is likely that the components with a molecular weight of $106 + n \times 14$ are monoalkyl benzenes.

Hence, compounds C, D and E are all probably alkenyl benzenes.

D and E, on account of their retention times and mass spectra, would appear to be identical with the components D and E of the n = 1 copolymer.

Components F and G cannot be related to any structure because no parent peaks are apparent in their mass spectra.

n = 4 Copolymer

Table 12 shows the parent molecular and fragment ion peaks of the mass spectra of the product components A - Q shown in figure 13c.

TABLE 12

PRODUCT	PARENT PEAK	PROMINENT ION PEAKS IN DECREASING ORDER OF MAGNITUDE							
A	118	118	117	103	78	51	77	115	
B	132, 118	117	91	118	115	105	103		
C	132, 134	91	117	92	105	103	132	115	134
D	146, 132	105	91	117	115	131	103	146	
E	132, 148	117	91	115	132	105	103	131	148
F	148, 146	91*	93	131	117	115	105		
G	160	104	118	91	103	115	117	145	131
H	162	105	91	119					
I	162	91	133	105					
J	160	104	91	117	105	129	131	118	115
K	174	91	119	131					
L	174	91*	118	117	104	115	174	131	132
M	174, 176	105	91	117	118	115			
N	174	105	118	91	131				
O	188	131	91	117	105	115			
P	178, 192	91	103	116	117	115	105	192	178
Q	196	105*	91	104	117	115	131	196	

Product A is α-methyl styrene.

Product B is a mixture of β-methyl styrene and an alkenyl benzene (104 + 2 x 14).

Product C appears to be a mixture of isobutyl and secondary butyl benzenes together with an alkenyl benzene of molecular weight, 132.

All the compounds with molecular weights of 132, 146, 160, 174

or 188 are probably alkenyl benzenes. However, because of the randomising of the double bonds in the mass spectrometer, very few conclusions can be made from their mass spectra as to possible structures. Component L, on the other hand, contains a very strong ion peak at 91 and is, hence, very likely to contain the Ph - CH_2 - group.

The compounds with molecular weights of 148 and 162 are probably alkyl benzenes. The alkyl benzene part of product E, from the mass spectrum, might be 2-phenyl pentane. Similarly, from their mass spectra, product F is mostly 1-phenyl pentane, product H appears to be 2-phenyl hexane and product I is 3-methyl-3-phenyl pentane.

n = 5 Copolymer

Table 13 gives the parent molecular and fragment-ion peaks of the mass spectra of the compounds A - Q in figure 13d.

TABLE 13

PRODUCT	PARENT PEAK	FRAGMENT ION PEAKS IN DECREASING ORDER OF MAGNITUDE									
A	118	118	117		103	78	51	77	115		
B	118	117	118		91						
C	132, 134	91	117		105	92	132	103	115	134	
D	146	105	91		131	146	117	115			
E	132	117	91		115	132	92	131			
F	146	91	105		106	92	117	115	131		
G	148	91	92		148	105					
H	160, 162	105	91		118	106	103	115	117	131	
I	162	105*	91		106	162	103				
J	160	105*	91		103	150	148	149	151		
K	160	91	104		105	117	115	131	132		
L	160	91	104		117	92	105	115	131	132	160
M	174	105	91		118	131	103	106	117	159	174
N	188, 186	91	104		105	117	92	118	115	145	
O	188	105	118		91	131	117	103			
P	188	131	91		117	115	105	104	119		
Q	188	91	92	97	188	118	117				

Compound A is α-methyl styrene and compound B is β-methyl styrene.

Compound C is a mixture of isobutyl and secondary butyl benzenes together with an alkenyl benzene.

Compounds D, E, F, K, L, M, N, O, P and Q are probably all monoalkenyl benzenes. Compounds G and I are monoalkyl benezenes and compound H appears to be a mixture of the two. By comparing the mass spectrum of compound G with the mass spectra of standard compounds, G was found to be 1-phenyl pentane. By the same process, I was found to be 2-phenyl hexane. The monoalkyl benzene part of product H could not be identified in this way. Compound J is a mixture of an alkenyl benzene and 1,5 dibromopentane. The dibromo compound is unreacted starting material.

The two products M and Q are by far the most abundant of the 'non-common' products, M, in fact, being present in similar quantities to α-methyl styrene.

n = 6 Copolymer

Table 14 shows the parent molecular and fragment ion peaks of the mass spectra of the products A - G shown in figure 13e.

TABLE 14

PRODUCT	PARENT PEAK	PROMINENT FRAGMENT IONS IN DECREASING ORDER OF MAGNITUDE						
A	118	118	117	103	78	51	77	115
B	118	117	118	91				
C	132, 134	91	105	117	115	103	132	
D	132, 146	105	105	91	117	115	131	132
E	132	117	115	91	132	131		
F	162	105	91	106				
G	160	91	104	105	117	115		

Compounds A and B are α- and β-methyl styrene respectively. Product C is a mixture of isobutyl benzene, secondary butyl benzene

and an alkenyl benzene of molecular weight, 132.

Products D, E and G are all probably monoalkenyl benzenes whereas compound F is a monoalkyl benzene. Comparison with known mass spectra showed this compound to be 2-phenyl hexane.

n = 10 Copolymer

Table 14 shows the parent molecular and fragment ion peaks of the mass spectra of the products A - H shown in figure 13f.

TABLE 15

PRODUCT	PARENT PEAK	PROMINENT FRAGMENT IONS IN DECREASING ORDER OF MAGNITUDE								
A	118	118	117	103	78	51	77	115		
B	118, 132	117	91	118	115	92	104	132		
C	132, 146	91	117	105	132	115	131	146		
D	148, 132	117	91	92	132	115	131	105	148	133
E	162, 160	105*	118	91	106	103	115	119	162	160
F	162	105*	91	106	162					
G	174, 162	118	105	91	104	117	119			
H	174	104	91	117	92	106	118			

Compound A is α-methyl styrene and product B is a mixture of β-methyl styrene and an alkenyl benzene of molecular weight, 132. Products C and H are also probably monoalkenyl benzenes whereas products D, E and G appear to be mixtures of one monoalkyl and one monoalkenyl benzene in each case. Comparison with the mass spectra of authenticated compounds showed that compound F is 2-phenyl hexane. The alkyl benzene part of product D appears to be 1-phenyl pentane. The mass spectrum is modified by peaks from the 132 compound, however, the retention time on the G.L.C. is very similar to that of product G of the n = 5 copolymer which is 1-phenyl pentane.

The alkyl benzene components of products E and G could not be identified. This was primarily due to the modification of the spectra

by the monoalkenyl benzenes also present.

The conclusions to be drawn from the mass spectra are rather limited. Firstly, all the copolymers produce a number of 'non-common' products, most of which are probably monoalkenyl benzenes and some of which are monoalkyl benzenes. Second the copolymers with n = 4 and n = 5 produce the greatest number of these products. Third it is clear that the production of mass spectra alone is not an efficient method of compound identification. For the above products, this is because of the randomisation of the double bonds within the mass spectrometer which gives rise to unexpected fragment-ion peaks. Also, for the alkenyl benzenes of molecular weight 132, 146, 160, 174 and 188, there are very few spectra available in the literature for comparison purposes. On the other hand, most of the above product components are available in such small quantities that it was only by using mass spectrometry that any useful data could be obtained.

Information as to the nature of the double bonds was, however, obtained by the investigation of the infrared spectra of the whole volatile liquid fraction. Figure 14 shows a typical spectrum of this fraction. The spectra are very similar to those produced by the corresponding low molecular weight fractions. All contain peaks at 1642 cm^{-1}, 1630 cm^{-1}, 1300 cm^{-1}, 990 cm^{-1}, 965 cm^{-1}, 910 cm^{-1} and 890 cm^{-1}. The relative intensities of the 1642 cm^{-1} and the 1630 cm^{-1} peaks vary with each copolymer. The 1642 cm^{-1}, 990 cm^{-1} and 910 cm^{-1} peaks show the presence of the $-CH=CH_2$ group, and the 1630 cm^{-1} and 890 cm^{-1} peaks show the presence of the $Ph-\overset{|}{C}=CH_2$ group. The latter of these entities exists for the most part as α-methyl styrene. The

FIGURE 14

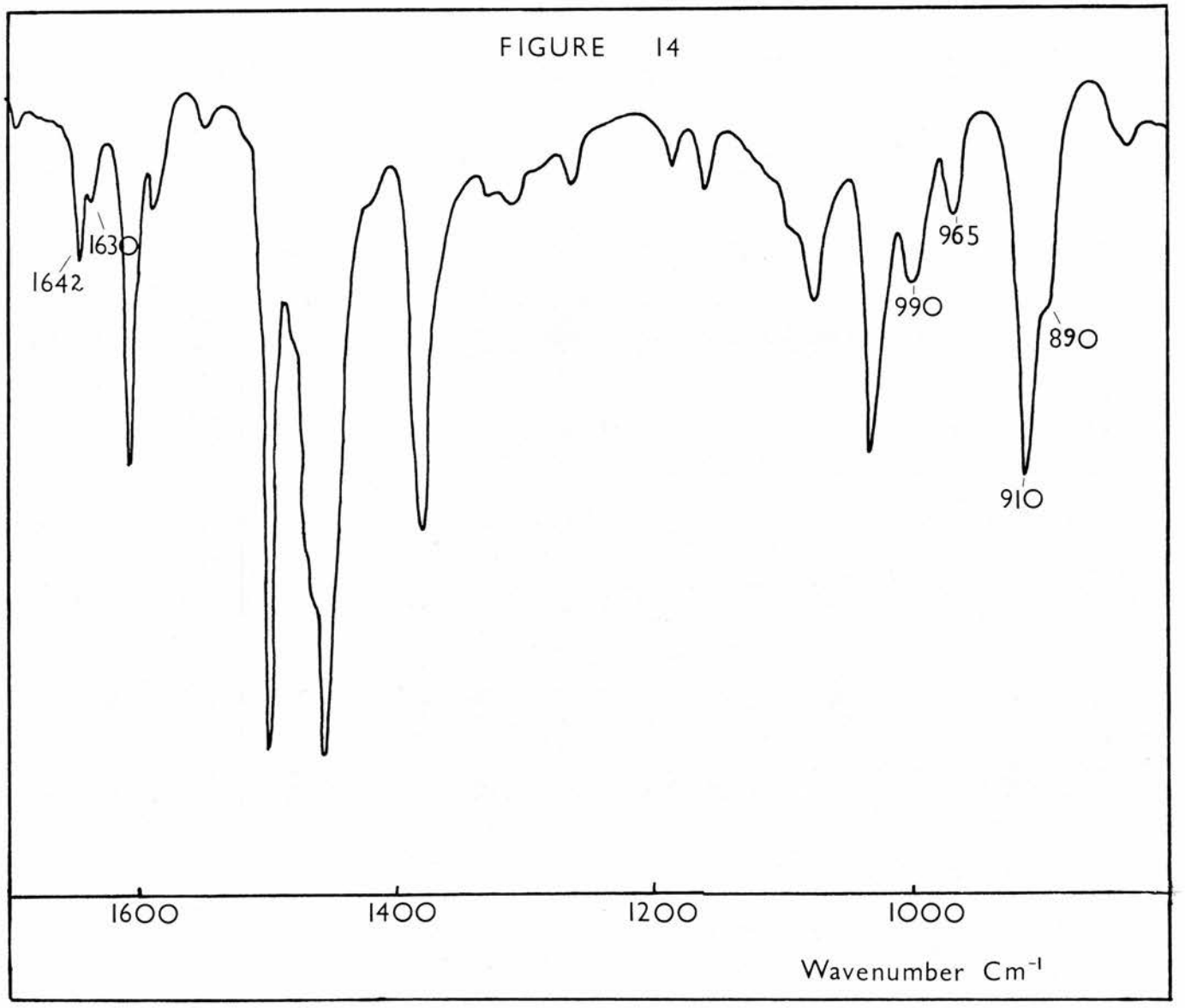

peaks at 965 cm^{-1} and 1300 cm^{-1} imply that a trans $\begin{smallmatrix} H \\ \diagdown \\ \quad C = C \\ \diagup \quad \diagdown \\ \quad\quad H \end{smallmatrix}$ group is present. On the other hand, no evidence can be found for a cis $\begin{smallmatrix} H \quad\quad H \\ \diagdown \quad \diagup \\ \quad C = C \\ \diagup \quad \diagdown \end{smallmatrix}$ group in any of the spectra.

The Gaseous Fraction

This fraction was also analysed qualitatively the G.L.C. - mass spectrometer system. The gases were injected onto the G.L.C. column in the manner previously described. The carrier gas flow rate was 20 ml/minute and the column temperature was 30°C. A mass spectrum was produced for each product and the gases were identified by comparison with standard spectra. The gases produced by each copolymer were, in many instances, the same.

The above method did not show the presence of methane. Methane was found to be present by conducting the degradation with the apparatus, shown in figure 8A attached directly to the mass spectrometer. The other gases, the volatile liquid, and low molecular weight fractions were trapped as before. The methane, however, was drawn straight into the mass spectrometer where it was identified.

The quantity of the gases was small in comparison with the amount of volatile liquid produced. The largest gaseous fraction was found for the n = 1 copolymer, and the least for the n = 4 and n = 5 copolymers.

Table 16 shows the gases produced by each copolymer during thermal degradation at 350°C for four hours.

For all cases, methane and ethylene are the most abundant of the gases. The structures of butane, butene, pentene, pentadiene, hexane and hexadiene could not be fully determined because of the great similarity in the mass spectra of the isomers.

TABLE 16

n / PRODUCT	1	3	4	5	6	10
Methane	✓	✓	✓	✓	✓	✓
Ethylene	✓	✓	✓	✓	✓	✓
Propane	✓	✓	✓	✓	✓	✓
Propene	✓	✓	✓	✓	✓	✓
Butane			✓			✓
Butene	✓	✓	✓	✓	✓	✓
Butadiene		✓	✓	✓	✓	✓
Pentene	✓	✓	✓	✓	✓	✓
Pentadiene	✓	✓	✓	✓	✓	✓
Hexane		✓			✓	
Hexene		✓			✓	
Hexadiene		✓			✓	

General Conclusions

The Residues are very similar in their structures to the undegraded polymers. They contain a very small degree of unsaturation which appears to be present as the isolated - $CH = CH_2$ group.

The Low Molecular Weight Fractions retain many of the structural features of the undegraded polymers. They contain a greater degree of unsaturation than the residues. The unsaturation is present as various functions, in particular, isolated - $CH = CH_2$, $\begin{matrix} R \\ \diagdown \\ \quad C = CH_2 \\ \diagup \\ R' \end{matrix}$ and $\begin{matrix} H \\ \diagdown \\ \quad C = C \\ \diagup \quad \diagdown \\ R \quad\quad R' \end{matrix}$ (H on the lower carbon). The species found are, for the most part, dimeric in nature, but higher molecular weight analogues are also present.

The Volatile Liquid Fractions contain a number of products which are common to all of the copolymers. These 'common' products are the more volatile, lower molecular weight species of the fraction and their contribution to the whole fraction is always greater than 70% by weight. The remaining products vary from copolymer to copolymer but nearly all appear to be monoalkyl or monoalkenyl benzenes. The same three kinds

of carbon-carbon double bond which are present in the low molecular weight fraction also exist in this fraction although the Ph-$\dot{C}$ = CH_2 is now much more obvious. This is primarily due to the presence of α-methyl styrene.

The Gaseous Fractions contain a number of unexpected products, particularly in the cases of the n = 1 and 3 copolymers. This suggests that a certain amount of secondary reaction can take place during degradation.

Conditional Variations

The variation of the product fractions with temperature was studied by conducting a series of degradations for four hours at 296°C, 350°C and 369°C. Table 17 shows the relative percentages of the four fractions for the above conditions.

TABLE 17

TEMPERATURE	% RESIDUE	% LOW M.W. FRACTION	% VOLATILE LIQUID FRACTION	% GASEOUS FRACTION
296°C	86.0	13.5	0.5	0.0
350°C	67.0	27.8	4.3	0.9
369°C	51.5	41.7	6.2	1.1

U.V. and ^{1}H N.M.R. spectroscopy showed that the residues were all very similar to the undegraded polymer. The infrared spectrum of the residue produced at 296°C showed no trace of a peak at 1642 cm^{-1}, however, this peak together with a slight extension of the peak at 910 cm^{-1} were both present in the spectra of the other two residues.

Using the Pye 104 G.L.C., the low molecular weight fraction obtained from the 296°C decomposition, was shown to consist of three products, all of which had similar retention times under the conditions

used. The largest of these products had the same retention time as

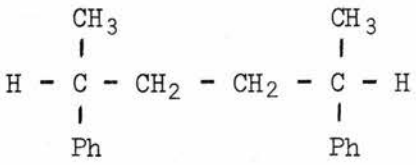

The infrared spectrum of this fraction was very similar to the spectrum of the undegraded polymer. In particular, no peaks were found in the 1600 cm^{-1} - 1700 cm^{-1} region showing that no carbon-carbon double bonds were present. The mass spectrum showed a large parent molecular peak at 238 and a small one at 252 together with a large number of fragment-ion peaks, the largest of which were at 105 and 91. Hence this fraction consists of three products, all of which appear to be dimer-like, one being the saturated dimer shown above. The other two also appear to be saturated.

Under the same conditions as used above, both of the other low molecular weight fractions were shown on the Pye 104 G.L.C. to contain at least eight products. The relative amounts of each were very similar for both cases. The infrared spectra were also very similar, each containing peaks at 1642 cm^{-1}, 1300 cm^{-1}, 990 cm^{-1}, 965 cm^{-1}, 910 cm^{-1} and 890 cm^{-1} showing the presence of the three types of double bond described previously. The mass spectra contained prominent peaks at 278, 264, 252, 250, 238 showing that a number of dimer-like species were present. Hence, at 350°C and 369°C, the low molecular weight fractions are very similar, the only difference being the amounts produced.

The volatile liquid fraction produced at 296°C contained α-methyl styrene and the products which were assigned the letters, M and Q in table 13. No evidence was found for any other products although this

was probably due to the fact that only a minute amount of this fraction was formed.

The volatile liquids produced at the other two temperatures contained all the 'common' and 'non-common' products of the n = 5 copolymer which have been previously mentioned for the 350°C decomposition. The relative amounts of each product were the same for both temperatures, the only variation being in the total amount present.

No gases were produced at 296°C. At 350°C and 369°C, however, gases were produced. These gases which are given in table 16 for the decomposition at 350°C, were the same for both cases although the quantity of methane was greater from the 369°C degradation.

Hence it would appear that at 296°C, very little breakdown occurs. At higher temperatures, decomposition gives rise to a number of products, many of which are unsaturated. The nature of these products is very similar at 350°C and 369°C although the relative amounts of each fraction are different.

The variation of the product fractions with time was effected at 350°C. The results showed that most of the breakdown occurs within the first hour and the relative proportions the low molecular weight, volatile liquid and gaseous fractions do not vary appreciably at any of the time intervals. This is summarised in table 18.

TABLE 18

TIME IN HOURS	% RESIDUE	% LOW M.W. FRACTION	% VOLATILE LIQUID FRACTION	% GASEOUS FRACTION
½	80.2	17.0	2.4	0.4
1	75.3	20.9	3.2	0.6
2	70.3	24.9	4.0	0.8
4	67.0	27.8	4.3	0.9

C. Kinetics of Degradation

The Apparatus

The apparatus, which is illustrated in figure 15, is a C.I. Electronics Micro-Force Balance. The balance, which is a null type, has a maximum capacity of one gram and can be operated over a number of weight ranges.

The principle of operation is based on an electric bridge circuit which is maintained in balance by the servo system. When a sample is suspended from the balance arm, the torque produced by the sample weight is electromagnetically balanced by the Balance Head Unit. This unit is illustrated in figure 16A. A displacement of the balance arm causes excess current to flow through one of the photocells. This is because displacement of the balance arm results in a change in the relative illumination on each photocell which unbalances the resistances causing the current to flow. The current is amplified and passed through a movement coil, restoring the arm to its original position. The bridge circuit is illustrated in figure 16B.

The current flow associated with the restoring force is directly proportional to the applied weight and operates a meter in the Control Cabinet. It also provides an electical output for the Recorder.

The Control Cabinet can function over five weight ranges, range 5 corresponds to a full-meter deflection of 10^{-1} grams, range 4 to 10^{-2} grams, range 3 to 2.5×10^{-3} grams, range 2 to 2.5×10^{-4} grams and range 1 to 2.5×10^{-5} grams.

The Ratio Box also contains five range positions. The value of the range on the Control Cabinet together with the value of range on the ratio box determines the weight corresponding to full scale

FIGURE 15

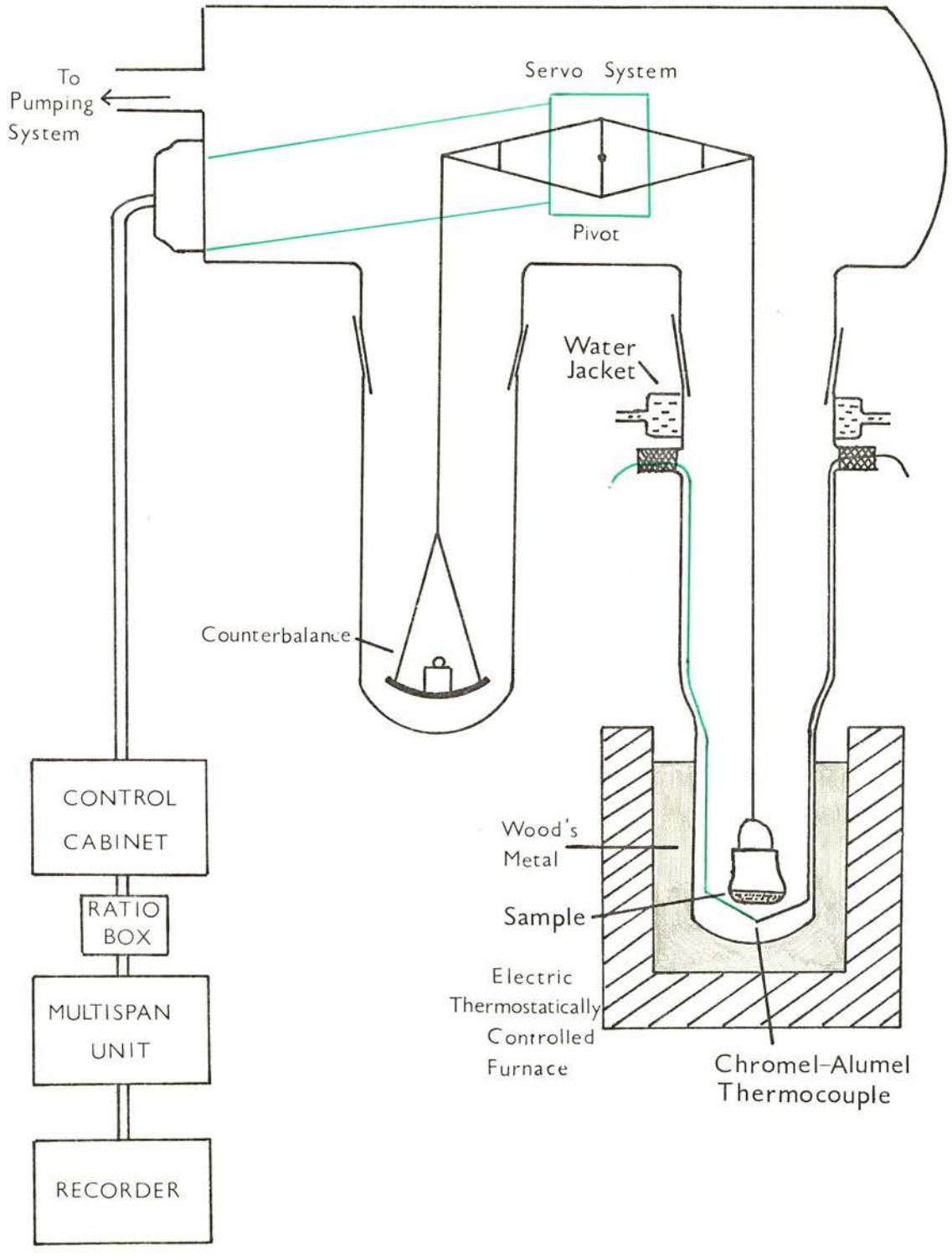
To
Pumping
System
Servo System
Pivot
Water
Jacket
Counterbalance
CONTROL
CABINET
RATIO
BOX
MULTISPAN
UNIT
RECORDER
Wood's
Metal
Sample
Electric
Thermostatically
Controlled
Furnace
Chromel-Alumel
Thermocouple

FIGURE 16 A

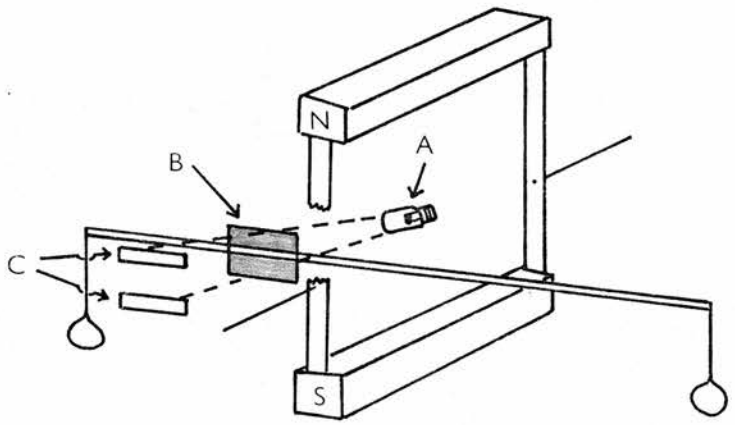

A – lamp

B – shutter

C – photocells

FIGURE 16 B

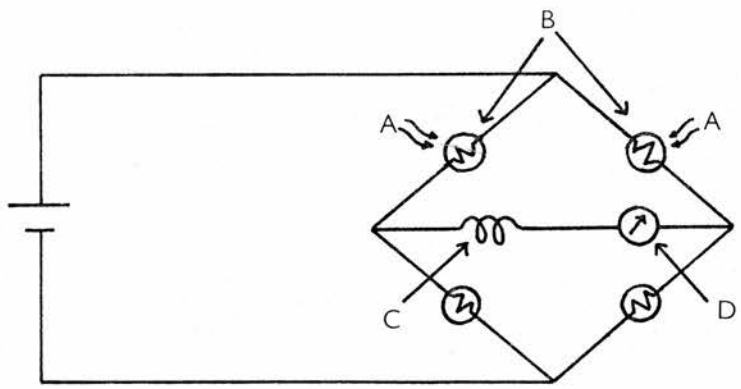

A– light focussed on photocells
B– photocells
C– balance movement coil
D– indicating meter

deflection on the Recorder. For example, a value of 4 on each corresponds to a full scale deflection on the Recorder of 4×10^{-3} grams.

The Multispan Unit allows weight changes which are greater than the weight corresponding to full scale deflection, to be followed. The unit detects when the pen of the recorder has reached one end of the scale and then returns it to the other. This process can be repeated eight times, effectively increasing the apparent chart width by a factor of nine.

The pumping system consisted of a double stage mercury diffusion pump and an Edwards single stage rotary oil pump. This allowed pressures of 1.33×10^{-2} $N.m^{-2}$ to be attained as measured on a Penning Ionisation gauge.

The sample container is a small glass tube which has a slight constriction at the open end. This constriction minimises the loss of undegraded polymer by splashing out of the sample container during degradation.

The sample is situated just above a chromel/alumel thermocouple. Visual display of the thermocouple output was shown on a Solartron digital voltmeter. The two thermocouple wires are taken out of the vacuum chamber through two small glass tubes packed with "Araldite" which maintained the good vacuum.

The sample is surrounded by a medium walled glass tube with a diameter slightly larger than that of the sample container. This tubing could be heated to a temperature of $600^{\circ}C$.

The heating system is a thermostatically controlled Woods Metal bath which could be raised around or lowered from the sample by means of a lab-jack. The molten metal ensured good contact with the glass

tube, which surrounds the sample, so that isothermal conditions could be reached with minimum time delay.

A water jacket was constructed and placed on the apparatus as shown. This aids the condensation of the involatile degradation products on the side of the glass tube. Otherwise, these species could condense on the balance arm or the Balance Head Unit and give rise to spurious results.

Method of Operation

After the apparatus had been zeroed, the sample container was suspended from the right hand end of the balance arm. This was counterbalanced by placing weights in a pan suspended from the left hand end of the arm.

Standard weights were then placed in the sample container and each weight range on the Control Box was callibrated so that it corresponded to full scale deflection on the meter.

The weight range was set equal to four, both on the Control Cabinet and on the Ratio Box. This corresponded to a full scale deflection equivalent to 10 mg. on the Control Cabinet meter and 4 mg. on the Chart Recorder. 10 mg. of polymer were weighed into the sample container which was suspended from the balance arm as shown in figure 15. The surrounding tube was replaced and the apparatus evacuated. When the good pressure was reached, the furnace, which had been preheated to the required temperature, was raised around the sample. For a temperature setting of 350^{o}C, 341^{o}C was reached in three minutes, 347^{o}C in four minutes and fully isothermal conditions in five minutes. The degradation was then allowed to proceed for a period of four hours with the resulting production of a weight versus time plot on the Chart Recorder.

Errors Involved in Isothermal Thermogravimetry

Daniels[21] has investigated all the possible sources of error as applied to the study of isothermal thermogravimetry using a micro-balance. The most serious experimental error involves raising the sample to the equilibrium temperature with a minimum of time delay. This was overcome to a certain extent by having a furnace which could be preheated and then raised around the sample. In this way, the heat-up period was only four minutes. However, for all the copolymers, degradation started to occur before the equilibrium temperature had been reached.

Changes of pressure within the system influence the apparent weight of the sample. Changes in pressure did occur in the kinetic analysis of the polymers. The changes were, however, small and occurred before the sample had reached the equilibrium temperature. By the time isothermal conditions prevailed, the pressure had been restored to its original value.

Apparent weight losses caused by buoyancy effects and thermomolecular flow[22] were kept to a minimum by the use of low pressures.

The effect of the sample size is often an important factor in the rate of weight loss[23]. As the sample is primarily heated by radiation, only the top surface of the sample is heated directly, the rest of the sample being heated by conduction through the sample or its container. This may lead to erroneous results through uneven heating. For the case of thick samples, the diffusion of products out of the sample may lead to errors in the measured rate. For the case of the polymers under investigation, the results obtained using two different sample sizes, 5 mg and 10 mg,were identical so a standard weight of 10 mg was used in each case.

Condensation of the ejected products on the wire supporting the sample container was a further source of error. This was minimised by using a very thin wire and also by keeping as much of the wire as possible surrounded by the furnace.

Analysis of Results

The method of processing the results of kinetic experiments performed under isothermal conditions was described in chapter 1. The major problem of this method was in the measurement of accurate values of $\frac{dC}{dt}$ from the thermogram. This was overcome by the derivation of a new equation based on equation (i)

$$\frac{dC}{dt} = k\ f(C) \qquad \text{(i)}$$

$$\frac{dC}{f(C)} = kdt$$

Hence,

$$F(C) = kt + K \qquad \text{(x)}$$

where F(C) is a function of C resulting from the integration of f(C) and K is a constant. At t = 0, F(C) = 0 hence K must be equal to zero. Substitution of equation (iv) in equation (x)

$$F(C) = Ae^{-E/RT} \cdot t$$

Thus,

$$\ln t = \ln[F(C)] - \ln A + \frac{E}{RT} \qquad \text{(xi)}$$

For a particular percentage degradation, F(C) is assumed to be a constant for all temperatures of decomposition. Hence for a series of thermograms, and by taking the same percentage degradation for each, a plot of ln t versus $\frac{1}{T}$ yields a straight line with a slope of $\frac{E}{R}$.

Equation (xi) was tested by investigating the kinetics of

breakdown of poly-α-methyl styrene. This polymer was chosen because there are a number of values of the energy of activation reported in the literature of which, the following have been collected under isothermal conditions:

Jellinek[24] - 189 k. J./mole

Brown and Wall[25] - 272 k. J./mole

Madorsky[26] - 230 k. J./mole

Madorsky[27] - 230 k. J./mole.

Because of the problem of the occurrence of some degradation before the sample had reached the equilibrium temperature, the initial weight of the polymer was taken as the weight which remained in the sample container after the furnace had been in position for four minutes. For the temperatures used, the loss was always less than 1 mg from a starting weight of 10 mg.

Figure 17 shows a plot of log t versus $\frac{1}{T}$ for 10, 20, 30, 40, 50, 60, 70 and 80 per cent degradation of poly-α-methyl styrene at 312, 316, 323, 334, and 339°C. The table included on the figure shows the energies of activation in k J./mole calculated for each percentage degradation. The average of 244.0 k J./mole compares favourably with the values of Madorsky.

Analysis of the Head to Head Homopolymer

Figure 18 shows a plot of log t versus $\frac{1}{T}$ for various percentage degradations of head to head poly-α-methyl styrene. The polymer decomposes at much lower temperatures than the equivalent regular polymer. Also, unlike the regular polymer, the energy of activation increases markedly with increasing percentage degradation. This implies

FIGURE 17

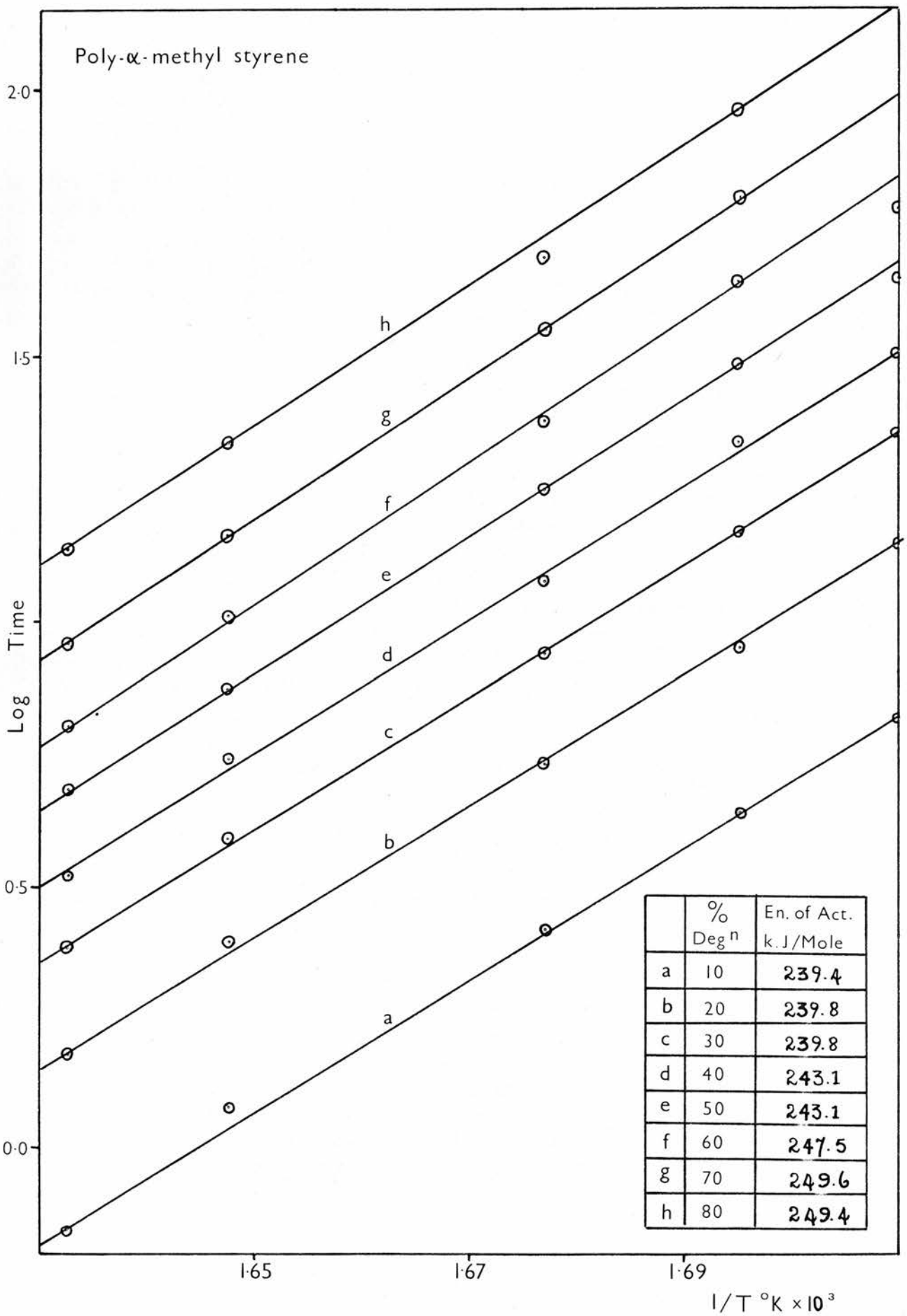

	% Deg n	En. of Act. k.J/Mole
a	10	239.4
b	20	239.8
c	30	239.8
d	40	243.1
e	50	243.1
f	60	247.5
g	70	249.6
h	80	249.4

FIGURE 18

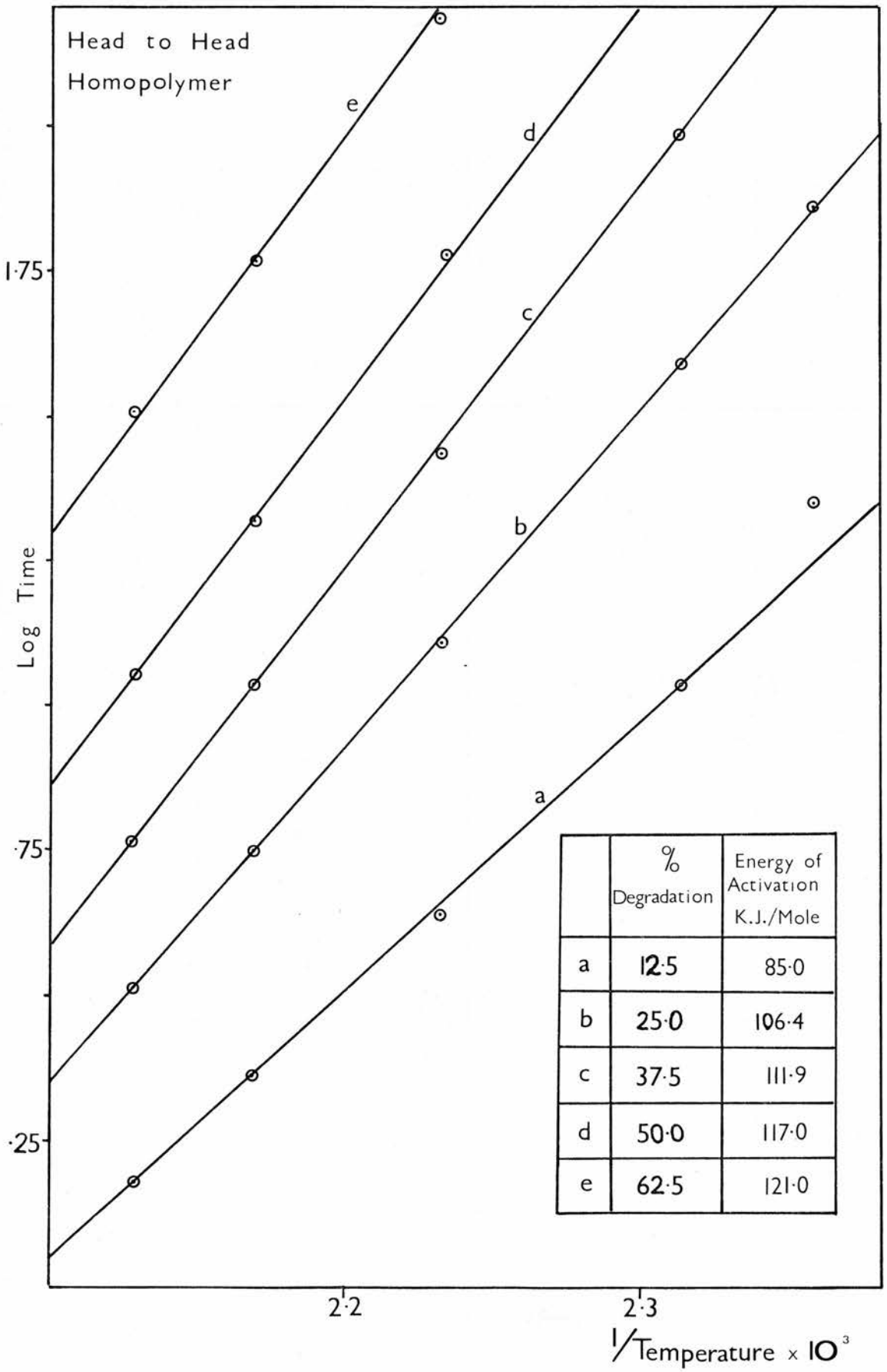

	% Degradation	Energy of Activation K.J./Mole
a	12·5	85·0
b	25·0	106·4
c	37·5	111·9
d	50·0	117·0
e	62·5	121·0

that more than one reaction is occurring during degradation.

For the case of normal poly-α-methyl styrene, W_o was taken as that weight which remained in the sample container four minutes after the furnace had been raised. Because only one reaction takes place during this degradation, whatever initial weights are taken, the calculated energy of activation will always be of the same magnitude. However, because the energy of activation of the head to head homopolymer changes continually with extent of degradation, a constant weight of 8 mg out of an initial weight of 10 mg was taken as the W_o. At all temperatures of decomposition no more than 2 mg of sample were lost before isothermal conditions had been attained. Had the weight after four minutes of heating been taken as W_o, then the values of W_o would be different for each temperature used. Hence, the relative extents of each type of reaction occurring would probably be different in each case and F(C) would not be a constant. On the other hand, the use of 8 mg as W_o assumes that the extent of each type of reaction in producing 8 mg is the same at all the temperatures of decomposition. The only proof of the validity of this assumption lies in the fact that good straight lines are produced using equation (xi).

Because different reactions are occurring during degradation, then the undegraded polymer is very unlikely to be exactly similar to the polymer remaining after 2 mg have been lost. Therefore the percentage degradations shown in figure 18, which are based on a W_o of 8 mg, are not absolute values. However, the main purpose of the kinetics of the head to head homopolymer is to show that more than one reaction is occurring.

The energy of activation calculated from a polymer decomposition process would normally be related to a particular bond energy within

the polymer. However, for the case of head to head poly-α-methyl styrene, the occurrence of more than one type of reaction implies that at least two types of bond scission are taking place. At low percentage degradation, the activation energy of 85 k J./mole is very small in comparison with the normal bond strengths of the carbon-carbon (335 - 369 k J./mole)[28] and carbon-hydrogen (382 - 436 k J./mole)[28] single bonds, the only two types of breakable bond in the polymer. Even at 62.5% decomposition, the value is still relatively low. Hence the scission reactions must be occurring at weak bonds within the molecule.

At the higher values of percentage degradation, the values for the energies of activation are very similar. This suggests that in the later stages of decomposition, one reaction prevails.

Hence, it may be concluded that in the degradation of head to head poly-α-methyl styrene, at least two types of bond are being broken. Also, the energies of activation for all the processes occurring are very low. Finally, the bond energy associated with one of the chain breaking processes is probably in the region of 120 k J./mole.

The Copolymers

Figures 19 - 24 show the plots of log t versus $\frac{1}{T}$ for various percentage degradations of the n = 1, n = 3, n = 4, n = 5, n = 6 and n = 10 copolymers respectively. From the figures, it is evident that the kinetics of breakdown of the copolymers, with the exception of the n = 1 case, bear a close resemblance to each other. The n = 1 copolymer decomposes at lower temperatures and the associated energies of activation are also lower.

For the calculation of the results, a W_o of 8 mg out of an initial weight of 10 mg was taken. Hence, as with the head to head homopolymer,

FIGURE 19

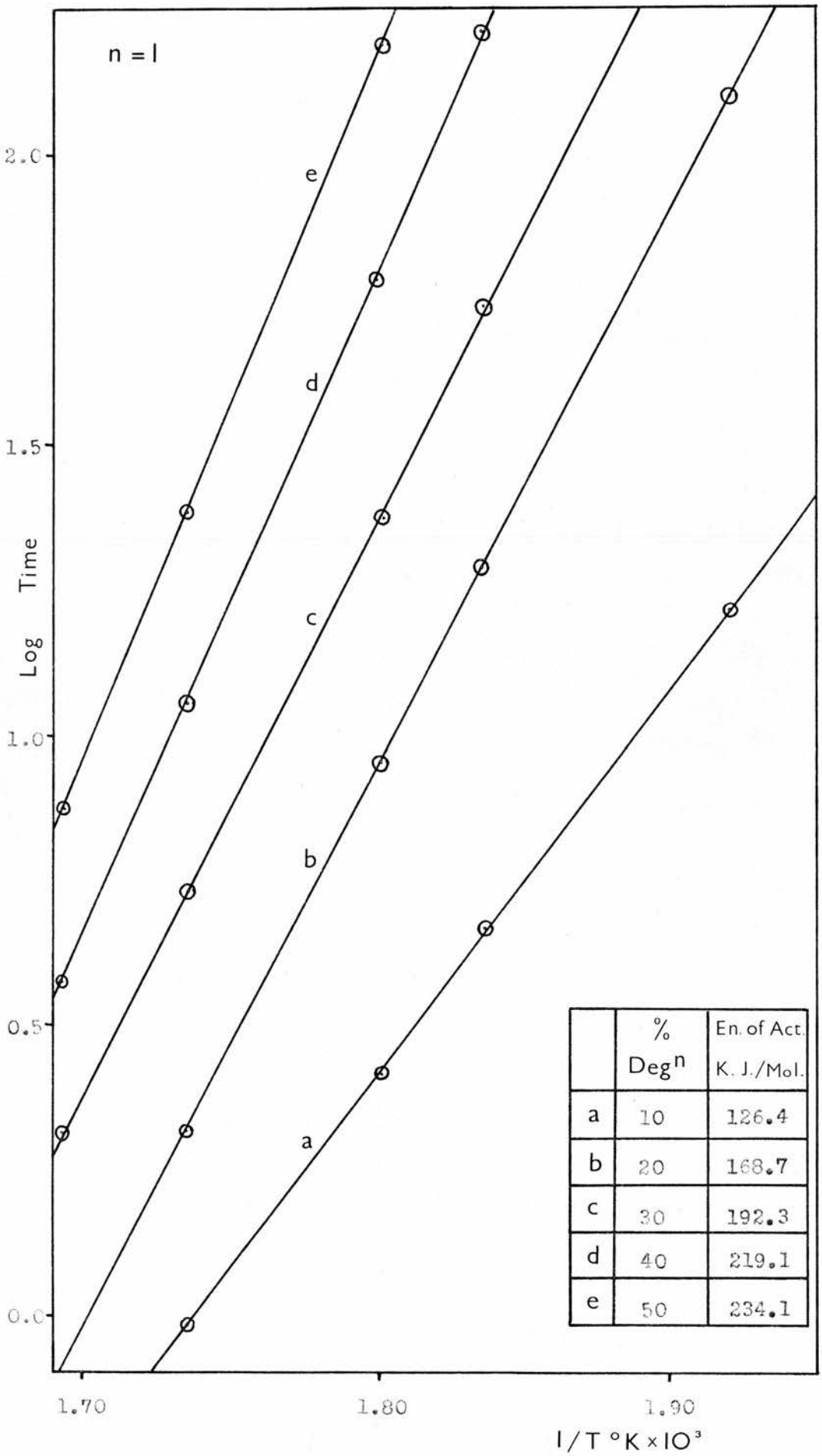

	% Deg^n	En. of Act. K. J./Mol.
a	10	126.4
b	20	168.7
c	30	192.3
d	40	219.1
e	50	234.1

FIGURE 20

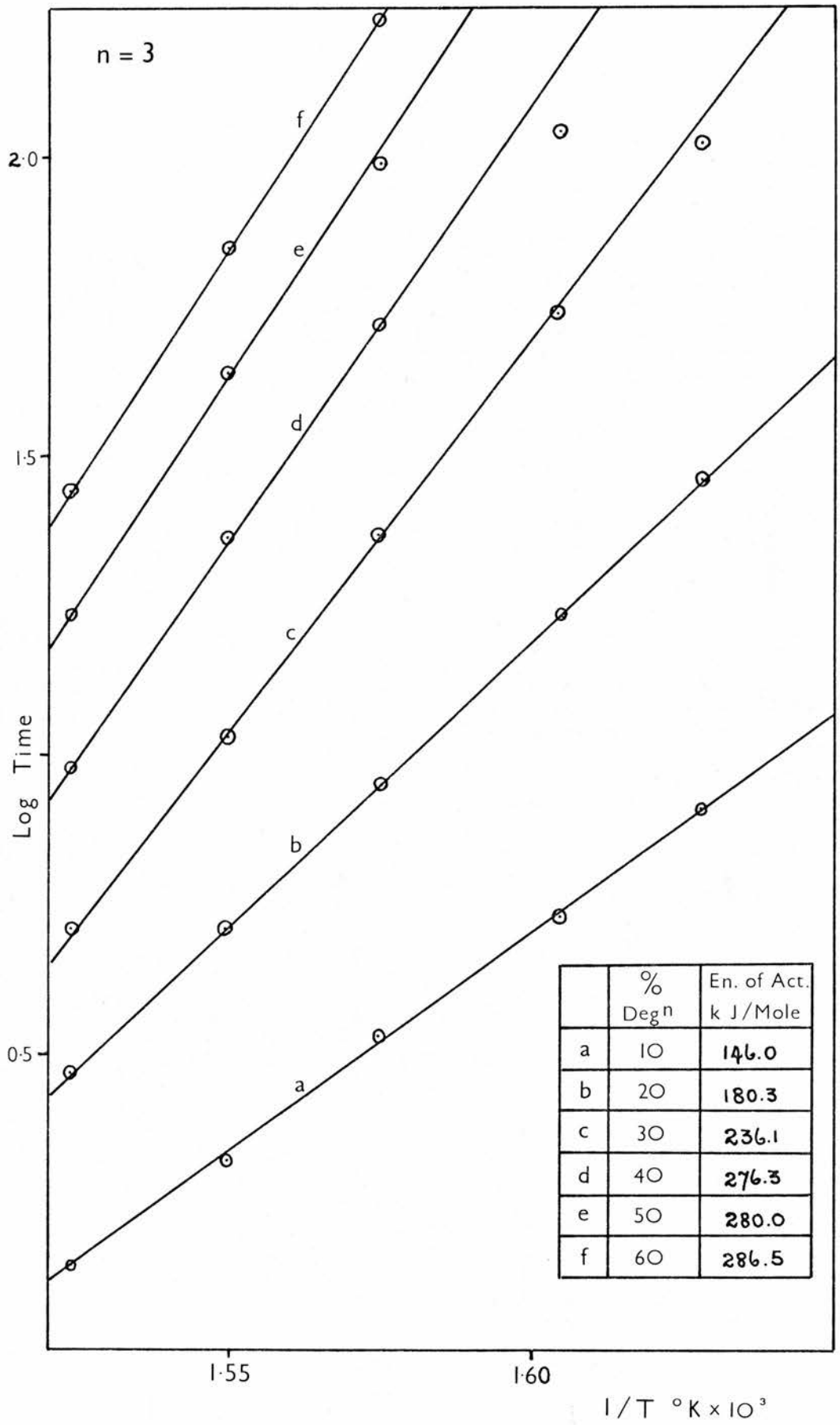

	% Degⁿ	En. of Act. k J/Mole
a	10	146.0
b	20	180.3
c	30	236.1
d	40	276.3
e	50	280.0
f	60	286.5

FIGURE 21

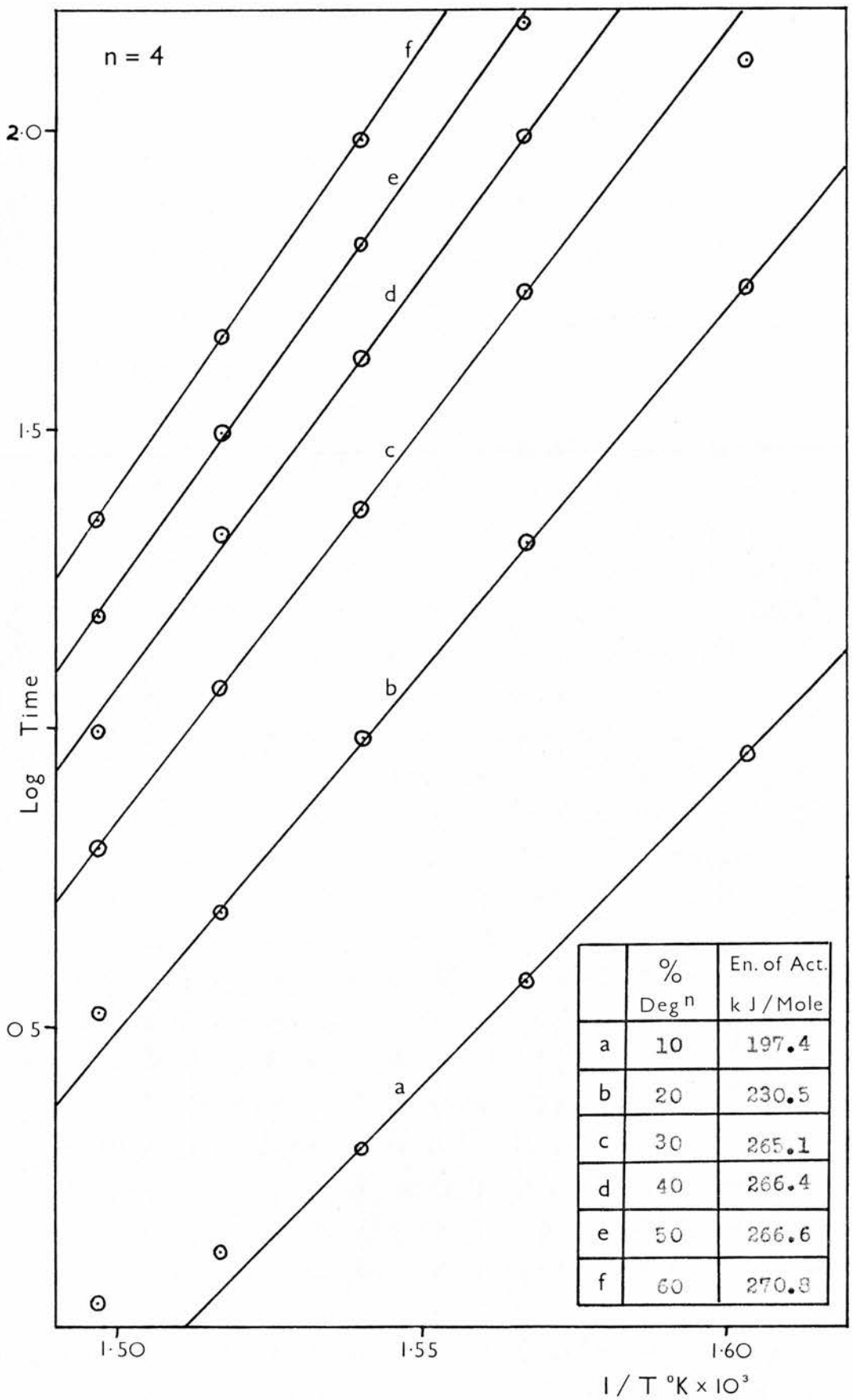

	% Deg^n	En. of Act. k J / Mole
a	10	197.4
b	20	230.5
c	30	265.1
d	40	266.4
e	50	266.6
f	60	270.8

FIGURE 22

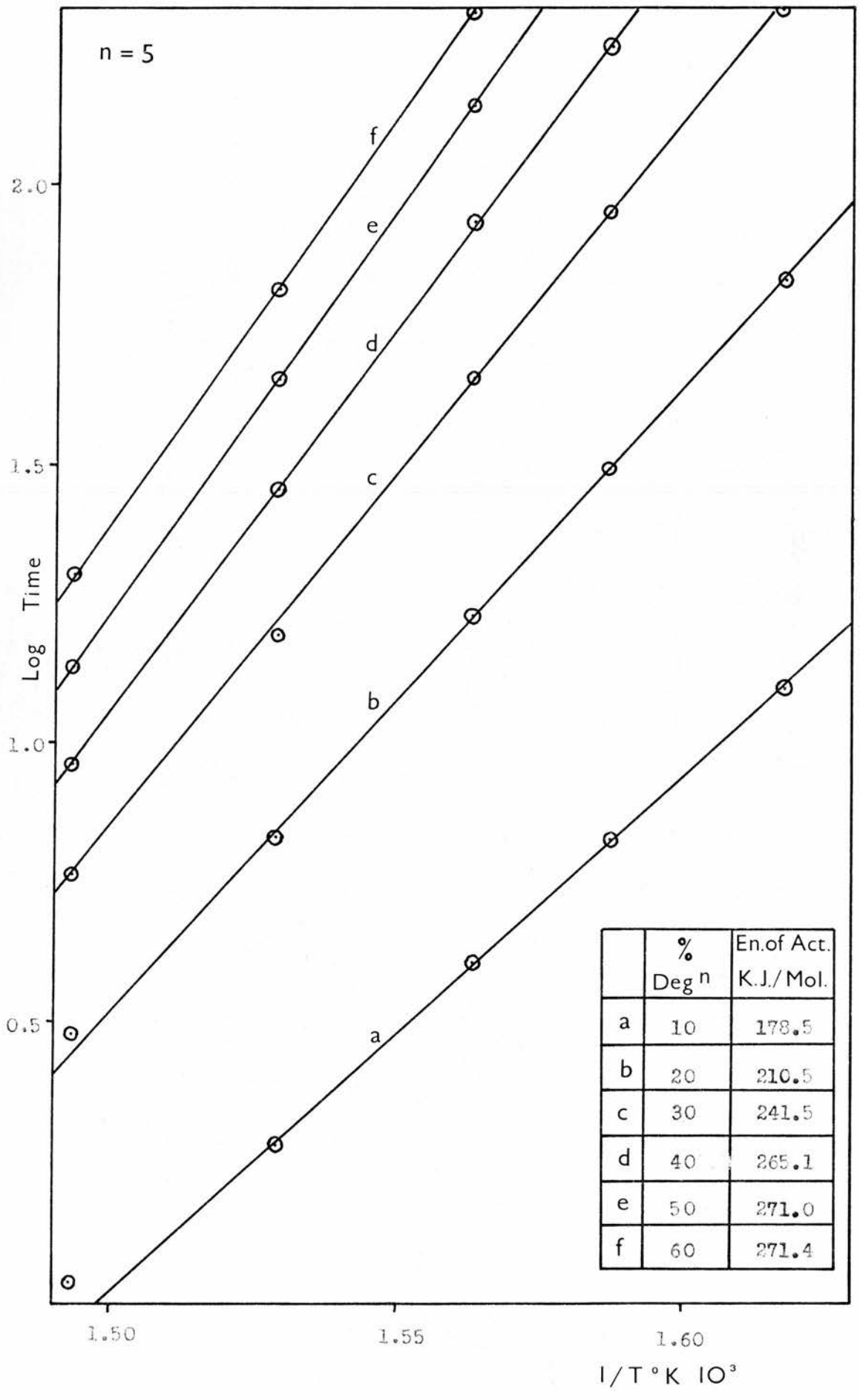

	% Deg n	En.of Act. K.J./Mol.
a	10	178.5
b	20	210.5
c	30	241.5
d	40	265.1
e	50	271.0
f	60	271.4

FIGURE 23

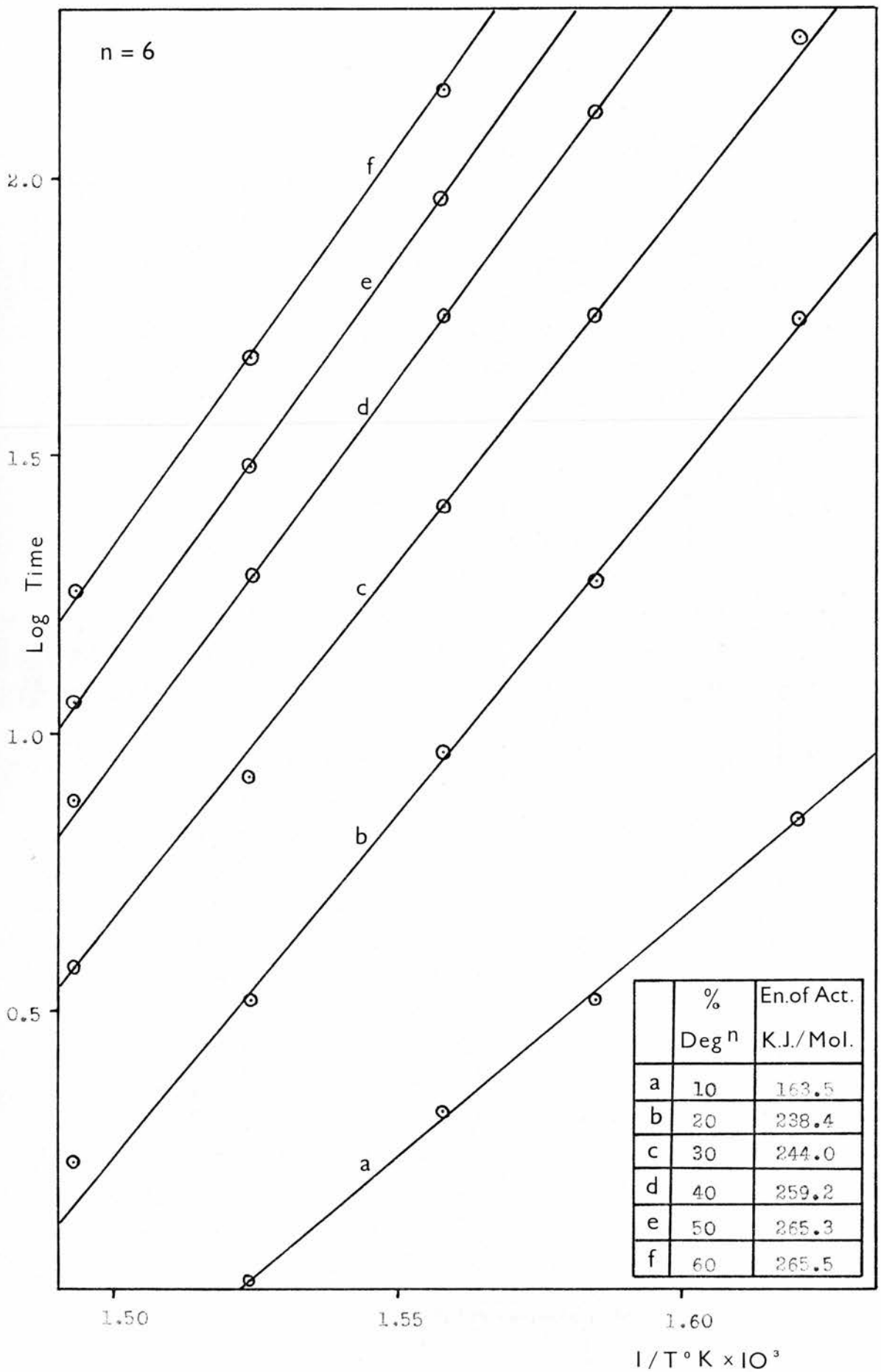

	% Deg n	En.of Act. K.J./Mol.
a	10	163.5
b	20	238.4
c	30	244.0
d	40	259.2
e	50	265.3
f	60	265.5

FIGURE 24

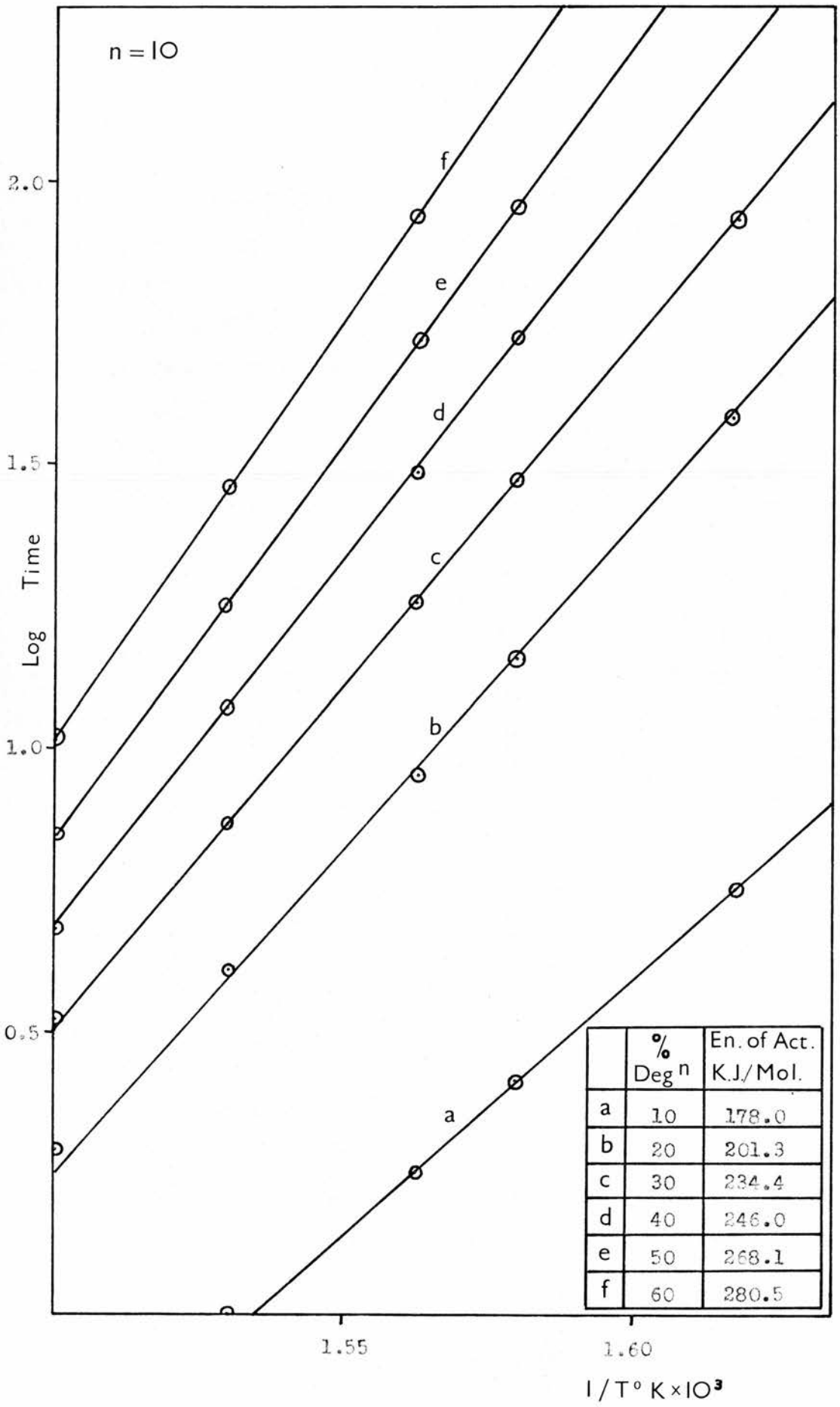

	% Deg n	En. of Act. K.J./Mol.
a	10	178.0
b	20	201.3
c	30	234.4
d	40	246.0
e	50	268.1
f	60	280.5

the values of the percentage degradations are not absolute.

In all cases, the energy of activation, E, increases with increasing decomposition. Therefore more than one type of reaction is occurring in all the breakdown processes. For the n = 1 copolymer, E is very small at low percentage degradation in comparison with the normal energy needed to break a carbon-carbon or carbon-hydrogen single bond. However, at 50% degradation, the value of E is in the same order as that of normal poly-α-methyl styrene.

The copolymers with n = 3, 4, 5, 6 and 10 all have relatively low energies of activation at low percentage decompositions, however, as the latter increases beyond 40%, E becomes relatively constant and has a value in the region 265 - 285 k J./mole. This value is similar to the energy required to homolytically dissociate the C - R bond of

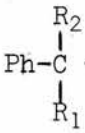

where R_1 and R_2 are hydrogen or alkyl groups and R is an alkyl group. Table 19 gives the dissociation energies associated with the weekest bond in some of the alkyl benzenes.

TABLE 19

R_1	R_2	R	BOND DISSOCIATION ENERGY[29] OF C - R IN Ph CR_1R_2 - R IN k.J./MOLE
H	H	CH_3-	302
H	H	C_2H_5-	289
H	H	iC_3H_7-	281
H	H	tC_4H_9-	264
H	CH_3	CH_3-	256
CH_3	CH_3	CH_3-	252

Hence, it may be concluded that the copolymers with n = 3, 4, 5, 6 and 10 all have very similar kinetic behaviour. The possible presence of weak bonds in the polymer is shown in all cases by the low energies

of activation in the early stages of decomposition. The tendency of the energies of activation of all the copolymers to approach a constant value after 40% decomposition implies that in the later stages, one type of reaction predominates. Furthermore, these activation energies are of the same order of magnitude as the energies needed to break the C - R bond of Ph CR_1R_2 - R.

Hence, the results obtained from the analysis of the kinetics of the head to head homopolymer and the copolymers only give qualitative hints as to the pattern of decomposition.

D. Molecular Weight Changes

The variation of molecular weight with extent of degradation was found to be very similar for all the investigated polymers. Figure 25 shows a plot of molecular weight (taken relative to the initial molecular weight) versus percentage decomposition for the n = 5 copolymer. This curve shows that the probable degradation reaction is based on random scission of the main chain bonds.

FIGURE 25

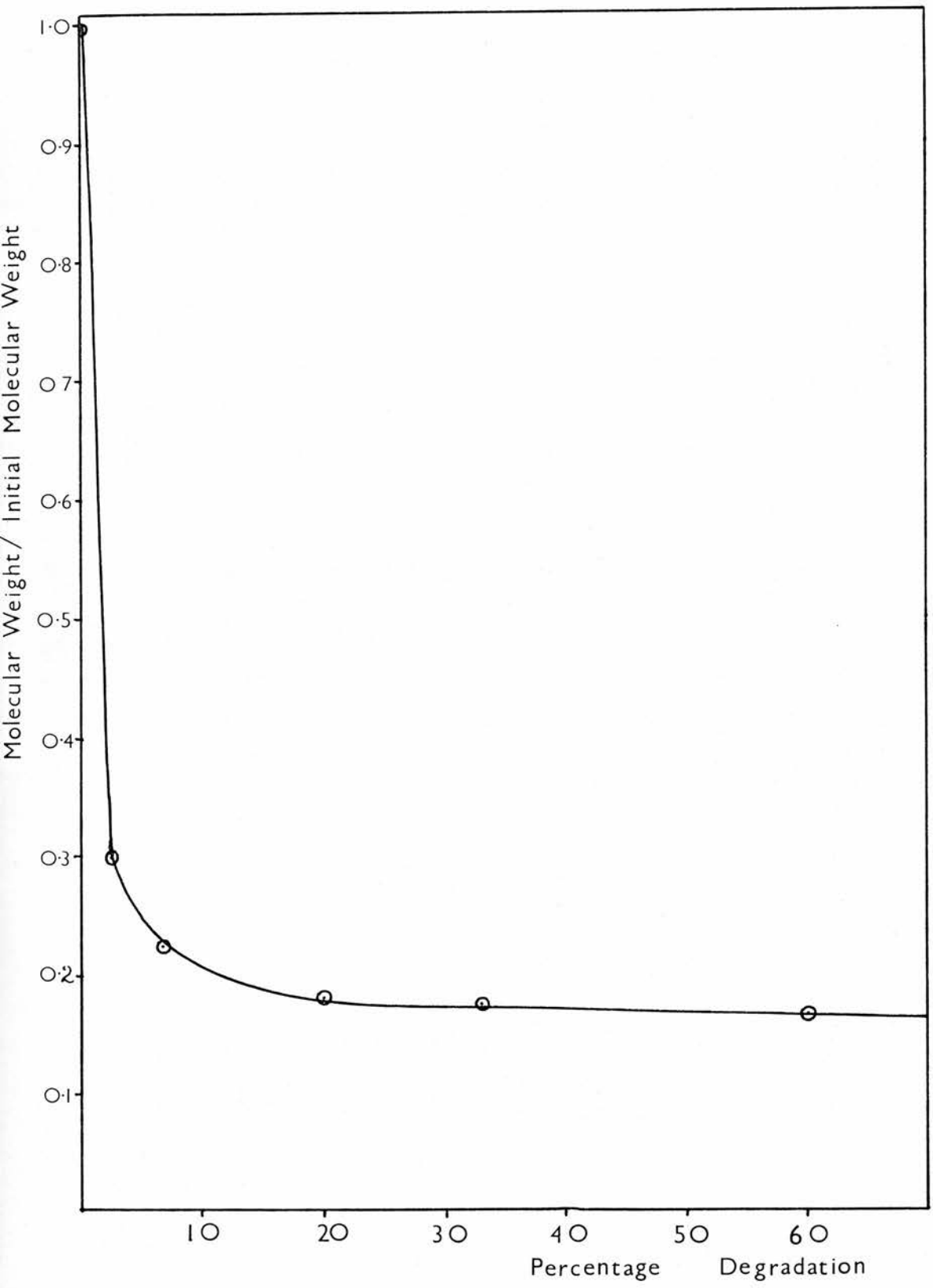
1·0
0·9
0·8
0·7
0·6
0·5
0·4
0·3
0·2
0·1
Molecular Weight/ Initial Molecular Weight
10
20
30
40
50
60
Percentage Degradation

CHAPTER 3. DISCUSSION

The thermal degradation of polymeric stystems almost invariably involves the production of radicals. Therefore, it is convenient, at this stage, to mention a few of the relevant properties of radicals.

The preferred geometry of tricoordinated carbon radicals has been shown by E.S.R.[30,31] spectroscopy, to exist in a planar or near planar configuration. However, this is not such a rigid condition as is to be found with carbonium ions.

The stability of related radicals tends to follow the sequence: tertiary is more stable than secondary which is, in turn, more stable than primary. For example, with respect to stability

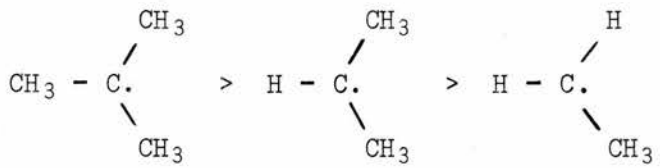

This is due to hyperconjugation which occurs to a greater degree in the case of the tertiary radical

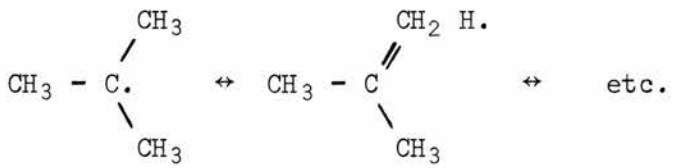

However, the tertiary butyl radical is not as stable as the primary benzyl radical. This is because the odd electron of the benzyl radical can be delocalised in the benzene ring. This has a greater stabilising effect than hyperconjugation.

Any specific stabilisation of a free radical carbon atom by substituents leads to a decrease in the bond dissociation energy (B.D.E.). This is illustrated by the following examples:

			B.D.E.
$CH_3 - CH_3$	→	$2\ CH_3.$	369 k J./mole[28]
$CH_3 - \underset{\displaystyle CH_3}{\overset{\displaystyle CH_3}{\overset{\displaystyle \vert}{\underset{\displaystyle \vert}{C}}}} - CH_3$	→	$CH_3. + {\cdot}C(CH_3)_3$	335 k J./mole[28]
$C_6H_5\ CH_2 - CH_3$	→	$CH_3. + C_6H_5CH_2.$	302 k J./mole[28]
$C_6H_5\ C(CH_3)_2 - CH_3$	→	$CH_3. + C_6H_5C(CH_3)_2.$	252 k J./mole[29]
$CH_2 = CH - CH_2 - CH_3$	→	$CH_3. + CH_2 = CH - CH_2.$	335 k J./mole[28]

Once a radical has been formed, it can react in a variety of ways. There are good reviews by Stirling[32] and Pryor[33] on this very subject. Some of the possible radical reactions will be mentioned briefly.

Combination

$$R. + R'. \rightarrow R - R'$$

where R. and R'. are two radicals.

Combination is an energetically favourable reaction as the heat of formation of a new bond is liberated. This is a characteristic of long life radicals rather than short lived ones.

Abstraction

$$R. + R'H \rightarrow RH + R'.$$

This very common reaction is also referred to as 'transfer'. The new radical R'. is often more stable than R. and this provides the driving force for the reaction. Hence, it follows that the greater the stability of R'., the easier the abstraction.

Disaproportionation

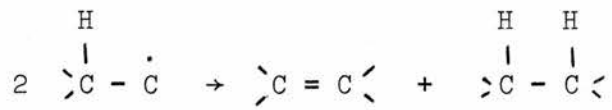

This reaction is energetically favourable as two new bonds are being formed and only one is broken.

Addition to Multiple Bonds

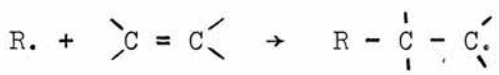

This reaction is of importance in the degradation process with respect to the possible occurrence of secondary reactions.

Rearrangement

Rearrangement of radicals is not an uncommon phenomenon. A considerable amount of research has been directed to their study[34,35,36] One such rearrangement, namely that of the neophyl radical [34,37,38], may well be relevant to this thesis.

The energy of activation for migration of a phenyl radical to an adjacent primary radical is only 33.5 k J./mole[38] in the gas phase.

Fragmentation

where M is a non radical species. This process usually involves the breaking of a bond within the molecular chain with the formation of a

more stable radical and a stable molecule.

The Reaction Mechanisms

From the results obtained from the anlysis of the decomposition products, it is clear that the thermal breakdown of head to head poly-α-methyl styrene and the α-methyl styrene/hydrocarbon copolymers is of a complex nature. This is confirmed by the analysis of the kinetics. The change in molecular weight with percentage decomposition suggests that the chain breaking process is random scission followed by little or no 'unzipping'. The possible mechanisms of breakdown will be considered for each polymer in turn.

The Head to Head Homopolymer

The N.M.R. of the original polymer (figure 3) shows the existence of two possible configurations. These are shown below in their probable preferred conformations:

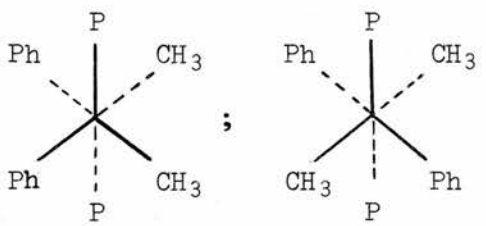

A B

Where P is the remainder of the polymer chain.

The methyl groups of structure A were assigned to the peak at 9.0τ and those of structure B, to the peak at 9.5τ[17].

The N.M.R. spectra of the residues obtained at all temperatures of decomposition, did not contain a detectable peak at 9.5τ (figure 10). This suggests that scission of the single bond between the two tertiary carbon atoms of structure B, is occurring during degradation. This results in the production of two tertiary radicals, both of which are

stabilised by resonance with the phenyl ring.

The other head to head structure, A, may also give rise to the same radicals. However, the continued existence of the peak at 9.0τ in the N.M.R. spectra of the residues implies that scission of the carbon-carbon bond of structure B preferentially occurs.

The analysis of the kinetics of thermal decomposition of this polymer showed that the energy of activation at all degrees of conversion was small compared to that for conventional poly-α-methyl styrene. This suggests that the energy needed to break certain bonds within the polymer, with the resulting production of volatiles, is probably relatively small.

Representations of the two structures, A and B, by molecular models are shown in figure 26. From the figure, it is clear that a certain amount of steric strain must exist within the polymer molecule. Scission of the carbon-carbon bond in either structure to produce two radicals, not only gives rise to two relatively stable tertiary radicals but also leads to reduction of the steric strain within the polymer chain. Hence, it is likely that the energy needed to break these bonds will be relatively small. The fact that structure B is lost first probably means that it contains greater steric strain.

The two radicals produced by the above bond scission are basically identical and can act in one of three ways. Firstly they can abstract a hydrogen from another carbon atom. This is not a likely occurrence as there is no possible abstraction that gives rise to a more stable radical and hence the process has no driving force. Second, they can disproportionate giving rise to three possible terminal groups.

FIGURE 26

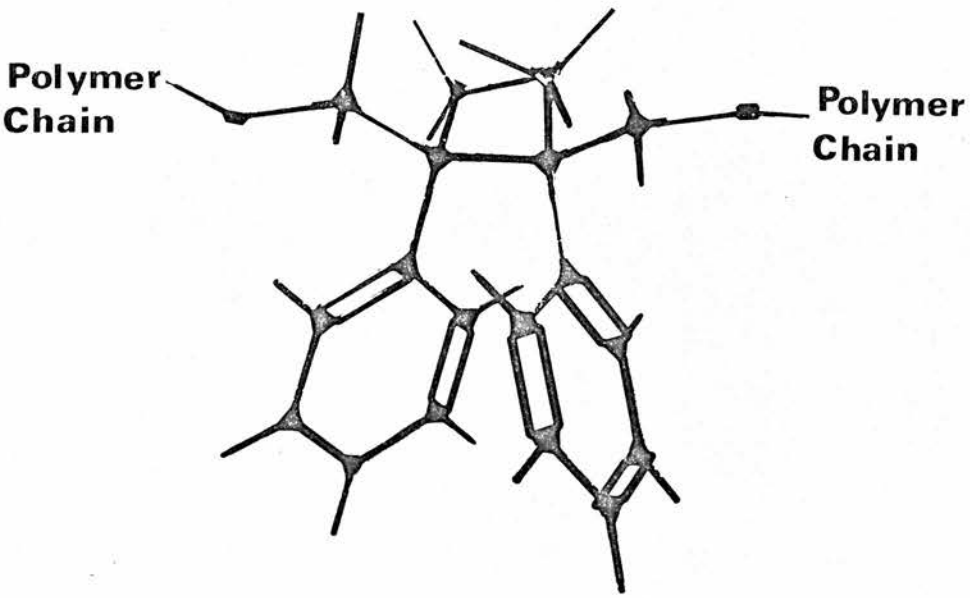

STRUCTURE A

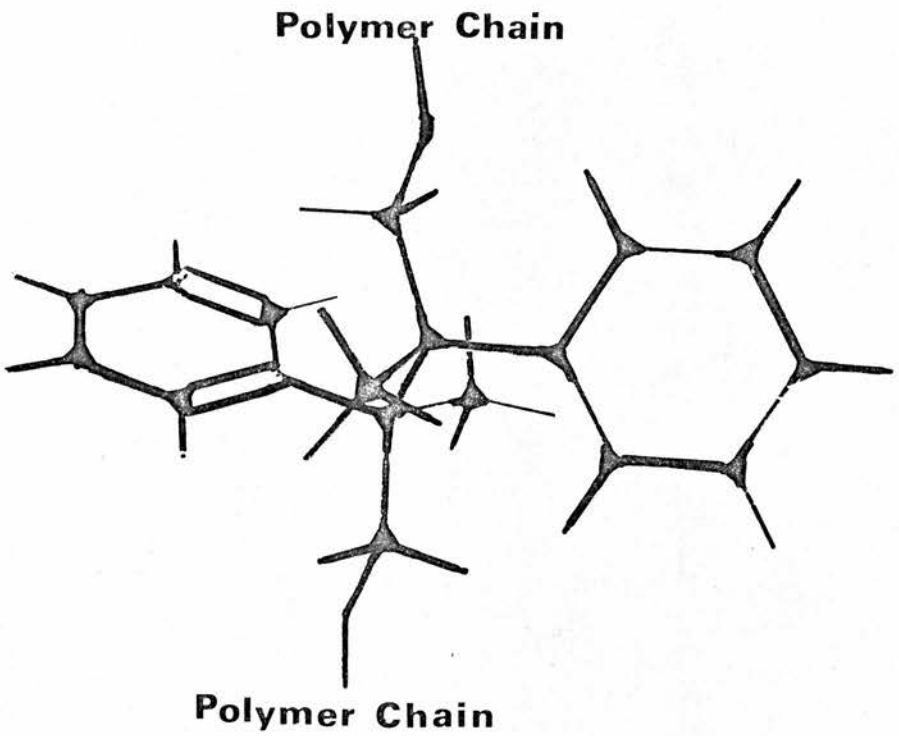

STRUCTURE B

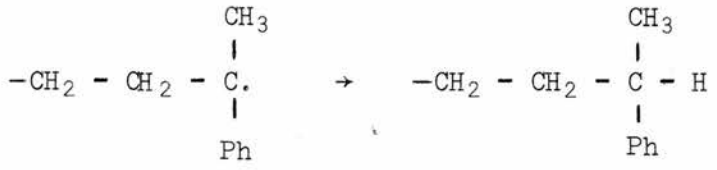

or

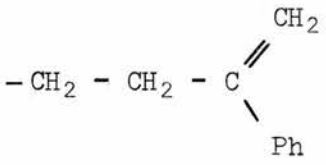

or

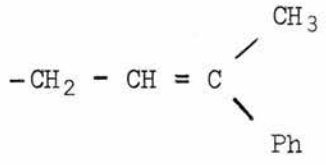

Third, the radicals may depolymerise producing one α-methyl styrene molecule with the resulting production of a primary radical.

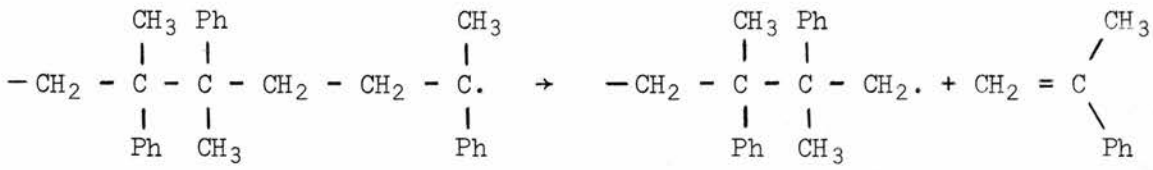

This is less likely to occur than the disproportionation reaction because of the production of a primary radical from a much more stable tertiary radical. However the increased conjugation of the resulting monomer unit makes the process energetically feasible.

The infrared spectra of the residues (figure 11B) showed a significant peak at 1630 cm^{-1}. This together with a shoulder at 890 cm^{-1} implied the presence of $\begin{matrix} R \\ | \\ Ph \end{matrix} > C = CH_2$ where R is an alkyl group. No evidence could be found for the presence of a $\begin{matrix} Ph \\ \diagdown \\ \quad C = CH - \\ \diagup \\ CH_3 \end{matrix}$ group which would be expected to absorb in the 1660 cm^{-1} region. Hence, it appears that the disproportionation reaction leads to

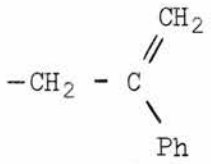

as the unsaturated end group.

With the above terminal group, scission of the first head to head linkage from the end leads to the following radical

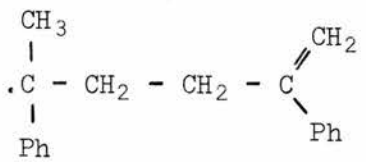

If this radical 'unzips' one unit, then α-methyl styrene and a phenallyl radical are formed. The phenallyl radical, although a primary radical, is stabilised by resonance with the double bond. The likely reaction of the phenallyl radical is the abstraction of a hydrogen atom from the chain thus forming α-methyl styrene.

The production of monomer in high yield at all temperatures of decomposition, suggests that the 'unzipping' of one monomer unit, with the production of a primary radical from a tertiary radical, must occur to a marked extent. The resulting primary radical may abstract a hydrogen atom or 'unzip' another monomer unit (see figure 27). The 'unzipping' of a monomer unit results in the formation of a tertiary radical and is hence a favourable reaction. The abstraction of hydrogen by the primary radical can occur intra - or inter - molecularly. The first of these can take place via a five or six membered cyclic intermediate. Steric inhibition within the polymer chain renders this situation very unlikely. Intermolecular abstraction of hydrogen generally leads to the formation of a more stable radical. Two such abstractions

are possible, the first involves the tertiary hydrogen atom which exists at each end of the undegraded polymer chain. This gives a tertiary radical which is exactly similar to the tertiary radicals produced in the initial bond scission. The second, and less energetically favourable, abstraction involves the methylene groups within the polymer chain. This gives rise to a secondary radical which can internally fragment, (i), or disproportionate, (ii):

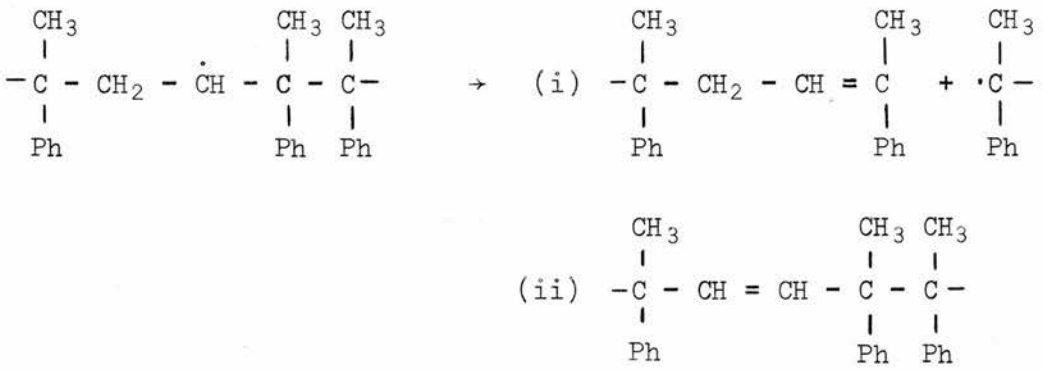

The fragmentation shown in the more likely of the two possible mechanisms because of the increased conjugation in the resulting end group. Disproportionation would also give the saturated form, however, the important point about both of these reactions is that neither of the above double bonds can be detected in the I.R. spectra of the three fractions. Hence, it must be assumed that abstraction of a methylenic hydrogen does not occur to a significant extent.

Hence, for the thermal degradation of head to head poly-α-methyl styrene, the decomposition involves the production of two relatively stable tertiary radicals. These radicals can disproportionate so that the unsaturated part contains the Ph - $\dot{C}$ = CH_2 group. On the other hand, these radicals can 'unzip' one monomer unit to form a primary radical. The primary radical may also 'unzip' one monomer unit, or it can abstract hydrogen from somewhere in the polymer chain. Monomer can

also be produced as a result of scission of the head to head linkage next to a terminal Ph - $\dot{C}$ = CH_2 group. The smaller of the two fragments can 'unzip' a monomer unit leaving a primary radical which is stabilised by allylic resonance and which can also give rise to α-methyl styrene.

The low molecular weight fraction is probably composed of dimeric, trimeric and tetrameric species, produced as a result of degradation and which are volatile at the temperature of the experiment. The residue is chemically very similar to the undegraded polymer. However, it contains a number of Ph - $\dot{C}$ = CH_2 groups resulting from the disproportionation reaction. The proposed mechanistic sheme is summarised in figure 27.

The Copolymers

Unlike the head to head homopolymer, the copolymers do not contain any bonds which, when broken, lead to two stable radicals. However, all have three different carbon-carbon single bonds which, on scission give rise to a primary and tertiary radical, the tertiary radical being further stabilised by delocalisation of the odd electron in the benzene ring. These scissions are summarised below:

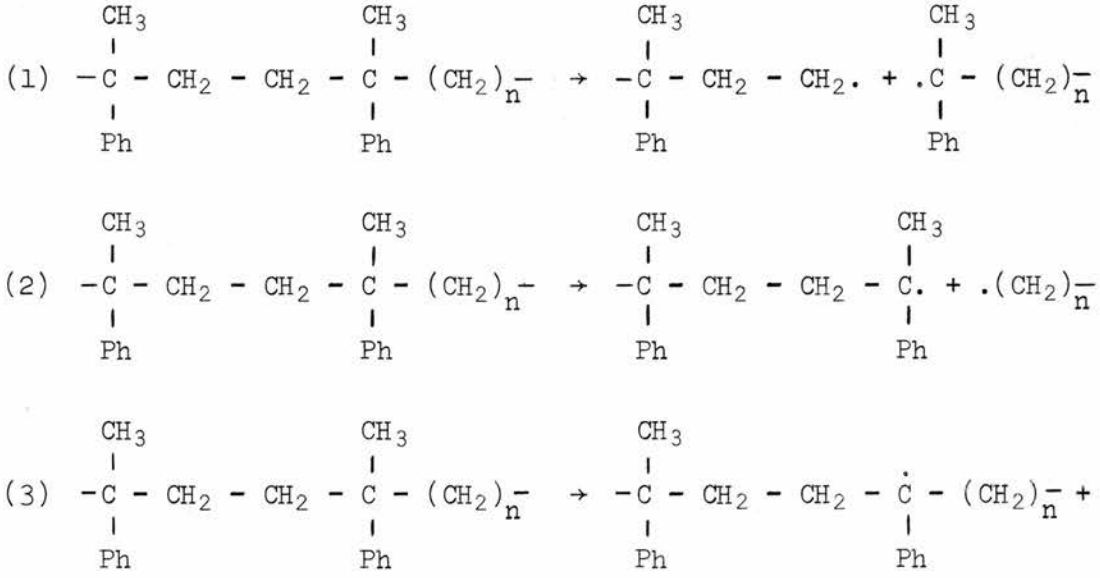

FIGURE 27

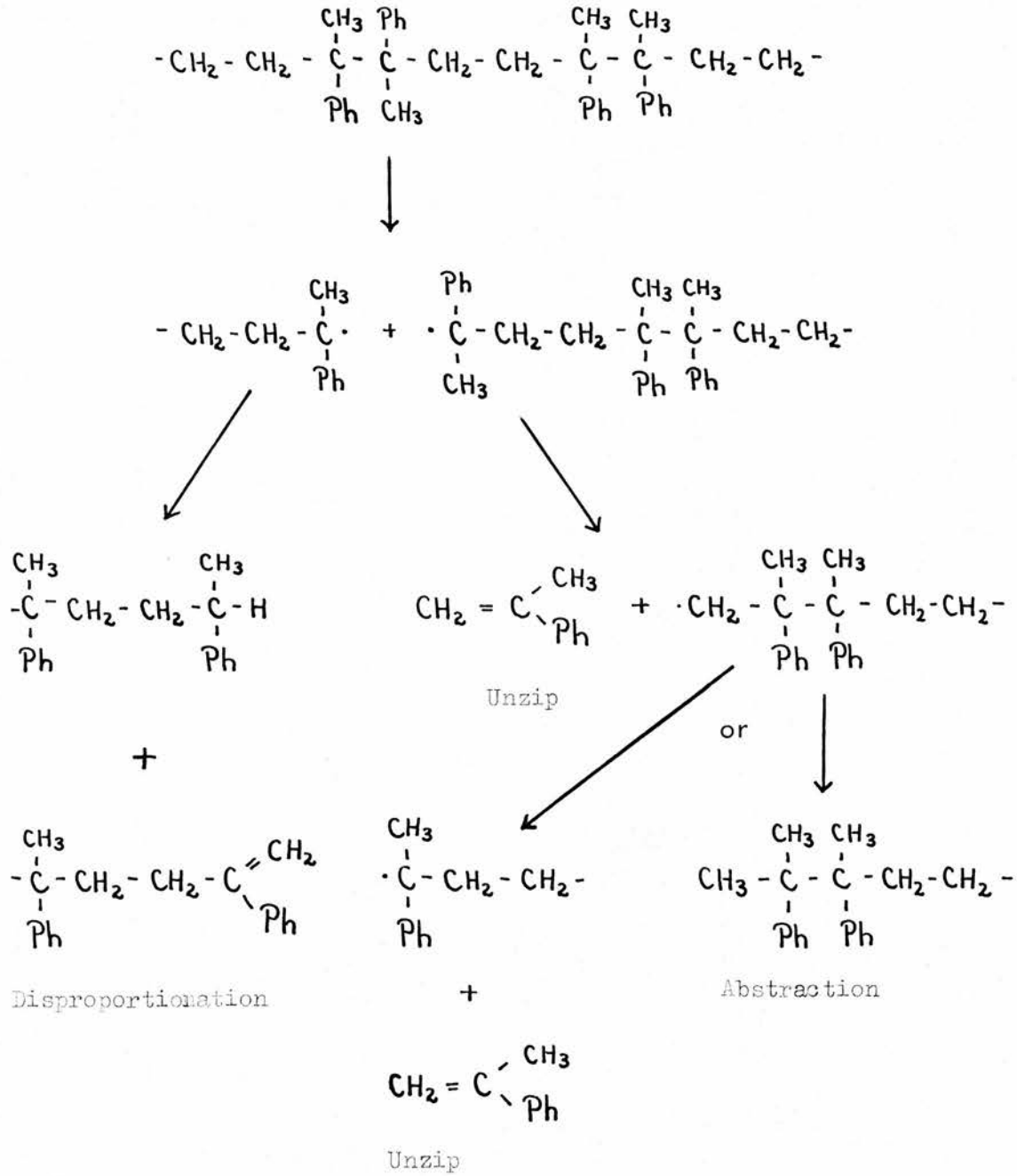

The other possible bond breakages give rise to two primary radicals or a phenyl and a tertiary radical, both of which are energetically less favourable.

n = 1 Copolymer

This polymer differs from the other copolymers in that it is much less thermally stable and produces far more α-methyl styrene in relation to the other volatile liquids.

The molecular chain can be broken at the three different bonds, as shown in figure 28, to produce a primary and a tertiary radical. The tertiary radical resulting from bond scission (1) (Figure 28(1)) can unzip one α-methyl styrene unit with the production of a similar tertiary radical. This is an energetically favourable step due to the increased conjugation in the α-methyl styrene produced and the formation of an equally stable radical. This second tertiary radical could similarly unzip, however, this would lead to a primary radical. This is not such a favourable reaction and it is possible that this particular radical would disproportionate. The primary radical formed by bond scission (1) can abstract hydrogen in the same way as was shown in the head to head homopolymer. On the other hand, this radical may produce ethylene with the formation of a tertiary radical which is exactly similar to the tertiary radical produced by the initial bond scission. A third possibility is that the primary radical disproportionates to form a saturated or unsaturated terminal group. The unsaturated function would be the isolated - $CH = CH_2$ group which was shown to be present, by I.R. spectroscopy, in the residue and low molecular weight and volatile fractions. The absorbtion however is weak in the spectra of all three fractions, therefore the

FIGURE 28 (1)

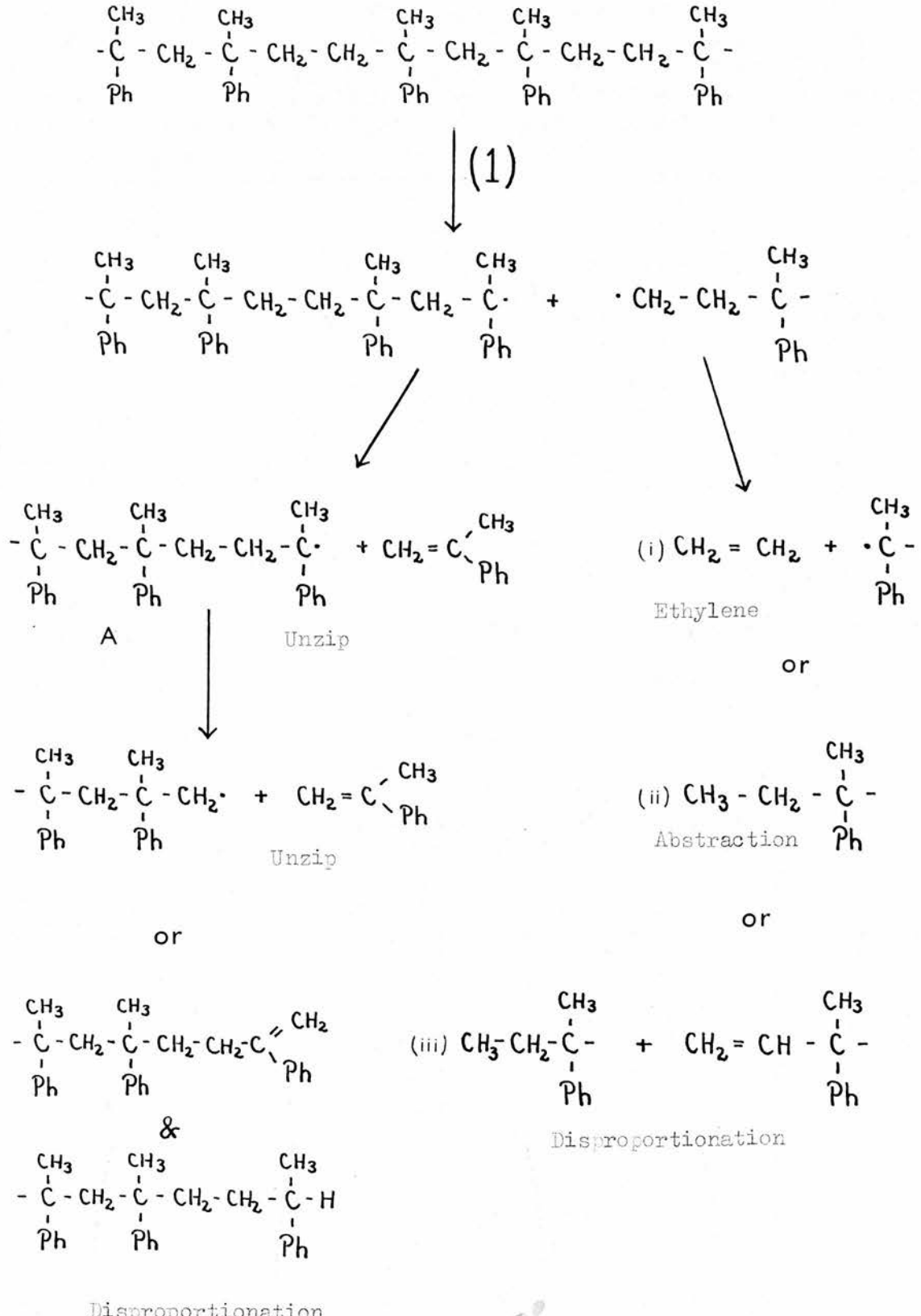
(1)
A
Unzip
Unzip
Ethylene
(i)
(ii)
Abstraction
(iii)
Disproportionation
Disproportionation
or
or
&

FIGURE 28 (2)

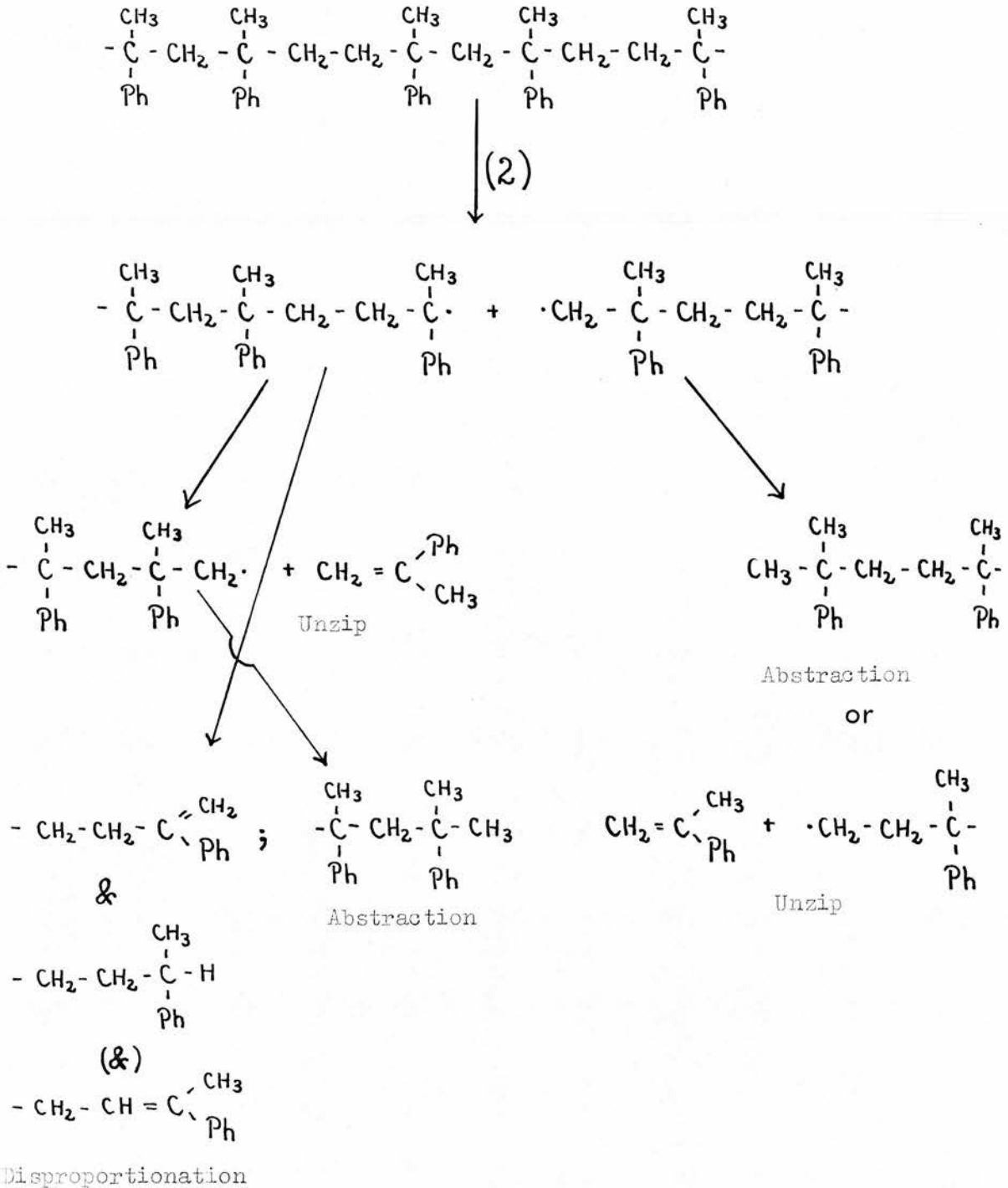
(2)
Unzip
Abstraction
or
Abstraction
Unzip
&
(&)
Disproportionation

FIGURE 28 (3)

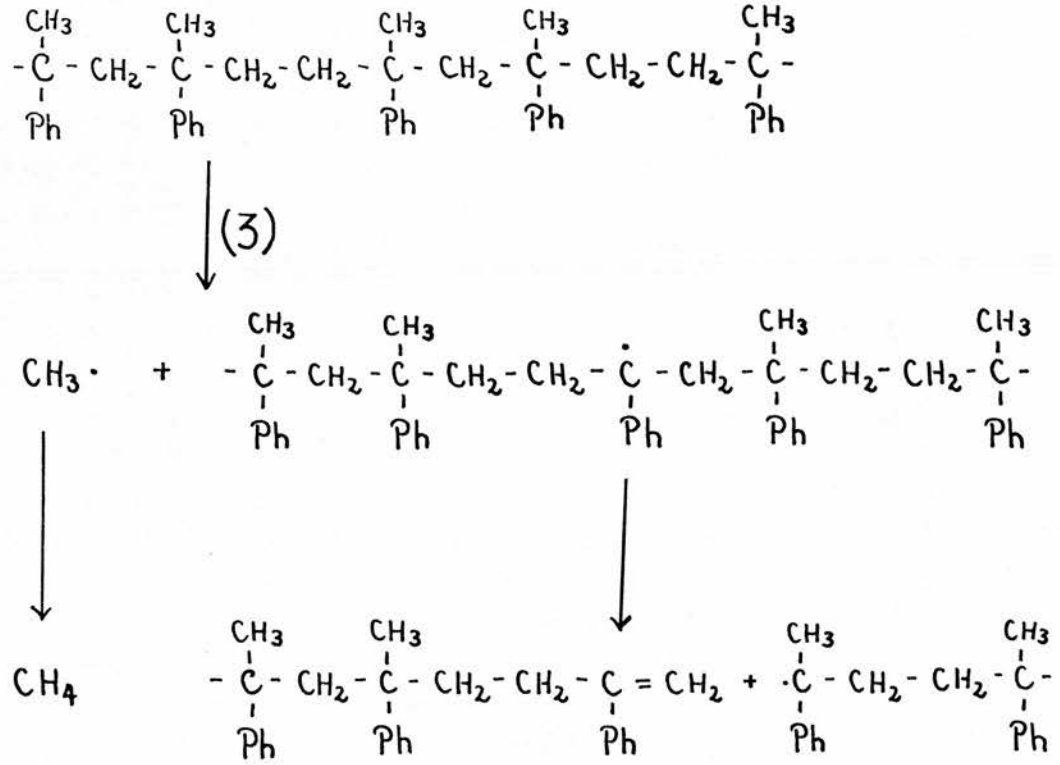
(3)
Fragmentation
or
&
& saturated equivalent
Disproportionation

disproportionation does not appear to be a common occurrence.

Bond scission (2) (Figure 28(2)) gives rise to a tertiary radical, which is identical with radical A (Figure 28(1)) produced by scission at bond (1), and a primary radical which is most likely to abstract a hydrogen atom from a suitable site. 'Unzipping' of a monomer unit from the primary radical is not as likely as this leads to another primary radical.

Scission at bond (3) (Figure 28(3)) results in a methyl radical which probably abstracts a proton forming methane. Alternatively, it can add to a double bond, this will be discussed in more detail in the subject of Secondary Reactions. The tertiary radical resulting from this bond breakage can fragment or disproportionate. Fragmentation can occur in two ways, the first gives rise to a tertiary radical and an end group which has increased conjugation. The second leads to the formation of a primary radical and a similar end group. The former reaction, being energetically more favourable, is considered the more likely to occur. Disproportionation, on the other hand, results in a trisubstituted carbon-carbon double bond or a saturated carbon-carbon single bond.

All three mechanistic schemes are summarised in figure 28. Route (1) appears to be the most prevalent judging by the quantity of α-methyl styrene produced. The low molecular weight fraction is probably made up of species which were produced by decomposition but which were volatile at the temperature of degradation.

n = 3 - 10 Copolymers

These polymers produce relatively large amounts of α-methyl styrene in comparison with the other volatile liquids, however, not

as marked as was found with the n = 1 copolymer. Other relevant features includes the peak at 1642 cm^{-1} in the infrared spectra of the residues and low molecular weight and volatile liquid fractions which is due to the isolated - CH = CH_2 group. Also in the I.R. spectra of the latter two fractions are peaks which may be assigned to Ph - $\overset{|}{C}$ = CH_2 and

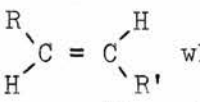

where R and R' are alkyl or aryl groups.

The molecular chains can be broken at the three possible bonds shown in figure 29. The primary radical produced by bond scission (1) (Figure 29(1)) can abstract hydrogen, produce ethylene or disproportionate in exactly the same way as the equivalent radical obtained in route (1) of the n = 1 polymer decomposition. The tertiary radical can disproportionate, or unzip one monomer unit forming a primary radical. The first of these possibilities is energetically more favourable, however, the latter, because of the relatively large amount of α-methyl styrene produced, cannot be discounted.

Scission at bond (2) (Figure 29(2)) results in the production of a primary radical which can abstract hydrogen or disproportionate. Both these processes lead to a saturated end group, the latter also giving rise to the isolated - CH = CH_2 group. The tertiary radical formed by this bond scission may disproportionate or 'unzip' one monomer unit. The disproportionation is again energetically more probable. However, should 'unzipping' occur, the primary radical produced can also 'unzip' a monomer unit with the resulting formation of a primary radical similar to that caused by the initial bond scission.

Bond scission (3) (Figure 29(3)) leads to the production of a methyl radical together with a tertiary radical. The methyl radical probably abstracts hydrogen forming methane although it may add to a

FIGURE 29(1)

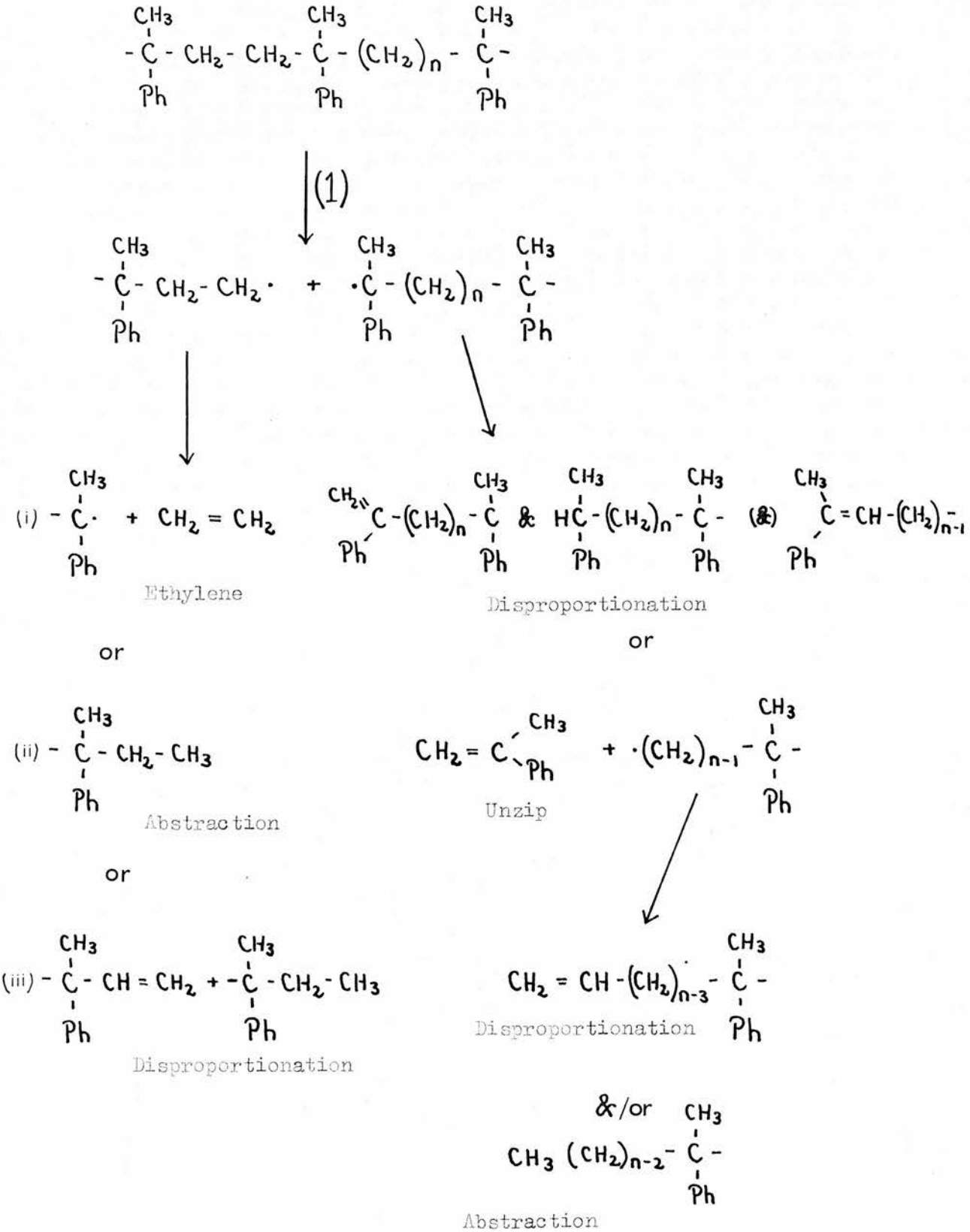
(1)
(i)
Ethylene
or
(ii)
Abstraction
or
(iii)
Disproportionation
Disproportionation
or
Unzip
Disproportionation
&/or
Abstraction

FIGURE 29 (2)

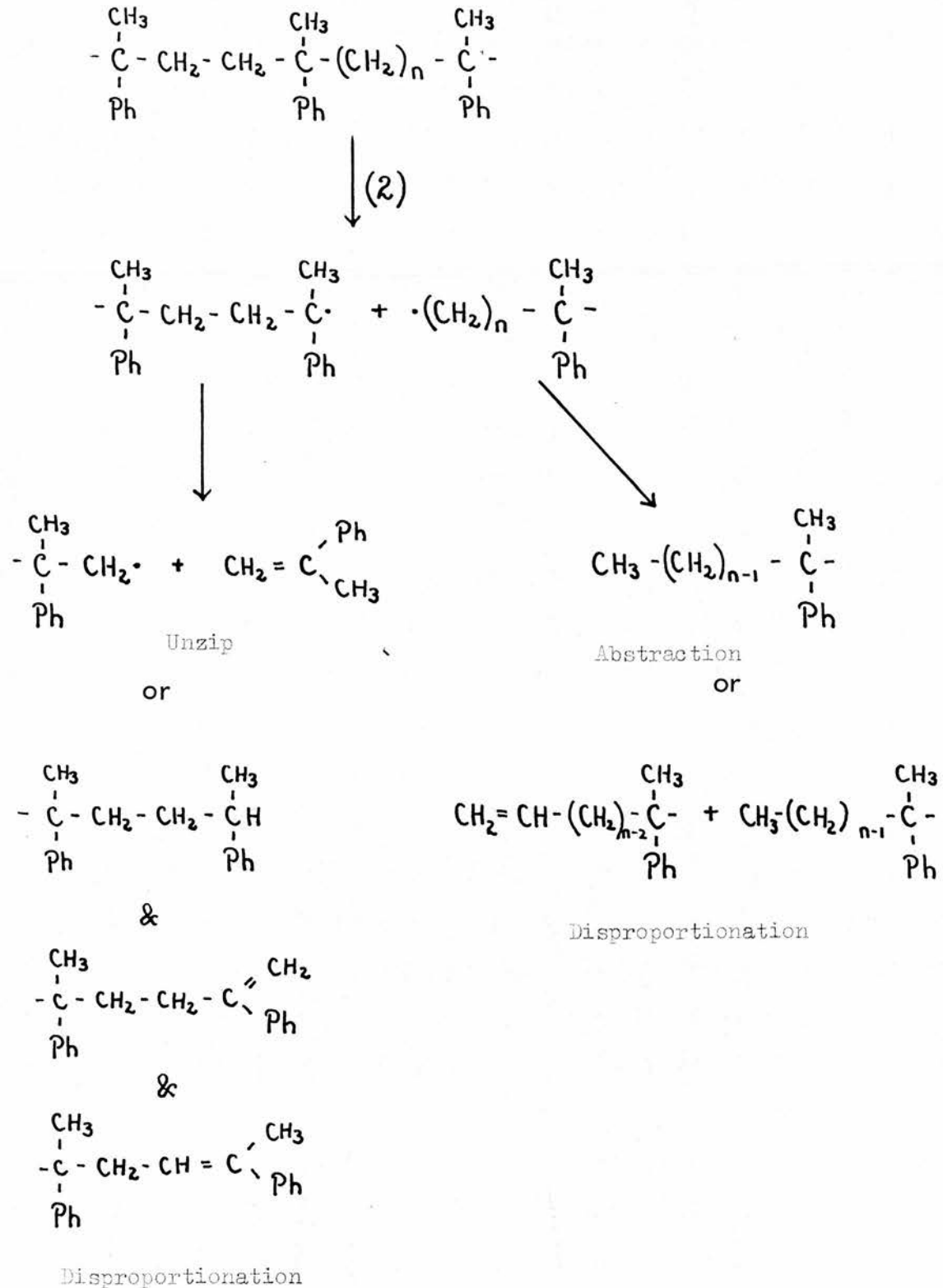
(2)
Unzip
or
Abstraction
or
&
&
Disproportionation
Disproportionation

FIGURE 29 (3)

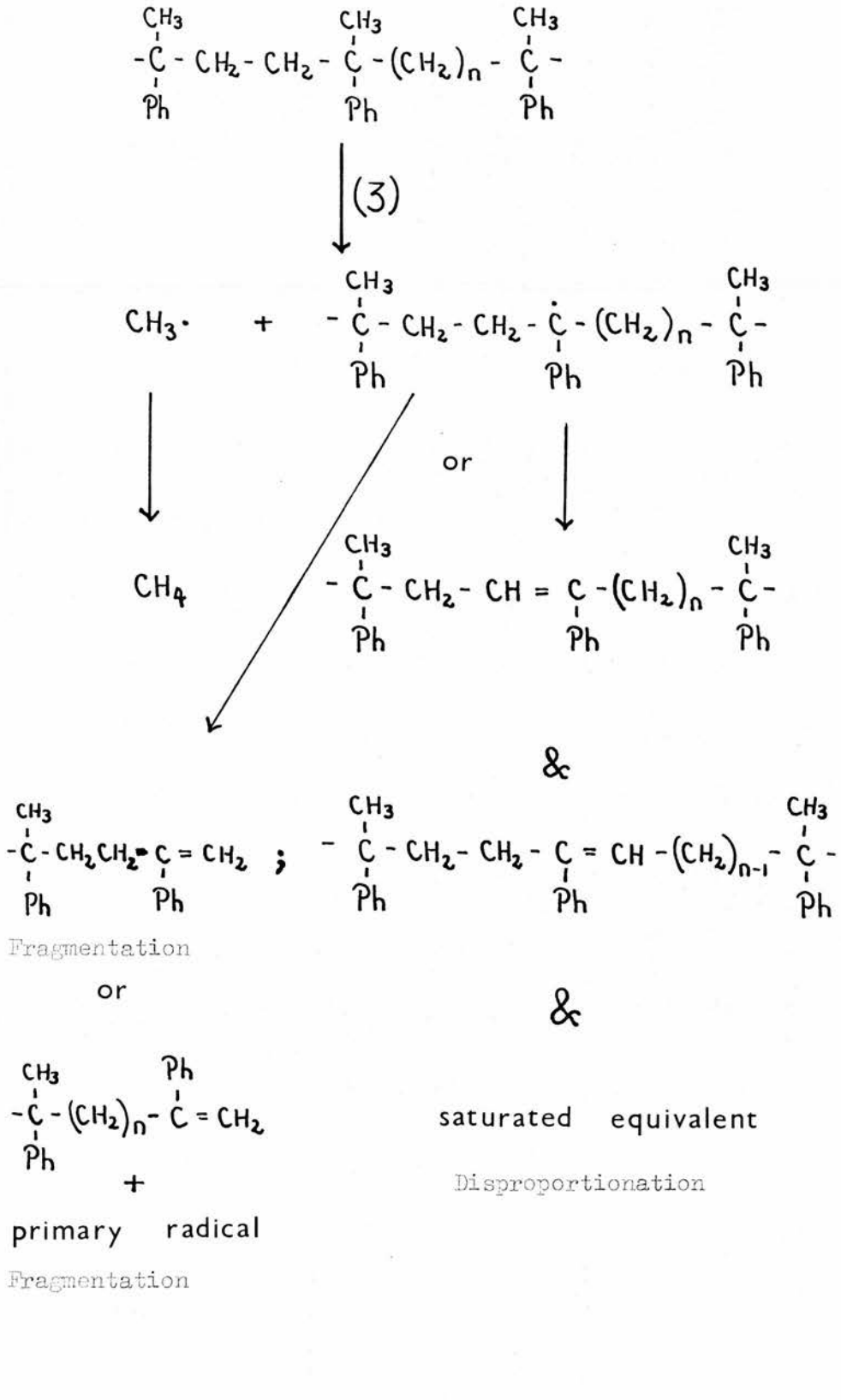
(3)
or
&
Fragmentation
or
&
saturated equivalent
Disproportionation
+
primary radical
Fragmentation

double bond. The tertiary radical may fragment or disproportionate. Fragmentation can only give a terminal group with increased conjugation, and a primary radical. Disproportionation leads to increased conjugation with the phenyl group or the incorportion of a tertiary hydrogen into the polymer chain.

The mechanistic schemes are summarised in figure 29.

The low molecular weight fractions from all of these copolymers again probably consist of species produced by degradation but which are volatile at the experimental temperature. The fractions include three types of double bond, the most prominent being that of the isolated $-CH=CH_2$ group.

Because of the findings of the head to head homopolymer, disproportionation of tertiary radicals of bond scissions (1) and (2) from all the copolymers is thought to result primarily in the $Ph-\dot{C}=CH_2$ group as the unsaturated species.

Hence, the above discussion although limited to the subject of the likely bond scissions followed by the probable reactions of the resulting radicals, has provided possible explanations for:

(i) The formation of α-methyl styrene, methane and ethylene.

(ii) The presence of $-CH=CH_2$.

(iii) The presence of $Ph-\dot{C}=CH_2$ and the possibility of the presence $\begin{matrix} Ph \\ CH_3 \end{matrix} > C=CHR$ and $\begin{matrix} R \\ Ph \end{matrix} \diagdown C=C \diagup \begin{matrix} R' \\ H \end{matrix}$ where R and R' are sections of polymer. Small peaks in the I.R. spectra of the residues and low molecular weight fractions at 1670 cm^{-1} show that either of, or both the latter two structures may be present. The presence of $Ph-\dot{C}=CH_2$ cannot be detected in the I.R. spectra of the residues, but it is certainly present in the volatile and low molecular weight fractions.

In all of the above scission reactions, a primary radical is produced. Such species are highly reactive, particularly the methyl radical. For this reason, abstraction of hydrogen, by these radicals, from somewhere along the polymer chain producing a more stable radical is a probable reaction. The most likely hydrogen to be abstracted is that of the chain ends which results in the production of a tertiary radical, further stabilised by resonance with the benzene ring

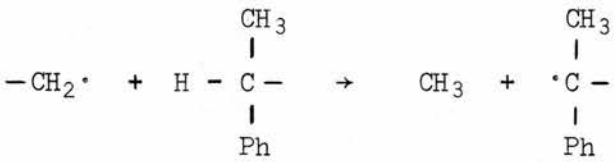

However, because the copolymers are in the form of a viscous liquid during degradation, then motion of the molecules is highly restricted. Hence, it is not unlikely that the abstraction of hydrogen to form secondary radicals also occurs

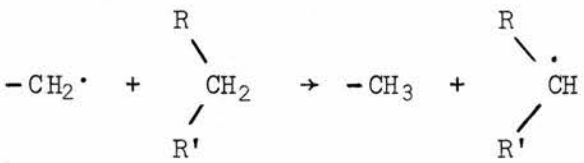

where R and R' are parts of the polymer chain. This second process of abstraction leads to the possibility of a number of different functions resulting from the subsequent fragmentation or disproportionation reactions. The larger the value of n, the greater the number of possible functions.

The preference for abstraction of tertiary hydrogen renders the production of the dimeric species of molecular weight, 238, which contains two such hydrogens, unlikely during degradation. Hence it is possible that the large amount of this dimeric species produced in the

decompositions was present in the undegraded polymer sample.

From the above treatments of the n = 1 and n = 3 - 10 copolymers, it is not easy to see how many of the volatile liquids and gases are formed. The next part of the discussion will deal with the possible mechanisms by which some of these entities are produced.

Secondary Reactions

With the exception of methane and ethylene, it is difficult to rationalise how products such as propene, propane, butene, pentene and pentadiene are formed by all the copolymers. It was concluded that from the n = 1 copolymers, these gases were very unlikely to be formed by direct decomposition. The reaction of the methyl radical with carbon-carbon double bonds has been studied by Gordon and McNesby[39,40]. Theyshow that in the gas phase, methyl radicals can add to ethylene. As it is probable that some of the methyl radicals leave the degrading polymer before reacting, it is conceivable that secondary reactions are possible in the decomposition apparatus. The addition to styrene is thirty times as fast as the addition to ethylene[41], this being due to the stability of the resulting radical. Hence, the addition to α-methyl styrene would also be expected to be fast. This process is also far more likely than abstraction if a choice is available. For[41]:

$$CH_3\cdot + \text{Iso-octane} \xrightarrow{k_1} CH_4 + \text{a secondary radical}$$

$$CH_3\cdot + A \xrightarrow{k_2} CH_3A\cdot$$

where A is an alkene, k_1/k_2 = 26 for ethylene and 796 for styrene where k_1 and k_2 are the rate constants for the above reactions. The possible secondary reactions of ethylene and α-methyl styrene with the methyl radical are shown below:

$$CH_3\cdot + CH_2 = CH_2 \rightarrow CH_3CH_2CH_2\cdot$$

$$CH_3\cdot + Ph\ C(CH_3) = CH_2 \rightarrow Ph\ \dot{C}(CH_3)(C_2H_5) \quad -(R)$$

The resulting radicals can react in a number of ways, the most likely being abstraction, combination or disproportionation. Abstraction is only relevant for the n-propyl radical which would produce propane. Disproportionation and combination are two competing processes. For unstable radicals combination is the dominant reaction but the reverse is true for stable radicals. The following examples illustrate this point for various radicals in the gas phase[42,43].

$CH_3\cdot + n\text{-}C_3H_7\cdot \rightarrow [CH_4 + C_3H_6]$ or C_4H_{10} pd/pc = 0.05

$2\ C_2H_5\cdot \rightarrow [C_2H_4 + C_2H_6]$ or C_4H_{10} pd/pc = 0.12

$2\ n\text{-}C_3H_7\cdot \rightarrow [C_3H_6 + C_3H_8]$ or C_6H_{14} pd/pc = 0.15

$C_2H_5\cdot + t\text{-}C_4H_9\cdot \rightarrow [C_2H_6 + C_4H_8]$ or C_6H_{14} pd/pc = 0.50

$2\ i\text{-}C_3H_7\cdot \rightarrow [C_3H_6 + C_3H_8]$ or C_6H_{14} pd/pc = 0.69

$2\ t\text{-}C_4H_9\cdot \rightarrow [C_4H_8 + C_4H_{10}]$ or C_8H_{18} pd/pc = 2.32

where $\frac{pd}{pc}$ is the relative probability of disproportionation to combination occurring.

This suggests that the n-propyl radical will preferentially combine with other radicals whereas the (ethyl-methyl-phenyl) methyl radical, R, will preferentially disproportionate. Hence, the n-propyl radical can give rise to propene and propane by disproportionation and butane by combination with a methyl radical. As butane is rarely found, it must be assumed that the secondary reactions of ethylene do not occur to a large degree.

Disproportionation of the aromatic tertiary radical, R, leads to

the formation of α-ethyl styrene, α,β-dimethyl styrene and isobutyl benzene. Of these, α-ethyl styrene is found in relatively large quantities. This is reasonable as the disproportionation of the tertiary radical by the head to head homopolymer gave rise to the $Ph - \overset{|}{C} = CH_2$ group rather than the $\overset{CH_3}{\underset{Ph}{\rangle}}C = CH -$ group. Therefore, it is possible that secondary reactions with α-methyl styrene do take place to a limited extent.

The above are not the only secondary reactions possible, for instance, the n-propyl radical could also add to α-methyl styrene with the resulting formation of an alkenyl benzene of molecular weight, 160, and 2-phenyl hexane.

Volatile Fragments

The most energetically favourable bond scissions of the polymer chain are those which produce a primary and tertiary radical. It is possible that some of the volatile liquid products are formed by breakage of bonds of similar energy occurring close to the end of the polymer chain. For example:

$$-CH_2 - CH_2 - \underset{Ph}{\overset{CH_3}{\underset{|}{\overset{|}{C}}}} - H \rightarrow -CH_2 - CH_2\cdot + \cdot\underset{Ph}{\overset{CH_3}{\underset{|}{\overset{|}{C}}}} - H$$

This terminal group which is present in all of the copolymers can form a radical which on disproportionation gives rise to styrene or ethyl benzene. The quantity of ethyl benzene produced during degradation is always greater than that of styrene. This could be due to the possible secondary reaction of styrene with the methyl radical. This process could give rise to the production of β-methyl styrene and

n-propyl benzene.

$$Ph - CH = CH_2 + CH_3\cdot \rightarrow Ph\dot{C}H - CH_2CH_3$$

Hence, because a number of different terminal groups are formed during thermal decomposition, it is easy to see that the possible products obtained by bond scissions occurring near the end of a polymer chain, are numerous. This process explains the presence of compounds containing the terminal - CH = CH_2 group in the volatile liquid fraction as this has been shown to be a probable terminal function in all the polymer decompositions.

Certain of the gaseous products may also be produced in the above manner. For example, the n = 3 copolymer probably contains the following terminal group:

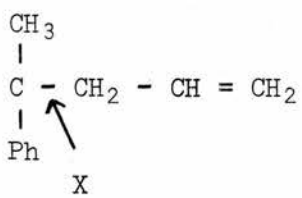

Scission at bond X produces a tertiary and a primary radical, however, the primary radical is stabilised by allylic resonance. Hence the bond dissociation energy for this reaction would be expected to be less than that needed for scission at any other bond within the chain. This is because the primary radical resulting from any other similar bond breakage would not be stabilised in any way. The allyl radical obtained is likely to lead to the formation of propene. The presence of significant quantities of hexene, pentene and butene from the n = 6, n = 5 and n = 4 copolymers respectively can be explained in a similar way. However, for these cases the resulting primary radical would have no added stability.

Rearrangements

The fact that some of the higher molecular weight components of the volatile liquid fractions contain large peaks at 91, attributable to Ph CH_2 -, in their mass spectra suggests that rearrangement of certain radicals may be occurring. All the copolymers can produce

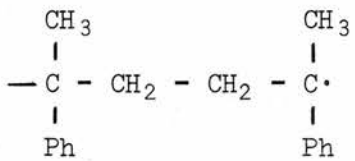

Should this radical unzip one monomer unit, then the resulting species is very similar to the neophyl radical, which was discussed in the early part of this chapter, and could act in the same way:

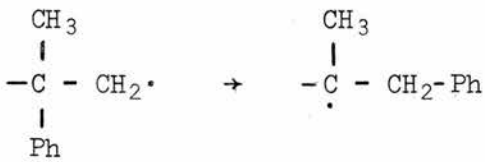

The resulting radical is very likely to disproportionate which can lead to the production of a saturated terminal group containing Ph - CH_2 -. However because of orientation difficulties within the viscous degrading polymer, this rearrangement would not be expected to take place to a significant extent.

Consequences of Abstraction

The presence of a trans carbon-carbon double bond has not been explained. However, it is probably formed by the disproportionation of secondary radicals, which were produced as a result of abstraction by the primary radicals which, in turn, resulted from the initial bond scissions.

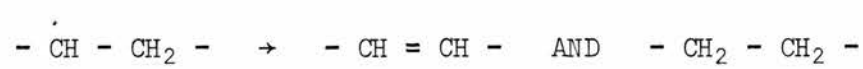

This process can also lead to the formation of the cis carbon-carbon double bond. The presence of this entity was not detected in the I.R. spectra of any of the fractions, however, this could have been due to masking of the relevant peaks.

Certain of the secondary radicals formed by the above abstraction can, alternatively, fragment. This is most favourable when the odd electron exists on a carbon atom which is next but one to a carbon atom attached to a phenyl group. This results in the formation of an isolated $-CH=CH_2$ group and a tertiary radical.

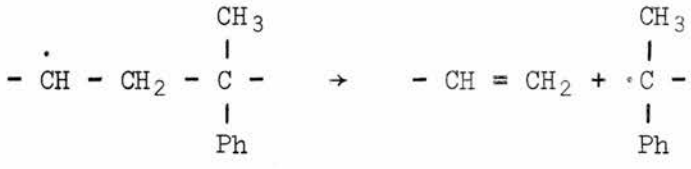

The above two reactions are concerned with radicals resulting from intermolecular abstractions. For certain of the copolymers, the production of a secondary radical from a primary radical by abstraction, can occur intramolecularly. The process involves the formation of a five or six membered cyclic intermediate. For the primary radicals resulting from the initial bond scissions, the formation of this cyclic intermediate is sometimes hindered by the phenyl and methyl groups in the chain. However, when $n \geq 4$, the primary radical produced by bond scission (2), figure 29, can form this intermediate without steric hindrance. For example, abstraction via six membered intermediate for n = 5 copolymer.

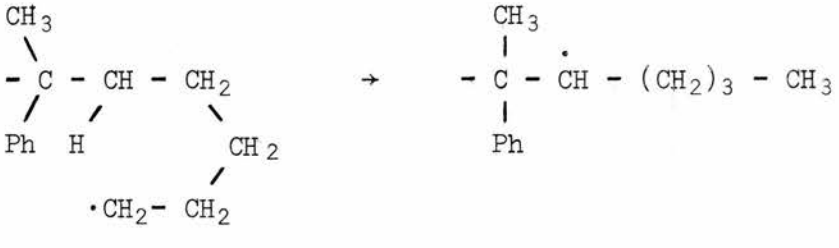

The secondary radical, resulting from this abstraction, can fragment or disproportionate in the same way as the similar radicals formed by intermolecular abstraction. Similar schemes can be produced for five and six membered cyclic intermediates, for all the primary radicals which are attached to at least three consecutive methylene groups.

The intramolecular abstraction of hydrogen by a primary radical to form a further primary radical, was used by Tsuchiya and Sumi[47] to explain certain of the products of the thermal degradation of poly-isobutylene at 345°C. Although this would appear to be an unlikely reaction, it could account for the α-ethyl styrene produced by all the copolymers.

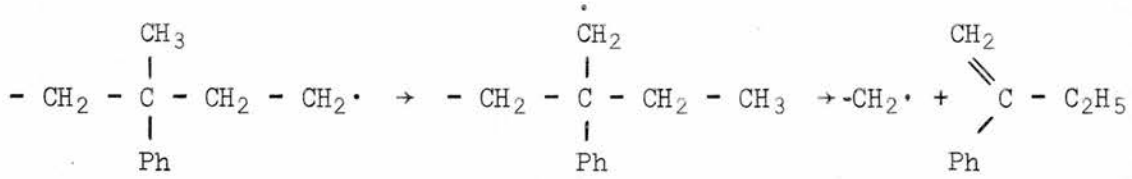

The above mechanistic postulations give possible explanations for some of the volatile liquid and gaseous products. They also show how the various carbon-carbon double bonds, present in the residue, and low molecular weight and volatile liquid fractions may be produced.

In the mass spectra of the volatile liquid and low molecular weight fractions, 131 is a very common fragment-ion peak. This could well be due to splitting out the Ph - $\dot{C}(CH_3)$ - CH = CH_2 group, a group shown to be possible by the mechanistic schemes. 117 is another common fragment-ion peak, this could be attributed to the Ph - C(=CH_2)-CH_2- group, another group shown to be possible by the mechanistic schemes. The possible presence of both of these functions in the afore-mentioned fractions was substantiated by the infrared spectra.

Hence, although some of the products have not been positively identified, it is possible from the mechanistic schemes to postulate structures for some of these compounds. For example, in the volatile liquid fraction produced by the n = 5 copolymer, a substantial quantity of a compound of molecular weight, 174, is present (component M). The large peak at 1642 cm^{-1} in the infrared spectrum of this fraction, suggests that this compound contains the isolated - CH = CH_2 group. The major peak in its mass spectrum is 105 which infers the presence of the Ph $CH(CH_3)$ group. Hence a possible structure would be:

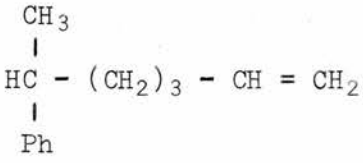

Both the terminal groups of this compound have been shown to be possible by the mechanistic schemes. Other compounds could be treated similarly.

The Polymers Investigated

The analysis of the kinetics of thermal decomposition of the polymers showed that head to head poly-α-methyl styrene was, by far, the least thermally stable. The n = 1 copolymer was also less thermally stable than the other copolymers. Comparison of the thermal stability of the other copolymers can best be considered using figure 30. This figure shows a plot of $\log_{10}$ (time) versus n, where time refers to the time taken for a polymer to reach a particular percentage degradation at 372°C and n refers to the copolymer. From the figure, it is clear that the n = 4 and n = 5 copolymers are the most thermally stable. However, it should be noted that the time taken to get to 60% degradation from 10% degradation is greatest for the n = 6 copolymer. Furthermore,

FIGURE 30

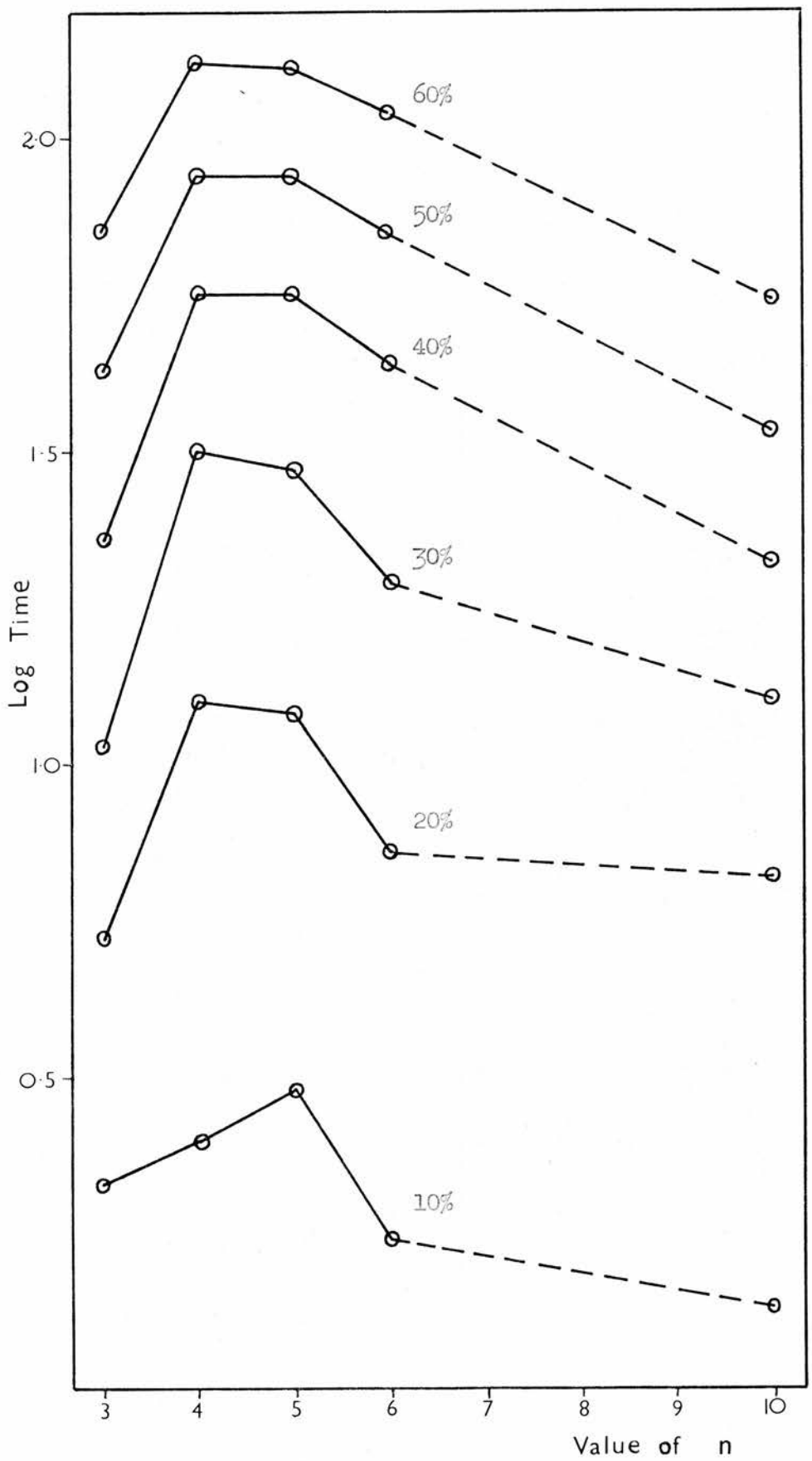

the times taken for this same change, for any of the copolymers, are very similar.

It should be mentioned that in the initial preparation of the copolymers, there are two side reactions which may occur. The first of these is a Wurtz type reaction[44] which may take place between two molecules of the dihaloalkane and lithium metal. This results in the formation of another dihaloalkane, however, this one contains twice as many methylene groups as its precursor.

$$X - (CH_2)_n - X + 2Li + X - (CH_2)_n - X \quad X - (CH_2)_{2n} - X$$

where X is a halide. An experiment was conducted under the conditions of the copolymer preparation, but with only the dihaloalkane and lithium present in the T.H.F. The resulting products consisted largely of unchanged dihaloalkane, however, a very small amount of the dimeric species was found but this was almost negligible in quantity. Hence, it may be assumed that the incorporation of longer, than expected, chains of methylene groups into the polymer structure is not an important side reaction.

The second side reaction involves the formation of the tetrameric dianion

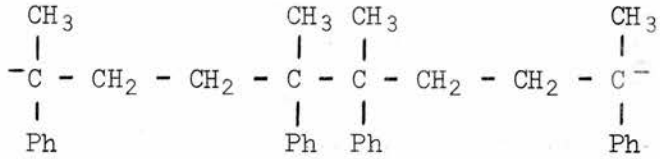

The preparation and comfirmation of the structure of this species have been carried out by Szwarc and co-workers[44,45]. The preparation requires that α-methyl styrene is reacted upon by sodium in the presence of T.H.F. at 0°C. It is reasonable to suppose that lithium would also effect the

reaction. Hence, it is possible that in the polymer preparation both the dimeric and tetrameric dianions may be produced. However, structure analysis of the copolymers only shows the presence of the dimeric species. On the other hand, it is not unlikely that small quantities of the tetrameric species have been incorporated into the polymer chain. This species contains a head to head linkage which was shown, in the case of the head to head homopolymer, to be a weak bond. This may be the reason behind the low energies of activation found for the early stages of all the polymer degradations.

PART ONE - BIBLIOGRAPHY

(1) Williams, C.G. from Slade, P.E. and Jenkins, L.T., 'Thermal Characterisation Techniques', Dekker, New York (1970)

(2) Angstrom, K., Ofersigt Kongl. Vetenskaps-Akad. Forh, 643 (1895)

(3) Urbain, M.G., Compt. Rend. 6, 347 (1912)

(4) Mikulinskii, A.S. and Gel'd P.V., Lavodskaya Lab., 9, 921 (1940)

(5) Kuhlman, W.H.F., Der Mechaniker, 18, 146 (1910)

(6) Dubois, P., Ph.D. Thesis, University of Paris, (1935)

(7) Gordon, S. and Campbell, C., Anal. Chem., 32, 271R (1960)

(8) Garn, P.D., 'Thermoanalytical Methods of Investigation', Academic Press, New York (1965)

(9) Lewin, S.Z., J. Chem. Educ., 39, A575 (1962)

(10) Cameron, G.G. and Fortune, J.D., Eur. Polymer J., 4, 333 (1968)

(11) Flynn, J.H. and Wall, L.A., J. Res. Natl. Bur. Std., 70A, 487 (1966)

(12) Friedman, H.L., J. Polymer Sci. (C), 6, 183 (1964)

(13) Tanner, J., Ph.D. Thesis, University of St. Andrews, (1969)

(14) Richards, D.H., Scilly, N.F. and Williams, F., Polymer, 10, 603 (1969)

(15) Szwarc, M., Nature, 178, 1168 (1956)

(16) Szwarc, M., Makromol. Chem., 35, 132 (1960)

(17) Richards, D.H., Scilly, N.F. and Williams, F., Polymer, 10, 611 (1969)

(18) Martin, A.J.P. and James, A.T., Biochem. J., 63, 138 (1956)

(19) Cornu, A. and Massot, R., 'Compilation of Mass Spectral Data', Heyden, (1966)

(20) Benyon, J.H., Saunders, R.A. and Williams, A.E., 'The Mass Spectra of Organic Molecules', Elsevier (1968)

(21) Daniels, T., Eur. Polymer J., 6, 773 (1970)

(22) Thomas, J.M. and Williams, B.R., Quart. Rev., 19, 231 (1965)

(23) Friedman, H.L., 'High Temperature Polymers', Arnold, London, p57 (1967)

(24) Jellinek, H.H.G., J. Polymer Sci., 4, 13 (1949)

(25) Brown, D.W. and Wall, L.A., J. Phys. Chem., 62, 848 (1958)

(26) Madorsky, S.L., J. Res. Natl. Bur. Std., 62, 219 (1959)

(27) Madorsky, S.L., J. Polymer Sci., 11, 491 (1953)

(28) Benson, S.W., J. Chem. Educ., 42, 502 (1965)

(29) Cottrell., T.L., 'The Strengths of Chemical Bonds', Butterworths, London (1956)

(30) Herzberg, G., Proc. Roy. Soc. (London), 262A, 291 (1961)

(31) Herzberg, G., Ann. Rev. Phys. Chem., 9, 327 (1958)

(32) Stirling, C.J.M., 'Radicals in Organic Chem.', Oldbourne Press, London (1965)

(33) Pryor, W.A., 'Free Radicals', McGraw-Hill, New York (1966)

(34) Curtin, D.Y. and Hurwitz, M.J., J. Am. Chem. Soc., 74, 5381 (1952)

(35) Urry, W.H. and Kharasch, M.S., J. Am. Chem. Soc. 66, 1438 (1944)

(36) Steinmetz, H. and Noyes, R.M., J. Am. Chem. Soc., 74, 4141 (1952)

(37) Urry, W.H. and Nicolaides, N., J. Am. Chem. Soc., 74, 5163 (1952)

(38) Seubold, F.H., J. Am. Chem. Soc., 75, 2532 (1953)

(39) Gordon, A.S. and McNesby, J.R., J. Chem. Phys., 31, 853 (1959)

(40) Gordon, A.S. and McNesby, J.R., J. Chem. Phys., 33, 1882 (1960)

(41) Szwarc, M. and Binks, J.H., 'Theoretical Org. Chem.', Kekule Symposium 1958, Butterworth, London, pp 271, 272, 278 (1958)

(42) Futtrell, J.H. and Terry, J.O., Can. J. Chem., 45, 2327 (1967)

(43) Futtrell, J.H. and Terry, J.O., Can. J. Chem., 46, 664 (1968)

(44) Wurtz, A., Ber., 20, 815 (1887)

(45) Lee, C.L., Smid, J. and Szwarc, M., J. Phys. Chem., 66, 904 (1962)

(46) Vrancken, A., Smid, J. and Szwarc, M., Trans. Faraday Soc., 58, 2036 (1962)

(47) Tsuchiya, Y and Sumi, K., J. Polymer Sci., 7 A1, 813 (1969)

(48) Ramey, K.C. and Statton, G.L., Makromol. Chem., 85, 287 (1965)

PART TWO

CHAPTER 1. INTRODUCTION

A. General and Historical

The confirmation of a postulated mechanism for a polymer degradation process depends on agreement between the observed and predicted rate laws. Hence, the study of the kinetics of polymer degradation has become instrumental as a means of elucidating the mechanism of breakdown. Early work in this field was carried out on cellulose and starches and this was concerned with the effects of chain scission on molecular weight. These are step reactions and various theoretical processes were put forward to describe them [1,2,3]. As new polymeric materials were studied, it became apparent that more complicated mechanisms involving chain processes were occurring. The first treatment of a chain process was by Simha, et al. [4,5]. They derived a set of differential equations to describe a general chain mechanism. Their treatment is based on the concept of initiation by chain scission followed by chain transfer or depropagation followed by termination. The same type of treatment has been extended by Boyd and co-workers [6,7,8], however they use a different method of solution of their equations. One point that both methods have in common is the application of the stationary state hypothesis to radical concentration in the solution of the rate equations. This hypothesis has been shown to be doubtful in its validity by MacCallum[9].

This part of the thesis is concerned with the evaluation of theoretical rate equations using a different approach to the one described above. Three cases will be considered; firstly, random scission of the main chain bonds with rapid evaporation of any species of less than a prescribed degree of polymerisation. Secondly, random

scission of main chain bonds followed by reverse polymerisation of a constant number of monomer units on both sides of the break together with rapid evaporation of any species of less than a prescribed degree of polymerisation. Thirdly, scission of a terminal bond only, followed by reverse polymerisation of a constant number of monomer units. All three cases are considered under isothermal conditions.

B. List of Symbols Used

P_o - Initial degree of polymerisation of the sample.

P - Degree of polymerisation of the sample at time t.

W_o - Initial weight of sample.

W - Weight of sample at time t.

N_x - Number of moles in the sample of degree of polymerisation 'x'

N - Number of moles in the sample at time t.

m - Molecular weight of the repeat unit.

t - Time of reaction.

k_s - Rate constant for scission reaction.

a - Degree of polymerisation of the largest molecule that can evaporate from the sample.

z - Number of monomer units produced when a molecule depolymerises (unzip length).

k_e - Rate constant for end initiation.

C. Kinetic Analysis

For any given polymer, the following relationship always applies:

$$W = m.N.P \qquad (i)$$

During the course of a reaction, the weight of the sample, the number

of moles, and the degree of polymerisation all vary continuously with time. Hence the following relationship must hold:

$$\frac{1}{m}\frac{dW}{dt} = N\frac{dP}{dt} + P\frac{dN}{dt} \qquad \text{(ii)}$$

In the following kinetic analyses, the sample is assumed to have a "most probable" distribution of molecular sizes. This is expressed mathematically by equation (iii):

$$N_x = \frac{N'}{P'}\left(1 - \frac{1}{P'}\right)^{x-1} \qquad \text{(iii)}$$

N' and P' are the number of moles and degree of polymerisation if a complete distribution were present. In the first two cases which considers an evaporatable size 'a', these are not experimental quantities and the above equation must be modified to incorporate the experimental values.

$$N = \sum_{x=a+1}^{\infty} N_x$$

$$= \sum_{x=a+1}^{\infty} \frac{N'}{P'}\left(1 - \frac{1}{P'}\right)^{x-1}$$

$$N = N'\left(1 - \frac{1}{P'}\right)^{a} .$$

$$P = \sum_{x=a+1}^{\infty} x N_x \Big/ \sum_{x=a+1}^{\infty} N_x$$

$$= \sum_{x=a+1}^{\infty} \frac{N'}{P'}\left(1 - \frac{1}{P'}\right)^{x-1} \Big/ \sum_{x=a+1}^{\infty} \frac{N'}{P'}\left(1 - \frac{1}{P'}\right)^{x-1}$$

$$P = P' + a .$$

$$N = N'\left(1 - \frac{1}{P-a}\right)^{a} .$$

Substituting in equation (iii):

$$N_x = \frac{N}{\left(1 - \frac{1}{P-a}\right)^{a}} \cdot \frac{1}{(P-a)} \cdot \left(1 - \frac{1}{P-a}\right)^{x-1} \qquad \text{(iv)}$$

CHAPTER 2. THEORECTICAL CALCULATIONS

This chapter will be subdivided into three sections, each of which is concerned with a different aspect of thermal degradation.

A. Random Scission - Evaporation Model

This section is concerned with random scission of main chain bonds followed by rapid evaporation of any species of less than a prescribed degree of polymerisation.

Molecular Population

If a molecule undergoes scission to produce two smaller molecules, then the molecular population increases by one. However, if the break occurs within a distance of 'a' repeat units from either end, then the smaller of the two molecules of size less than, or equal to, 'a', evaporates and the molecular population is unchanged. There will also be a fraction of molecules which when broken at certain bonds, will produce two fragments of size less than 'a' with a resulting decrease in population.

Thus,

$$\frac{dN}{dt} = \text{Rate of scission leading to an increase} - \text{rate of scission leading to a decrease.}$$

Only molecules with a degree of polymerisation, 'x', greater than 2a+1 can lead to an increase in population. Molecules with $x \geq 2a+2$ have $(x-2a-1)$ bonds which when broken lead to an increase in population. For a decrease in population $2a \geq x \geq a+1$, and any molecule in this region has $(2a+1-x)$ bonds which when broken lead to a decrease in population.

Thus,

$$\frac{dN}{dt} = k_s \text{ [Total number of bonds which when broken lead to and increase in population]}$$

$$- k_s \text{ [Total number of bonds which when broken lead to a decrease in population]}.$$

$$= k_s \cdot \sum_{x=2a+2}^{\infty} N_x \, (x-2a-1) - k_s \cdot \sum_{x=a+1}^{x=2a} N_x \, (2a+1-x)$$

N_x can be replaced by using equation (iv)

$$= k_s \frac{N}{(P-a)} \cdot \frac{1}{(1 - \frac{1}{P-a})^a} \left[\sum_{x=2a+2}^{\infty} (1 - \frac{1}{P-a})^{x-1} \, (x-2a-1) \right.$$

$$\left. - \sum_{x=a+1}^{x=2a} (1 - \frac{1}{P-a})^{x-1} \, (2a+1-x) \right]$$

By resolving the summations, the above equation reduces to:

$$= k_s \frac{N}{(P-a)} \cdot \frac{1}{(1 - \frac{1}{P-a})^a} \left[(P-a)^2 \, (1 - \frac{1}{P-a})^{2a+1} - \right.$$

$$\left. (P-a) \, (1 - \frac{1}{P-a})^a \, [2a-P+1+(P-a) \, (1 - \frac{1}{P-a})^{a+1}] \right]$$

This reduces to

$$\frac{dN}{dt} = k \, . \, N \, . \, (P - 2a - 1).$$

Weight of Sample

The rate of loss of weight, $- \frac{dW}{dt}$ is equal to the rate of production of volatile fragments multiplied by the weight of the volatile part.

$- \frac{dW}{dt}$ comprises three parts

a) Molecules for which $x \geq 2a+1$. Any molecule in this range has 2a

bonds which, when broken, lead to one molecule which can evaporate and one which cannot.

Rate of loss of weight due to a)

$$= k_s\, a(a+1)\ \frac{Nm}{P-a}\left[\frac{1}{(1-\frac{1}{P-a})^a}\right]_{x=2a+1}^{\infty}\sum (1-\frac{1}{P-a})^{x-1}$$

$$= k_s\, a(a+1)\ .\ Nm\ (1-\frac{1}{P-a})^a$$

From equation (i), $Nm = {}^{W}/_{P}$

$$\therefore\ -\frac{dW}{dt} = k_s\ .\ \frac{W}{P}\ a(a+1)\ \ (1-\frac{1}{P-a})^a$$

b) Molecules for which $a+1 \leqslant x \geqslant 2a$. In this region, any molecule has $(2a+1-x)$ bonds which on scission lead to complete removal of the molecule. When this occurs, the weight lost is equivalent to $x\ .\ m$.

Rate of loss of weight due to b)

$$= k_s\ \frac{Nm}{(P-a)}\cdot\frac{1}{(1-\frac{1}{P-a})^a}\ \ \sum_{x=a+1}^{x=2a}(1-\frac{1}{P-a})^{x-1}\ \ (2a+1-x)\ .\ x.$$

$$= k_s\ \frac{Nm}{P-a}\cdot\frac{1}{(1-\frac{1}{P-a})^a}\cdot(1-\frac{1}{P-a})^a\Big[[a(a+1)(1-(1-\frac{1}{P-a})^a)(P-a)]$$

$$-\sum_{n=2}^{a}(1-\frac{1}{P-a})^{n-1}\ \ (n-1)\ .\ n\Big]$$

c) Molecules for which $a+2 \leqslant x \geqslant 2a$. For this case, any molecule has $2(x-a-1)$ bonds which on scission lead to the loss of one fragment, whilst the other remains in the sample.

Rate of loss of weight due to c)

$$= k_s \frac{Nm}{P-a} \cdot \frac{1}{(1 - \frac{1}{P-a})^a} \sum_{x=a+2}^{2a} (1 - \frac{1}{P-a})^{x-1}(x-a-1)(x-a).$$

$$= k_s \frac{Nm}{P-a} \cdot \frac{1}{(1 - \frac{1}{P-a})^a} \cdot (1 - \frac{1}{P-a})^a \sum_{n=2}^{a} (1 - \frac{1}{(P-a)})^{n-1}$$

$$(n-1) \cdot n$$

The expression for the total rate of loss of weight is the sum of the three parts (a), (b) and (c) and solves out as

$$- \frac{dW}{dt} = k_s \cdot \frac{W}{P} \cdot a(a+1) \qquad \text{(vi)}$$

Figure 1 illustrates a plot of $dW/dt.W_o$ versus t for some values of P_o and a, and figure 2 shows a plot of percentage weight versus percentage molecular weight for the same values of P_o and a.

Degree of Polymerisation

From equations (ii), (v) and (vi), the following expression can be deduced for the rate of change of degree of polymerisation with respect to time:

$$- \frac{dP}{dt} = k_s \quad (P-a-1)(P-a). \qquad \text{(vii)}$$

The rate equation (vii) can readily be integrated resulting in the following expression for P in terms of t.

$$P = a + 1 + \frac{1}{\frac{e^{kt}}{c} - 1} \qquad \text{(viii)}$$

$$\text{where} \quad c = \frac{P_o - a - 1}{P_o - a}$$

Figure 3 shows a plot of $^1/_P$ versus $k_s.t.$ for various values of 'P_o'

FIGURE 1

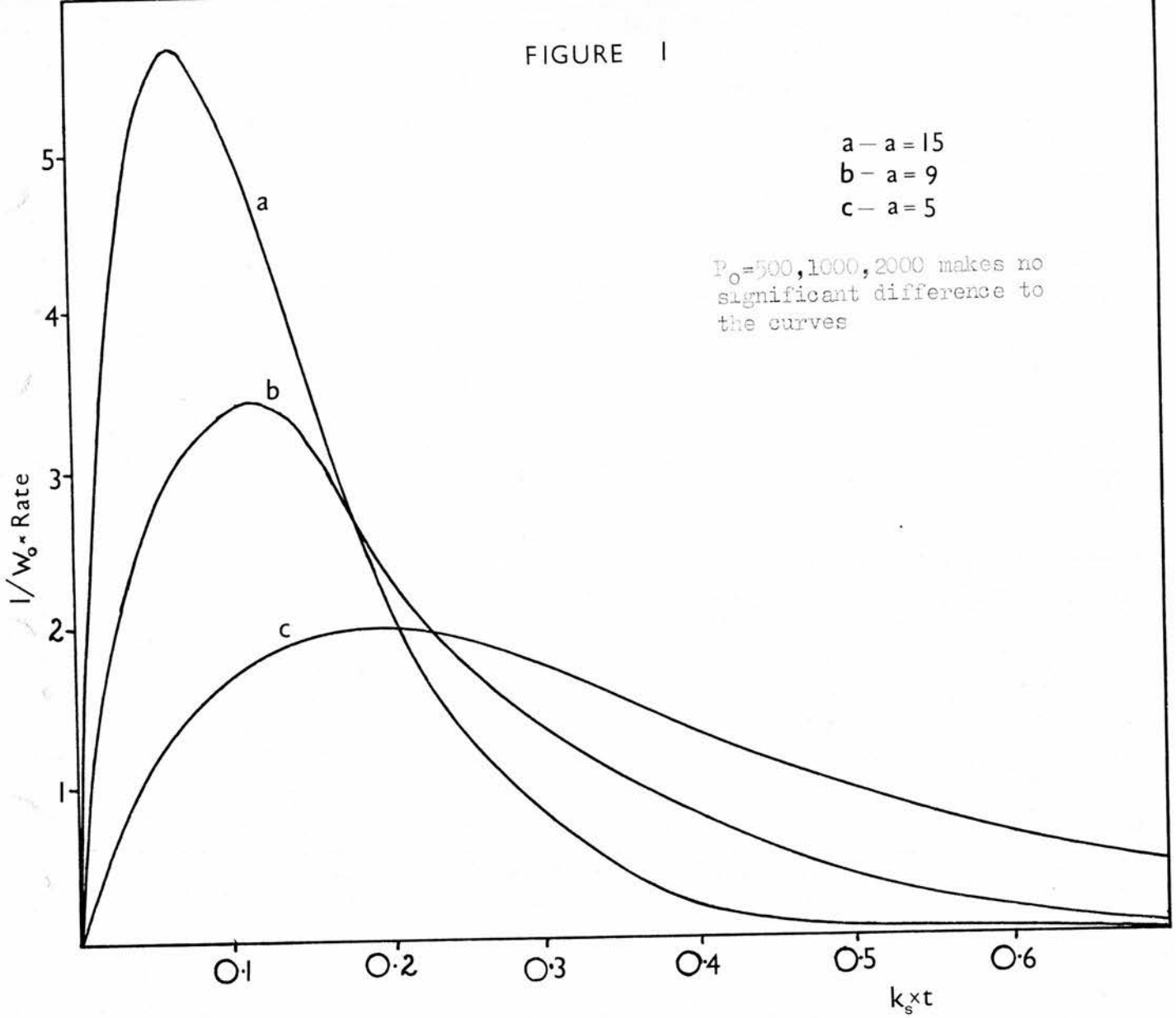
a — a = 15
b — a = 9
c — a = 5
P_o=500, 1000, 2000 makes no significant difference to the curves
1/W_o × Rate
5
4
3
2
1
a
b
c
0·1
0·2
0·3
0·4
0·5
0·6
k_s×t

FIGURE 2

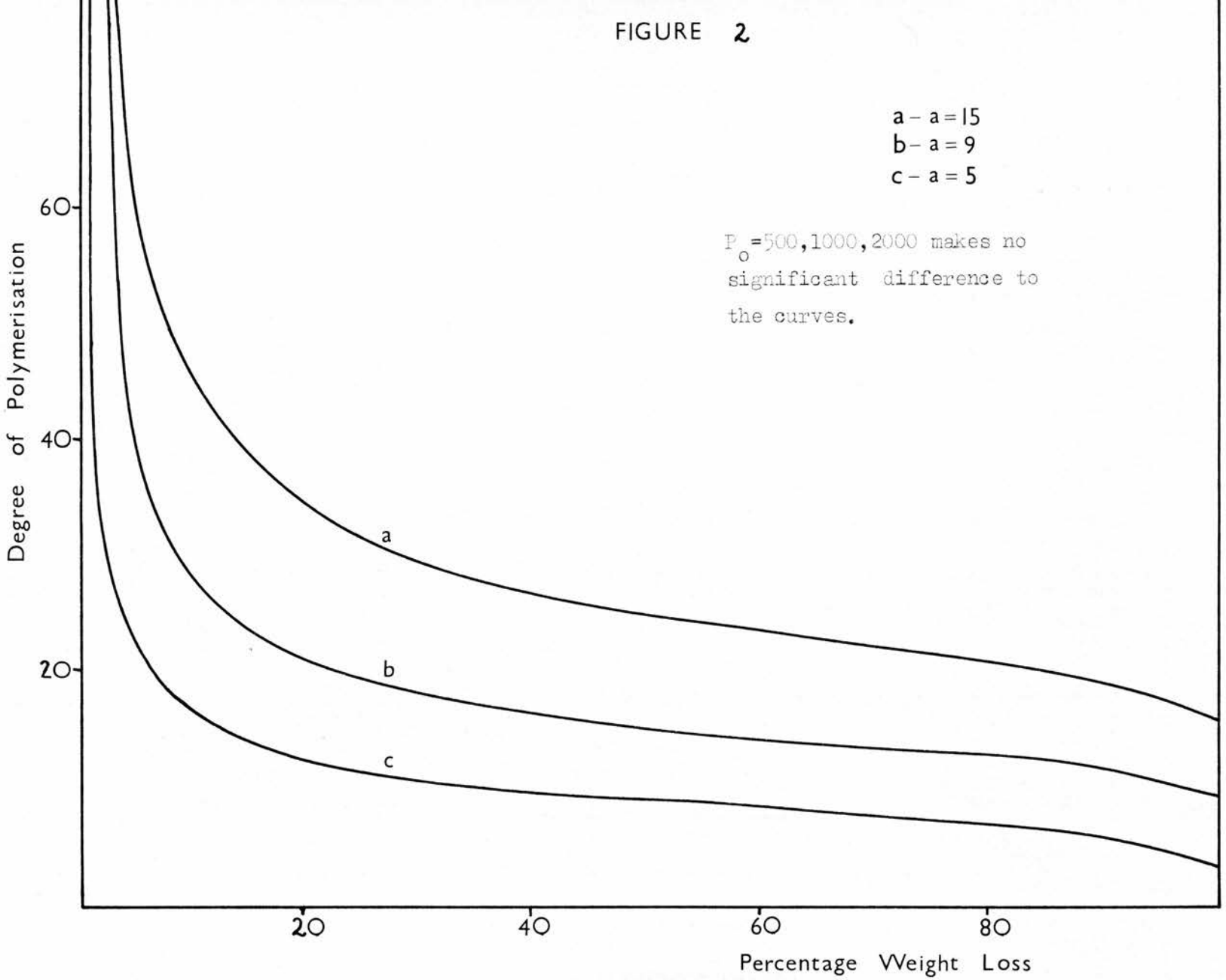
a – a = 15
b – a = 9
c – a = 5
P_o = 500, 1000, 2000 makes no significant difference to the curves.
Degree of Polymerisation
60
40
20
a
b
c
20
40
60
80
Percentage Weight Loss

FIGURE 3

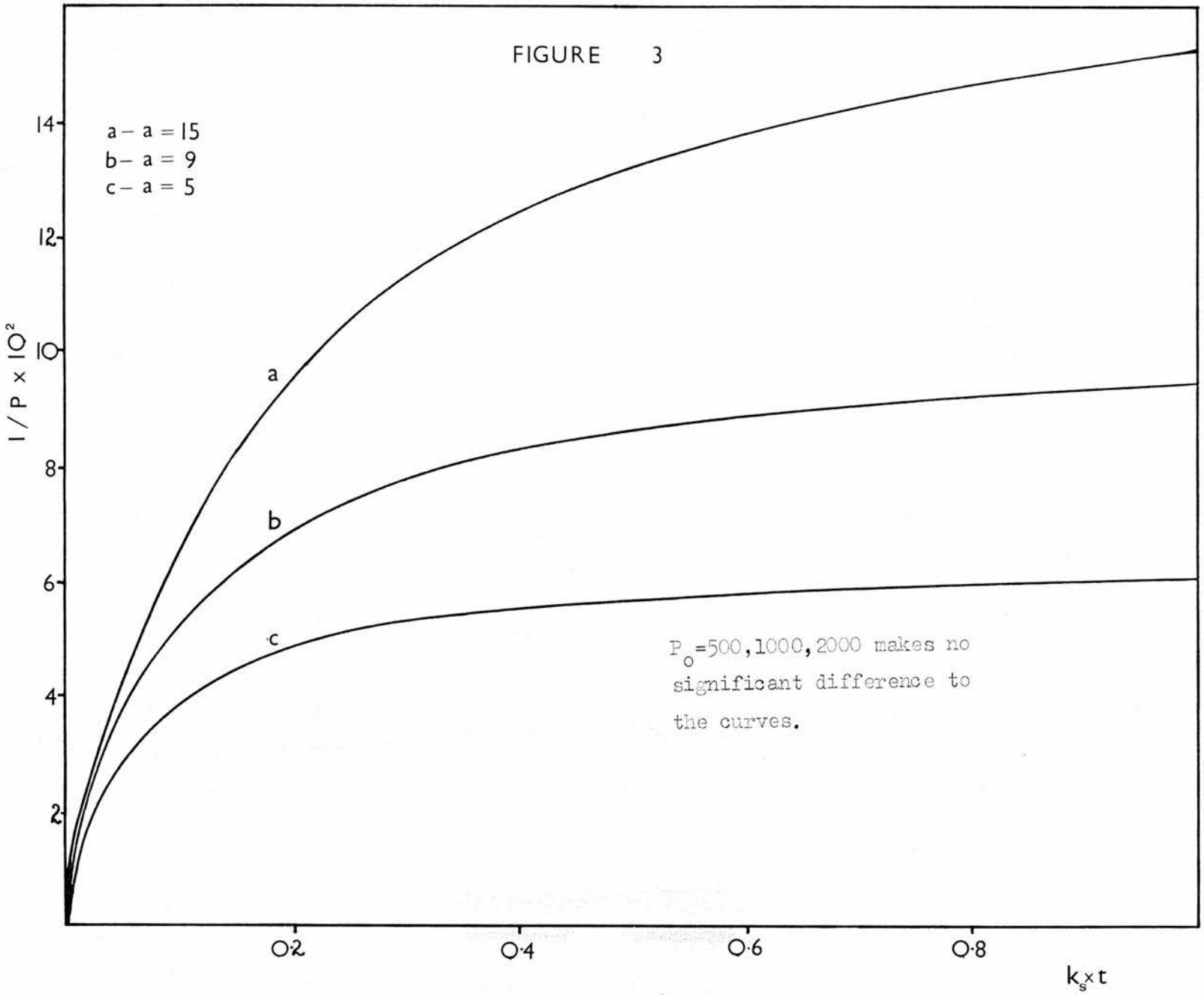
a – a = 15
b – a = 9
c – a = 5
1 / P x 10²
14
12
10
8
6
4
2
a
b
c
P₀=500, 1000, 2000 makes no significant difference to the curves.
0·2
0·4
0·6
0·8
kₛ x t

and 'a'. For most cases 'c' can be regarded as equal to 1, however for the limiting case of t = 0, it must be present.

Similarly, by substituting the P derived in equation (viii) in equation (vi) we can deduce the following expression for W in terms of t:

$$W = \frac{W_o\,[(a+1)e^{kt} - ac](P_o-a)}{P_o e^{(a+1)kt}}$$

Figure 4 shows a plot of $\frac{W}{W_o}$ versus $k_s.t$ for various values of 'P_o' and 'a'.

To test for the possible existence of a maximum value for the rate of loss of weight, $-\frac{dW}{dt}$ is differentiated with respect to time and set equal to zero.

$$-\frac{d^2W}{dt^2} = 0 = k\,.\,a(a+1)\left[\frac{1}{P}\,.\,\frac{dW}{dt} - \frac{W}{P^2}\,.\,\frac{dP}{dt}\right]$$

Solution of this equation results in the maximum rate of loss of weight occurring when the degree of polymerisation has a value of 2a+1.

The percentage decomposition corresponding to this maximum value for the rate of loss of weight can be calculated by integration of $\frac{dP}{dW}^*$ and substituting P = 2a+1 in the resulting equation.

$$\frac{dP}{dW} = \frac{(P-a-1)(P-a)P}{W.a\,(a+1)}$$

Integration of this equation between the limits W_o to W and P_o to P yields the following expression

$$\ln\,\frac{W}{W_o} = (a+1)\,\ln\,\frac{(P_o-a)}{(P-a)} + a\,\ln\,\frac{(P-a-1)}{(P_o-a-1)} + \ln\,\frac{P}{P_o} \qquad (x)$$

* $\frac{dP}{dW} = \frac{dP}{dt} \Big/ \frac{dW}{dt}$; both $\frac{dP}{dt}$ and $\frac{dW}{dt}$ are continuous functions and hence the above manipulation can be made.

FIGURE 4

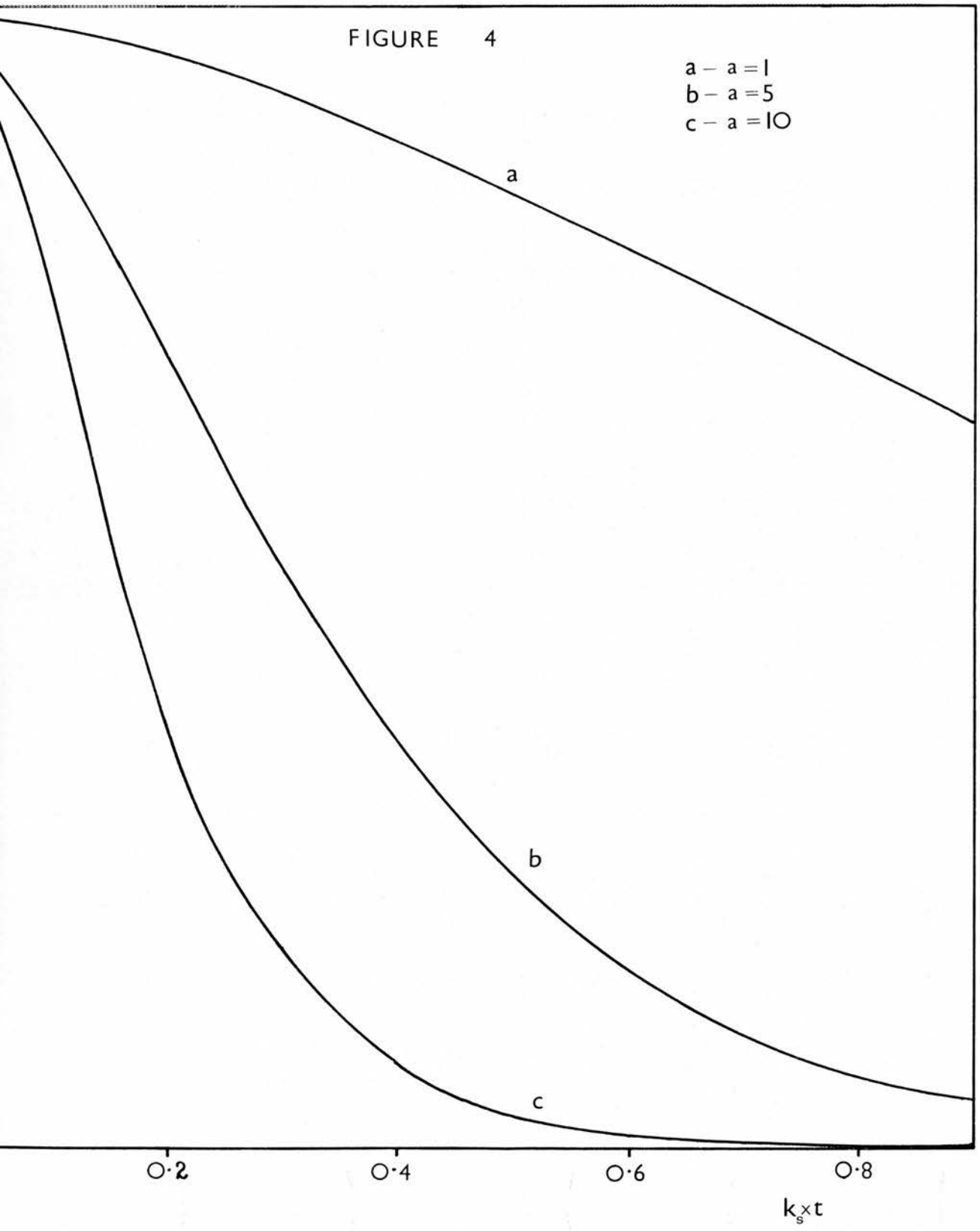

TABLE 1

a	P_o	$(1-W/W_o) \times 100$
1	100	25.00
3		26.13
4		26.18
5		26.20
6		26.18
7		26.14
10		25.90
20		24.30
1	500	25.00
5		26.32
10		26.38
11		26.38
12		26.38
13		26.38
20		26.35
1	1000	25.00
5		26.32
10		26.39
15		26.40
16		26.40
17		26.40
20		26.40

By substitution of P = 2a+1 in equation (x), the expression reduces to:

$$\frac{W}{W_o} = \frac{(2a+1)}{P_o} \cdot \frac{(P_o-a)^{a+1}}{(a+1)^{a+1}} \cdot \frac{a^a}{(P_o-a-1)^a}$$

The percentage degradation, $(1 - \frac{W}{W_o}) \times 100$, corresponding to the maximum rate of loss of weight, for various 'a' and 'P_o' values is summarised in Table 1.

B. Random Scission - Unzip Model

This section is concerned with random scission of main-chain bonds followed by reverse polymerisation of a constant number of monomer units and evaporation of any species produced of less than a prescribed degree of polymerisation. The molecules will be divided into three distinct groups:

Group 1 - Molecules of Degree of Polymerisation (D.P) greater than '2a+2z'

If a molecule in this group undergoes scission followed by depolymerisation of 'z' monomer units in both fragments, to produce two smaller molecules, then the molecular population has increased by one. The weight loss produced by such a bond scission is 2.z.m.

If, however, the scission occurs within a distance of 'a+z' units from either end of the molecule, then one volatile and one non-volatile fragment are produced. This results in the molecular population being unchanged and a weight loss of z.m from the larger fragment together with the whole weight of the smaller fragment.

Group 2 - Molecules with D.P from 'a+1' to 'a+z+1'

In this group, any bond scission leads to total evaporation of the molecule. This results in a decrease in molecular population of one unit and a weight loss corresponding to the size of the molecule.

Group 3 - Molecules with D.P from 'a+z+2' to '2a+2z'

The change in molecular population and weight for this group of molecules will be explained using the following diagram:

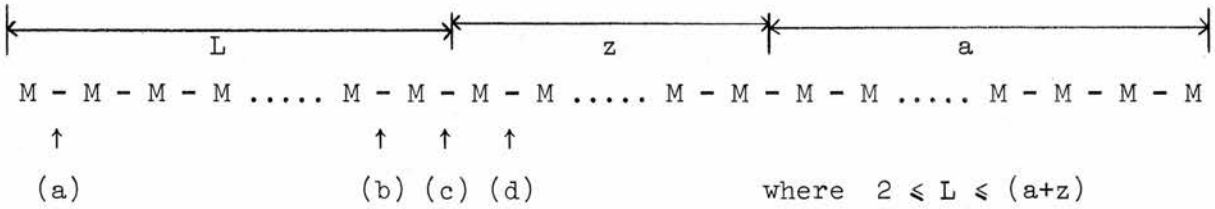

Firstly, consider scission of bond (a). For all possible values of 'L', this breakage results in evaporation of the monomer unit produced, together with reverse polymerisation of 'z' monomer units from the larger fragment. In all cases, a residue from this fragment results and the molecular population remains unchanged. The weight produced by the above scission is (z+1)m.

Secondly, consider scission of bond (b). This results in total loss of the smaller fragment together with reverse polymerisation of 'z' monomer units in the other with a residue of D.P 'a+1'. The molecular population remains unchanged and the weight loss is $[(L-1) + z].m$

Any bond between (a) and (b) will also result in total loss of the smaller fragment together with 'z' units from the larger fragment leaving a residue. Hence bond scission in this region always results in no change in molecular population. It must also be noted that this

region, (a) to (b), can be from either end of the molecule.

Thirdly, consider scission of bond (c). This results in total loss of the length 'L' and unzipping of 'z' units followed by evaporation of the residue 'a'. This results in a decrease in molecular population of one unit and a weight loss corresponding to the size of the molecule.

Finally, consider scission of bond (d). This results in total loss of the right hand fragment and if $L \leq (a+z-1)$, total loss of the left hand fragment. If $L = a+z$, then scission is equivalent to that at bond (b).

Molecular Population

Group 1

In this group, a molecule of D.P. 'x' contains (x-2a-2z-1) bonds which when broken lead to an increase in population of one unit.

Thus,

$$\frac{dN}{dt} = k_s \sum_{x=2a+2z+2}^{\infty} N_x \, (x-2a-2z-1)$$

$$= k_s \frac{N}{(1 - \frac{1}{P-a})^a} \cdot \frac{1}{(P-a)} \cdot \sum_{x=2a+2z+2}^{\infty} (1 - \frac{1}{P-a})^{x-1} \cdot (x-2a-2z-1)$$

On solving the above summation, the following result is obtained:

$$\frac{dN}{dt} = k_s \, N(P-a) \, (1 - \frac{1}{P-a})^{a+2z+1}$$

Group 2

In this group, all bonds undergoing scission lead to evaporation of both fragments and hence a decrease in population of one unit.

Thus,

$$\frac{dN}{dt} = - k_s \sum_{x=a+1}^{a+z+1} N_x \, (x-1)$$

$$= - k_s \frac{N}{(1 - \frac{1}{P-a})^a} \cdot \frac{1}{(P-a)} \cdot \sum_{x=a+1}^{a+z+1} (1 - \frac{1}{P-a})^{x-1} \cdot (x-1)$$

From the above summation, the following equation is obtained:

$$\frac{dN}{dt} = - k_s.N[\, a(1-(1 - \frac{1}{P-a})^{z+1}) + (P-a-1)(1-(z+1)(1 - \frac{1}{P-a})^z + z(1 - \frac{1}{P-a})^{z+1})]$$

Group 3

In this group, any molecule has (2a+2z+1-x) bonds which when broken lead to a decrease in population of one unit.

Thus,

$$\frac{dN}{dt} = - k_s \sum_{x=a+z+2}^{2a+2z} N_x.(2a+2z+1-x)$$

$$= - k_s \cdot \frac{N}{(1 - \frac{1}{P-a})^a} \cdot \frac{1}{(P-a)} \cdot \sum_{x=a+z+2}^{2a+2z} (1 - \frac{1}{P-a})^{x-1} \, (2a+2z+1-x)$$

$$= - k_s.N(1 - \frac{1}{P-a})^{z+1} \left[(a+z-1)(1-(1 - \frac{1}{P-a})^{a+z-1}) \right.$$

$$\left. - (P-a-1)\{(1-(a+z-1)(1 - \frac{1}{P-a})^{a+z-2} + (a+z-2)(1 - \frac{1}{P-a})^{a+z-1}\} \right]$$

Hence, the overall rate of change in population is obtained by addition of the three separate parts, 1, 2 and 3.

$$\frac{dN}{dt} = k_s.N(P-a)[\, 2(1 - \frac{1}{P-a})^{z+1} - \frac{P-1}{P-a}] \qquad \text{(xi)}$$

Weight of Sample

Group 1

In this group, a molecule of D.P. 'x' has (x-2a-2z-1) bonds which when broken lead to a weight loss of 2.z.m.

Thus,

$$-\frac{dW}{dt} = k_s \sum_{x=2a+2z+1}^{\infty} N_x .2z.m(x-2a-2z-1)$$

$$= k_s \frac{N}{(1-\frac{1}{P-a})^a} \cdot \frac{1}{(P-a)} \cdot 2z.m \sum_{x=2a+2z+1}^{\infty} (1-\frac{1}{P-a})^{x-1} (x-2a-2z-1)$$

$$= k_s \, N.m.2z \, (P-a)(1-\frac{1}{P-a})^{a+2z+1}$$

From equation (i), $Nm = \frac{W}{P}$

Hence,

$$-\frac{dW}{dt} = k_s \frac{W}{P} \cdot (P-a)(1-\frac{1}{P-a})^{a+2z+1} \cdot 2z$$

If, however, the break occurs within (a+z) units of either end of the molecule, the weight loss is z.m from the larger fraction and the whole weight of the smaller fragment.

Thus,

$$-\frac{dW}{dt} = k_s \sum_{x=2a+2z+1}^{\infty} N_x .2m. \sum_{n=z+1}^{2z+a} n$$

$$= k_s(a+z)(a+3z+1)m. \sum_{x=2a+2z+1}^{\infty} N_x$$

$$= k_s \frac{N.m}{(P-a)} \cdot \frac{1}{(1-\frac{1}{P-a})^a} \cdot (a+z)(a+3z+1) \sum_{x=2a+2z+1}^{\infty} (1-\frac{1}{P-a})^{x-1}$$

Hence,

$$-\frac{dW}{dt} = k_s \frac{W}{P}(a+z)(a+3z+1)\left(1 - \frac{1}{P-a}\right)^{a+2z}$$

Group 2

In this group, any bond scission produces total loss of the molecule and a weight loss corresponding to the size of the molecule. Hence, a molecule of D.P. 'x' has (x-1) bonds leading to a weight loss of x.m.

Thus,

$$-\frac{dW}{dt} = k_s \sum_{x=a+1}^{a+z+1} N_x.m.x(x-1)$$

$$= k_s \frac{N.m}{(P-a)} \cdot \frac{1}{\left(1 - \frac{1}{P-a}\right)^a} \cdot \sum_{x=a+1}^{a+z+1} \left(1 - \frac{1}{P-a}\right)^{x-1} \cdot x(x-1)$$

$$= k_s \frac{W}{P}(P-a)\left[\left(2P-2 + \frac{a^2-a}{(P-a)}\right) - \left(2P+2z+\frac{(a+z)(a+z+1)}{P-a}\right)\left(1 - \frac{1}{P-a}\right)^{z+1}\right]$$

Group 3

In this group, a molecule of D.P. 'x' contains (2a+2z+1-x) bonds which when broken lead to total removal of the molecule.

Thus,

$$-\frac{dW}{dt} = k_s \sum_{x=a+z+2}^{2a+2z} N_x.m.x(2a+2z+1-x)$$

$$= k_s \frac{N.m}{(P-a)} \cdot \frac{1}{\left(1 - \frac{1}{P-a}\right)^a} \sum_{x=a+z+2}^{2a+2z} \left(1 - \frac{1}{P-a}\right)^{x-1} \cdot x(2a+2z+1-x)$$

$$= k_s \frac{W}{P} (a+z+1)(a+z)(1 - \frac{1}{P-a})^{z+1}[1-(1 - \frac{1}{P-a})^{a+z-1}]$$

$$- k_s \frac{W}{P(P-a)} \cdot y^{z+1}[2+6y+12y^2+.....+(a+z)(a+z-1)y^{a+z-2}]$$

where $y = 1 - \frac{1}{P-a}$

Also, a molecule of D.P. 'x' has 2(x-a-z-1) bonds which when broken lead to total loss of the smaller fragment together with depolymerisation of 'z' monomer units from the larger fragment. The weight loss is (z+s)m where s is the number of monomer units in the smaller fragment.

Thus,

$$- \frac{dW}{dt} = k_s \sum_{x=a+z+2}^{2a+2z} N_x(x-a-z-1)(x-a+z).m$$

$$= k_s \frac{N.m}{(P-a)} \cdot \frac{1}{(1 - \frac{1}{P-a})^a} \sum_{x=a+z+2}^{2a+2z} (1 - \frac{1}{P-a})^{x-1}(x-a-z-1)(x-a+z)$$

$$= k_s \frac{W}{P} (P-a)(1 - \frac{1}{P-a})^{z+1}.2z. \left[1-\frac{(1+(a+z-1))}{P-a}(1 - \frac{1}{P-a})^{a+z-1}\right]$$

$$+ k_s \frac{W}{P(P-a)} \cdot y^{z+1} \cdot [2+6y+12Y^2+.....+(a+z-1)(a+z)y^{a+z-2}]$$

where $y = 1 - \frac{1}{P-a}$

Hence, the overall rate of loss of weight is obtained by addition of the five separate equations, two from Group 1, one from Group 2 and two from Group 3:

$$- \frac{dW}{dt} = k_s W(2P-2a-2 + \frac{a^2+a}{P} - 2(P-a)(1 - \frac{1}{P-a})^{z+1}) \qquad \text{(xii)}$$

Degree of Polymerisation

The rate of change of D.P. with time is obtained by substitution of equations (xi) and (xii) in equation (ii):

Thus,

$$-\frac{dP}{dt} = k_s(P-a-1)(P-a). \qquad \text{(xiii)}$$

This equation is identical with the equivalent expression in the 'Random Scission - Evaporation Model', equation (vii). In particular, it is independant of 'z'.

From equations (xii) and (xiii), the following expression for $\frac{dP}{dW}$ is obtained:

$$\frac{dP}{dW} = \frac{(P-a-1)(P-a)}{W[\,2P-2a-2 + \frac{a^2+a}{P} - 2(P-a)(1-\frac{1}{P-a})^{z+1}]} \qquad \text{(xiv)}.$$

Integration of equation (xiv) requires a complex procedure. Allocating values to P allowed corresponding ratios of $\frac{W}{W_o}$ to be calculated for various 'a', 'z' and P_o using a computer. The programme used for this manipulation was Integration by Modified Romburg Quadrature.[10] Figures 5 and 6 show plots of $\frac{P}{P_o}$ versus $\frac{W}{W_o}$, figure 5 shows the curves obtained when a fixed P_o is taken and the a/z ratio is varied. Figure 6 shows the curves produced by taking a fixed a/z ratio and varying P_o.

Differentiation of equation (xii) with respect to time and setting equal to zero gave an insoluble expression. Hence, to test for the possible existence of a maximum rate of loss of weight, appropriate values of P and $\frac{W}{W_o}$ were fed into equation (xii) and $\frac{1}{W_o}.\frac{dW}{dt}$ computed. The results of this process can be divided into two parts. Firstly,

FIGURE 5

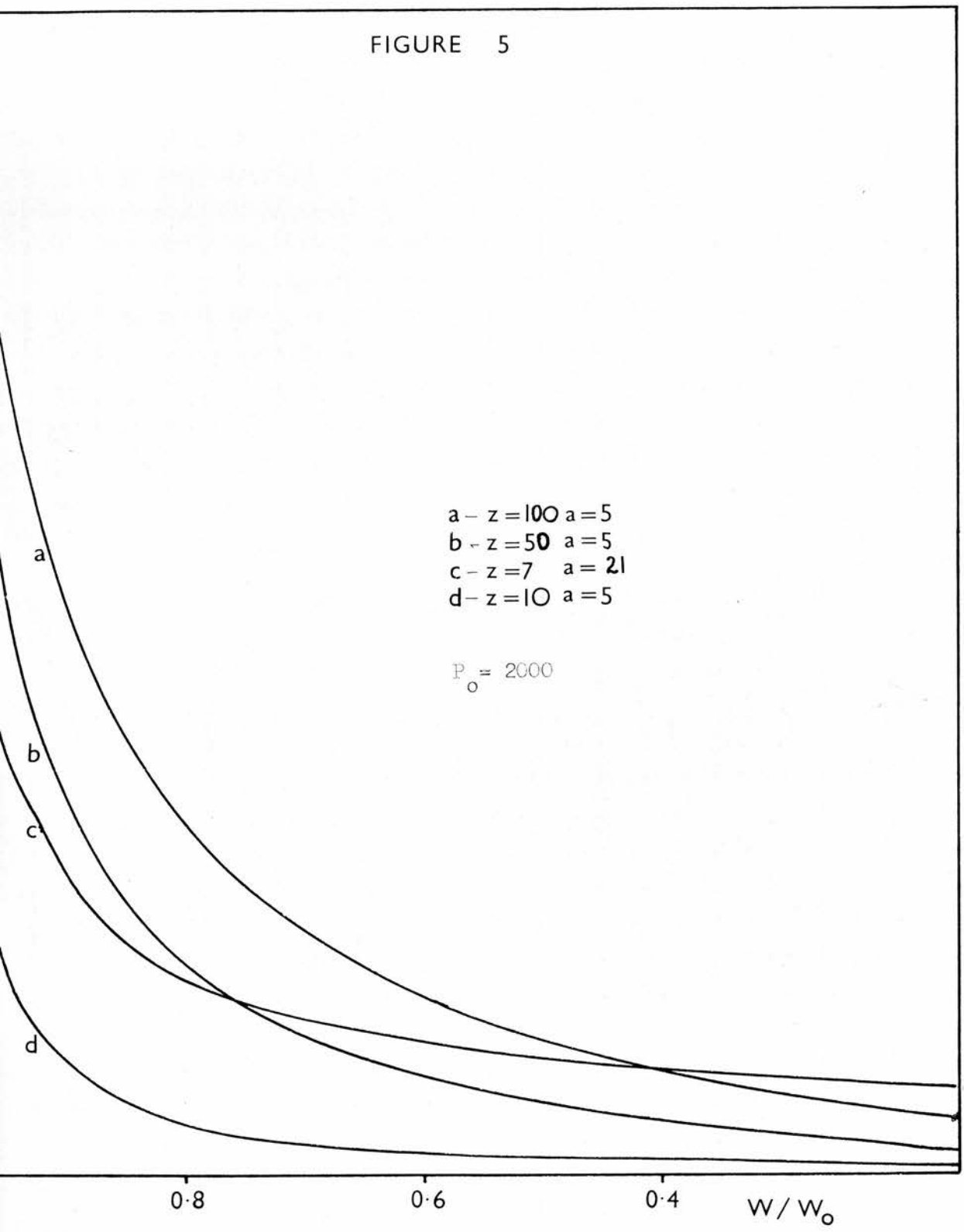

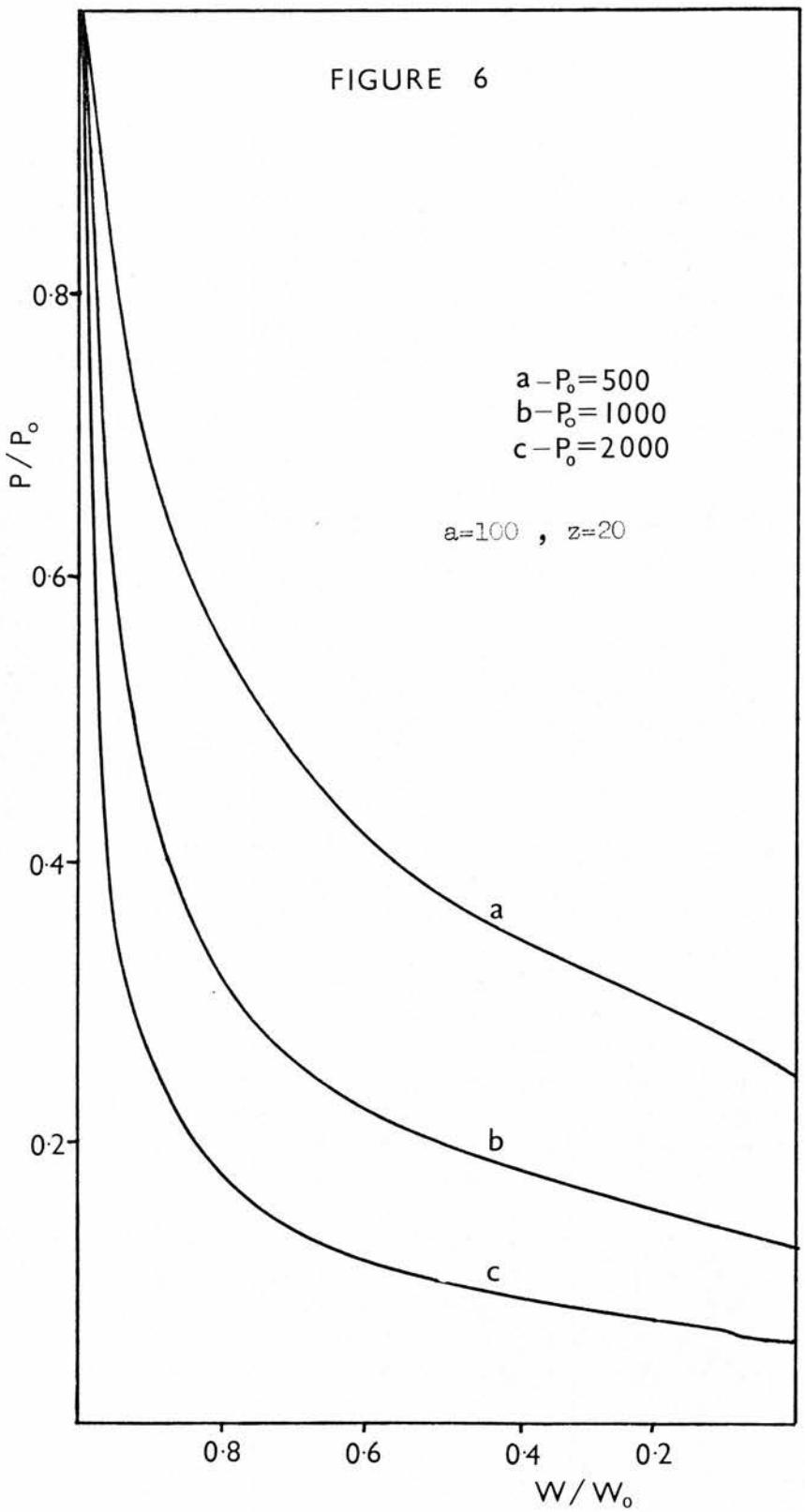
FIGURE 6
a – P_o = 500
b – P_o = 1000
c – P_o = 2000
a=100 , z=20
P / P_o
0·8
0·6
0·4
0·2
a
b
c
0·8
0·6
0·4
0·2
W / W_o

there is the case in which P_o is kept constant and the $\frac{a}{z}$ ratio is varied. If $\frac{a}{z} >> 2$ and 'a' is small compared to P_o then the maximum rate occurs at a percentage degradation of just less than 26.4%. As the $\frac{a}{z}$ ratio decreaes, then the percentage degradation corresponding to the maximum rate also decreases. For any value of P_o, if $\frac{a}{z} < 2$, then no maximum rate occurs. The value of $\frac{a}{z}$ corresponding to a maximum rate occurring at zero percentage degradation is always greater than or equal to two. The actual value depends on 'a' and P_o. Figure 7 shows a plot of percentage degradation corresponding to maximum rate versus $\frac{a}{z}$ ratio for z = 1 and P_o = 2000. Figure 8 shows a plot of $\frac{1}{W_o} \cdot \frac{dW}{dt}$ versus $\frac{W}{W_o}$ for various $\frac{a}{z}$ ratios and P_o = 2000.

Second, there is the case in which the $\frac{a}{z}$ ratio is kept constant and P_o is varied. As P_o decreases then the percentage degradation corresponding to the maximum rate also decreases. However, for any value of P_o and set values of 'a' and 'z', the maximum rate always occurs at the same degree of polymerisation.

Table 2 shows the degrees of polymerisation corresponding to the maximum rate for various 'a' and 'z' values.

Hence, for a = 100 and z = 20, the maximum rate of loss of weight always occurs at a D.P. of 342. If $P_o < 342$, then no maximum rate occurs and if P_o = 342, then the maximum rate occurs at zero percentage degradation.

The above results are all obtained without the use of any approximations. However, unlike the 'Random Scission - Evaporation Model', no equations have been obtained for W in terms of P or for the D.P. corresponding to the maximum rate. This, as has been stated previously, is because of the complexity of the mathematics involved

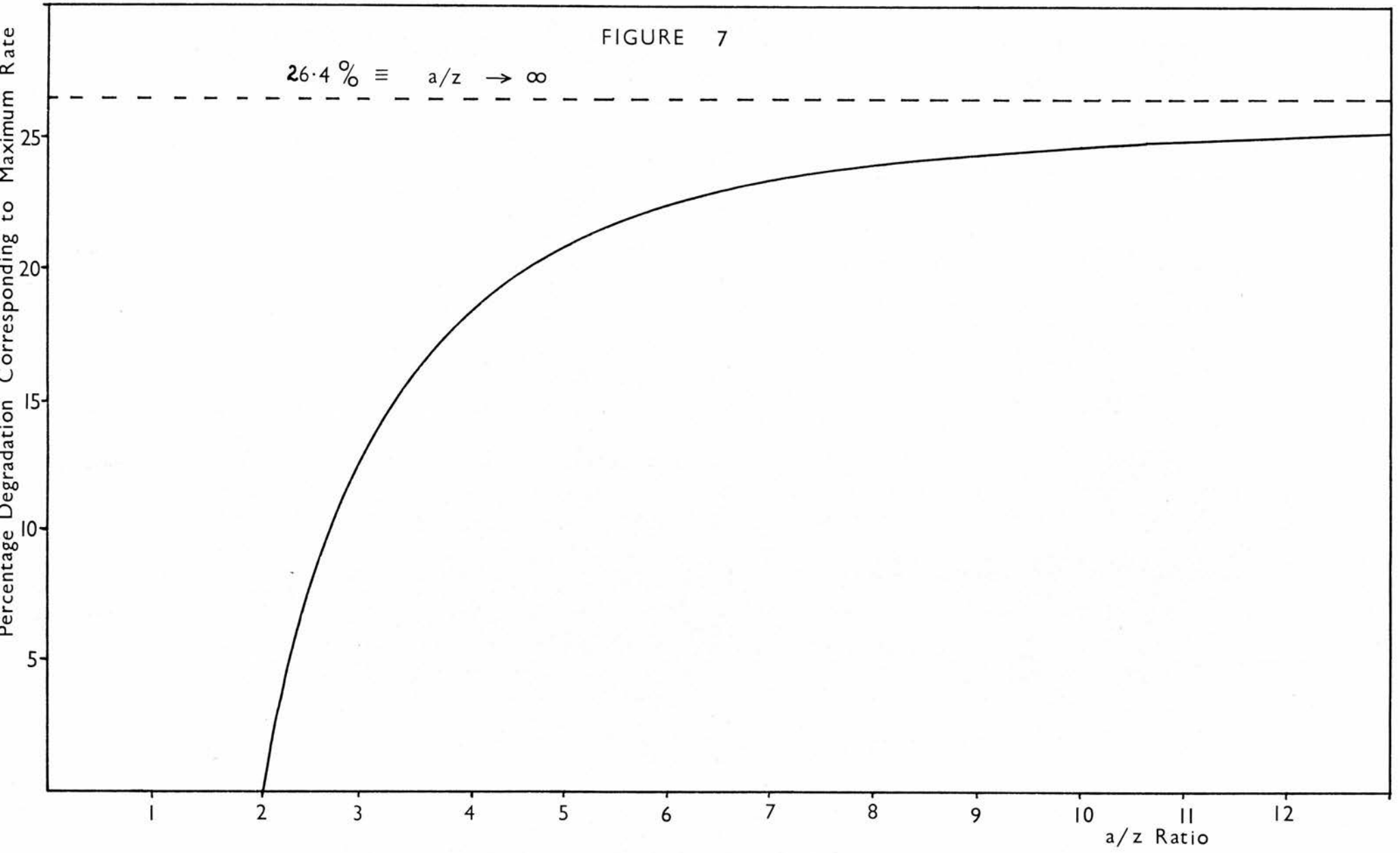
FIGURE 7
26·4 % ≡ a/z → ∞
Percentage Degradation Corresponding to Maximum Rate
25
20
15
10
5
1
2
3
4
5
6
7
8
9
10
11
12
a/z Ratio

FIGURE 8

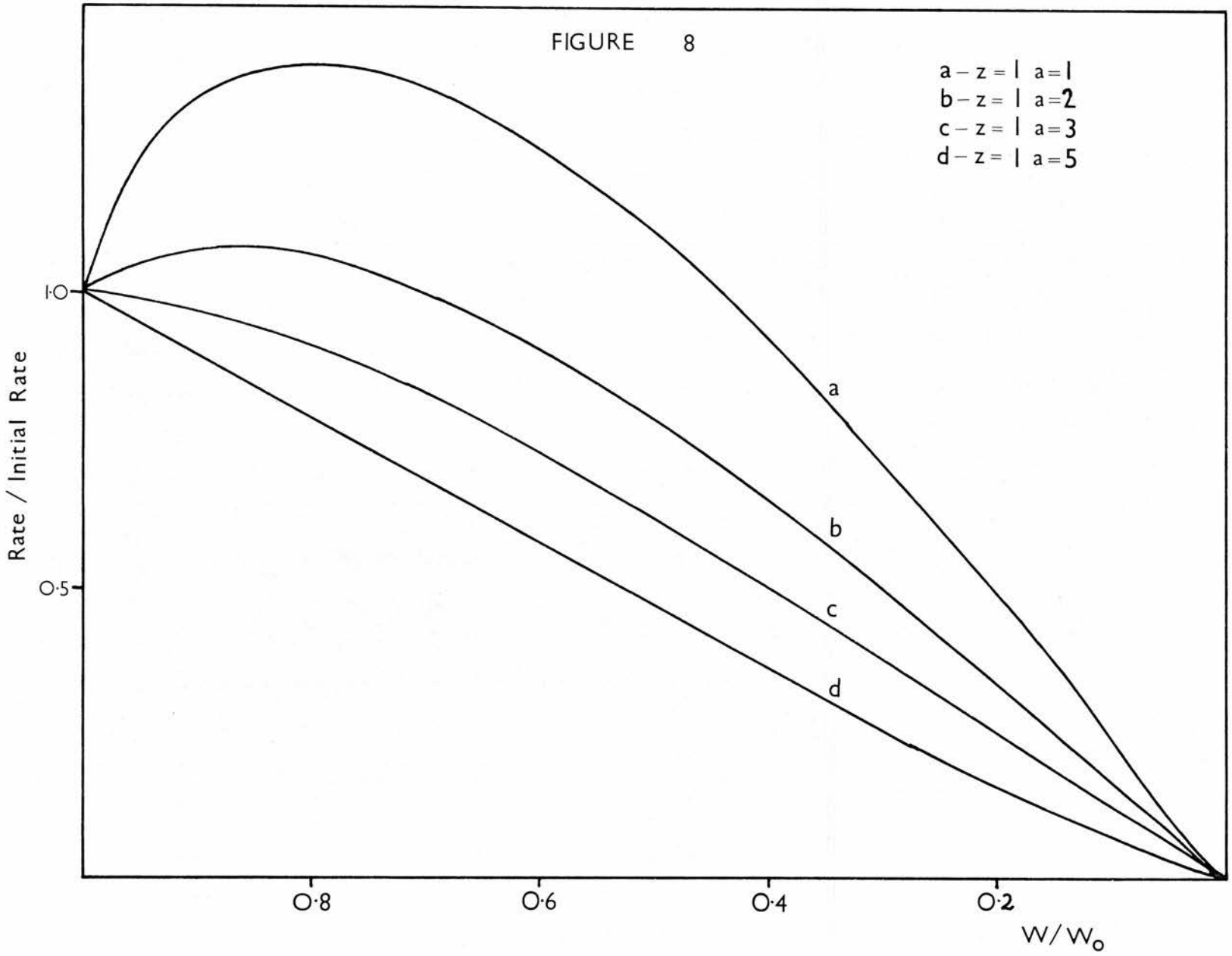
a – z = 1 a = 1
b – z = 1 a = 2
c – z = 1 a = 3
d – z = 1 a = 5
1·0
0·5
Rate / Initial Rate
a
b
c
d
0·8
0·6
0·4
0·2
W/W₀

TABLE 2

a	z	D.P. CORRESPONDING TO MAXIMUM RATE
3	1	20
4	1	17
5	1	18
10	2	35
9	3	63
21	7	146
90	9	227
90	18	309
100	20	342
150	50	1038

in producing such equations. However, when $z << (P-a)$ the function, $(1 - \frac{1}{P-a})^{z+1}$, can be approximated to $1 - (\frac{z+1}{P-a})$ and this allows the following expressions to be obtained:

D.P. Corresponding to Maximum Rate

$$- \frac{dW}{dt} = k_s W[2P-2a-2 + \frac{a^2+a}{P} - 2(P-a)(1 - \frac{1}{P-a})^{z+1}]$$

For $z << P-a$, $(1 - \frac{1}{P-a})^{z+1} \simeq 1 - (\frac{z+1}{P-a})$

Hence,

$$- \frac{dW}{dt} \simeq k_s W[\frac{a^2+a}{P} + 2z] \qquad (xv)$$

Differentiation of equation (xv) with respect to time and setting equal to zero leads to the following expression for the D.P. corresponding to the maximum rate:

$$P_{max} \simeq \frac{2a^2+a}{a-2z} \qquad \text{(xvi)}$$

where P_{max} is D.P. corresponding to maximum rate.

Table 3 shows the P_{max} values calculated using the above expression and those accurately calculated using the computer for various 'a' and 'z' values.

TABLE 3

a	z	P_{max} (computer)	P_{max} (equation (xvi))
3	1	20	21
4	1	17	18
5	1	18	18.33
10	1	26	25.9
10	2	35	35
9	3	63	57
21	7	146	129
90	9	227	226.25
90	18	309	301.67
100	20	342	335
150	50	1038	903

Close agreement is found for $\frac{a}{z} \geq 4$. It should also be noted that equation (xvi) is independent of P_o and that a maximum rate occurs if $P_o \geq \frac{2a^2+a}{a-2z}$. Equation (xvi) also predicts that no maximum rate occurs if $a \leq 2z$. This is very close to the condition found by using accurate computed values.

W in Terms of P

When $z << P-a$, $(1 - \frac{1}{P-a})^{z+1} \simeq 1 - (\frac{z+1}{P-a})$, and equation (xiv) can be approximated to:

$$\frac{dP}{dW} = \frac{(P-a-1)(P-a)}{W(\frac{a^2+a}{P} + 2z)} \qquad \text{(xvii)}$$

Integration of equation (xvii) between the limits P_o to P and W_o to W yields the following expression:

$$\ln \frac{W}{W_o} = (a+2z+1) \ln \frac{P_o-a}{P-a} - (a+2z) \ln \frac{P_o-a-1}{P-a-1} - \ln \frac{P_o}{P} \qquad \text{(xviii)}$$

Substitution of $P = \frac{2a^2+a}{a-2z}$ in equation (xviii) gives rise to the percentage degradation corresponding to the maximum rate . If $\frac{a}{z} \geq 4$, then the values of $(1 - \frac{W}{W_o})$ corresponding to maximum rate obtained from the above substitution are in good agreement with the values obtained accurately by the computer. Table 4 shows a comparison of the computed values of $(1 - \frac{W}{W_o})$ corresponding to the maximum rate with values obtained from equation (xviii) for $a = 100$, $z = 20$ and various P_o.

TABLE 4

P_o	$(1 - \frac{W}{W_o})$ computer	$(1 - \frac{W}{W_o})$ equation (xviii)
500	10.02	10.11
750	14.73	14.90
1000	16.52	16.80
2000	18.91	19.06
5000	20.01	20.19

C. End Initiation - Unzip Model

This section is concerned with initiation of depolymerisation at either of the terminal bonds of a molecule followed by reverse polymerisation of 'z' monomer units. The only species which is lost through evaporation is monomer and the rate of loss of monomer through evaporation is assumed to be greater than the rate of production.

Molecular Population

A molecule of D.P. 'x' is produced from depolymerisation of a molecule of D.P. 'x+z'. In the same way, a molecule of D.P. 'x' is lost by depolymerisation to produce a molecule of D.P. 'x-z'. This is summarised in the following equation for the rate of change in the number of molecules of D.P. 'x', $\frac{dN_x}{dt}$.

$$\frac{dN_x}{dt} = 2k_e (N_{x+z} - N_x).$$

Similar expressions can be written for other D.P.'s:

$$\frac{dN}{dt}(x-z) = 2k_e (N_x - N_{x-z})$$

$$\frac{dN}{dt}(x-z-1) = 2k_e (N_{x-1} - N_{x-z-1}).$$

From the above equations, it can be seen that some of the terms are appearing twice. On producing the overall rate of change of molecular population by summation of all possible equations of the above type, many of the terms cancel each other out. The only terms which do not cancel are those concerning D.P.'s of 'z+1' or less.

Thus,

$$\frac{dN}{dt} = -2k_e \sum_{x=2}^{z+1} N_x$$

From equation (iv)

$$N_x = \frac{N}{(P-a)} \cdot \frac{1}{(1-\frac{1}{P-a})^a} \quad (1-\frac{1}{P-a})^{x-1}$$

For the above case, a = 1.

Hence,

$$\frac{dN}{dt} = 2k_e \frac{N}{(P-1)} \cdot \frac{1}{(1-\frac{1}{P-1})} \cdot \sum_{x=2}^{z+1} (1-\frac{1}{P-1})^{x-1}$$

On solving the above summation, the following equation is obtained:

$$-\frac{dN}{dt} = 2k_e N(1-(1-\frac{1}{P-1})^z) \qquad \text{(xix)}$$

Weight of Sample

The rate of change of weight of the sample is best considered in two separate groups:

Molecules of D.P. of 'x+2' or Greater

For this group of molecules, initiation leads to reverse polymerisation of 'z' monomer units and a weight loss of z.m.

Thus,

$$-\frac{dW}{dt} = 2k_e \cdot z.m. \sum_{z+2}^{\infty} N_x$$

$$= 2k_e \cdot z.m. \frac{N}{(P-1)} \cdot \frac{1}{(1-\frac{1}{P-1})} \cdot \sum_{x=z+2}^{\infty} (1-\frac{1}{P-1})^{x-1}$$

$$= 2k_e \cdot z.m. \, N(1-\frac{1}{P-1})^z$$

From equation (i), $N.m = \frac{W}{P}$.

Hence,

$$-\frac{dW}{dt} = 2k_e \frac{W}{P} \cdot z \cdot (1-\frac{1}{P-1})^z$$

Molecules with D.P. of '2' to 'z+1'

For this group of molecules, initiation leads to total loss of the molecule and a weight loss corresponding to the size of the molecule.

Thus,

$$-\frac{dW}{dt} = 2k_e \cdot m \cdot \sum_{x=2}^{z+1} N_x \cdot x$$

$$= 2k_e \cdot \frac{N}{(P-1)} \cdot m \cdot \frac{1}{(1-\frac{1}{P-1})} \cdot \sum_{x=2}^{z+1}(1-\frac{1}{P-1})^{x-1} \cdot x$$

$$= 2k_e N \cdot m (P-1) [1+\frac{1}{P-1} - (1+\frac{z+1}{P-1})(1-\frac{1}{P-1})^z]$$

$$= 2k_e \frac{W}{P} (P-1) [1+\frac{1}{P-1} - (1+\frac{z+1}{P-1})(1-\frac{1}{P-1})^z].$$

The overall rate of change of weight is obtained by addition of the above two parts:

$$-\frac{dW}{dt} = 2k_e W [1-(1-\frac{1}{P-1})^z] \qquad \text{(xx)}$$

Degree of Polymerisation

From equations (ii), (xix) and (xx):

$$\frac{dP}{dt} = 0 \qquad \text{(xxi)}$$

Hence, the degree of polymerisation does not change with time and remains as P_o throughout. Substitution of P_o for P in equation (xx) gives rise to the following expression:

$$-\frac{dW}{dt} = 2k_e [1-(1-\frac{1}{P_o-1})^z] \cdot W \qquad \text{(xxii)}$$

$$= \text{Constant} \times W$$

Hence, for the 'End Initiation - Unzip Model' the rate of loss of weight with respect to time obeys first order kinetics with respect

to the weight of the sample.

The above mechanism requires that a bond is broken at the end of a polymer molecule and the larger of the two resulting species 'unzips' a definite number of monomer units. In practice, this process often involves the scission of the bond between the first monomer unit and the rest of the chain. There results a weight loss corresponding to the size of the molecule for molecules of D.P. $\leq z+2$, and a weight loss of $(z+1)m$ for molecules of D.P. $\geq z+3$. The change in molecular population involves the molecules with D.P. $\leq z+2$. The total effect of this particular modification is to replace z by z+1 in equations (xix) and (xx). $\frac{dP}{dt}$ remains equal to zero so $-\frac{dW}{dt}$ is still equal to a constant x W.

CHAPTER 3. DISCUSSION

The results obtained by the above treatment are in good agreement with previous workers results. The most recent of these treatments, that of Boyd[8], has been taken for comparison purposes.

For the Random Scission - Evaporation Model, the percentage degradation corresponding to maximum rate of 26.4% has also been deduced by Boyd[8], and by Simha and Wall[5]. Turning to practical applications, it would seem that none of the thermal decompositions of polymeric materials so far studied, proceeds by a simple evaporation - and - scission mechanism. Recent evidence[11] has shown that linear alkanes of degree of polymerisation greater that 47 evaporate without undergoing chemical change. On this basis, the maximum rate of loss of weight, by the Random Scission - Evaporation Model mechanism, would occur at a D.P. of about 95. This is much lower than is encountered experimentally.

The standard method of following the thermal breakdown of a polymer is by thermogravimetry. Wall, Flynn and Straus[11] have demonstrated that 'a', the D.P. of the largest fragment which can evaporate, is itself a complicated function of temperature. This factor must be taken into account when equation (vi) is applied to data collected during thermogravimetric experiments, particularly in the case of programmed thermogravimetry.

The expressions for $\frac{dW}{dt}$ and $\frac{dP}{dt}$ deduced for the Random Scission - Evaporation Model in this work are very similar to the equivalent equations produced by Boyd[8].

The effect of inclusion of unzipping along with evaporation was shown in the Random Scission - Unzip Model. The above work is more explicit than previous treatments. In particular, the effects of 'a' and 'z' on the percentage degradation corresponding to maximum rate are

shown to depend on the value of P_o and also on the $\frac{a}{z}$ ratio. This is in contrast with the Random Scission - Evaporation Model where the percentage degradation corresponding to maximum rate was a constant for all 'a' and P_o values. Furthermore, the degree of polymerisation corresponding to this maximum rate was a simple function of 'a'. For the Random Scission - Unzip Model, complex procedures were needed to produce accurate expressions for W in terms of P and for the degree of polymerisation corresponding to maximum rate, hence sample results had to be calculated using a computer. These results showed that as 'z' increased relative to 'a', the percentage degradation corresponding to maximum rate (P.D.C.M.R.) decreased. If 'a' and 'z' were kept constant and P_o decreased, the P.D.C.M.R. also decreased, however, under these conditions the degree of polymerisation corresponding to maximum rate, remained constant. Hence, eventually, a value of P_o is reached where no maximum rate is found.

By using approximations in the deduced rate of weight-loss, expressions were obtained for W in terms of P and for the D.P. corresponding to the maximum rate in terms of 'a' and 'z'. However, the approximations were only valid if $\frac{a}{z}$ was greater than, or equal to four, and 'z' was small compared to P.

The equations for $\frac{dP}{dt}$ produced in this work is very similar to the equivalent expression of Boyd[8]. In particular, both are independent of 'z' and equal to the equivalent expressions for $\frac{dP}{dt}$ obtained in the respective Random Scission - Evaporation Models. However, the expression for $\frac{dW}{dt}$ is different from that deduced by Boyd[8]

$$-\frac{dW}{dt} = k_s W\left[2P-2a-2 + \frac{a^2+a}{P} - 2(P-a)\left(1 - \frac{1}{P-a}\right)^{z+1}\right]$$

$$-\frac{dW}{dt} = k_s W\left[\frac{2(P-a)z}{z+P-a} + \frac{a^2+a}{P}\right] \quad - \text{ Boyd}^8.$$

Figures 9 and 10 show sample curves from the expressions of this work and from Boyd[8]. Figure 9 shows a plot of $\frac{P}{P_o}$ versus $\frac{W}{W_o}$ for various $\frac{z}{P_o}$ and $\frac{a}{P_o}$ ratios, a P_o of 2000 was used for the results of this work. Figure 10 shows a plot of rate, $(\frac{dW}{dt})$, divided by initial rate, $(\frac{dW_o}{dt})$, versus $\frac{W}{W_o}$ for the same selected values of $\frac{z}{P_o}$ and $\frac{a}{P_o}$.

From figure 9, it is evident that for $\frac{z}{P_o} = 0.01$ and $\frac{a}{P_o} = 0.05$, the two curves are almost identical. However, when $\frac{z}{P_o} = 0.1$, then for both $\frac{a}{P_o}$ ratios, the curves of Boyd and of this work show slight differences, particularly for the $\frac{a}{P_o} = 0.1$ ratio.

From figure 10, the findings of figure 9 are confirmed. Again for $\frac{z}{P_o} = 0.01$ and $\frac{a}{P_o} = 0.05$, the two curves are virtually superimposable. However, slight differences can be seen in the positions of the other two curves.

Hence, although the results calculated from this model are very similar to the equivalent results of Boyd, the treatment is far more specific in giving information as to the relative value of maximum rate.

The End Initiation - Unzip Model leads to some interesting points. Firstly the rate of loss of weight with time is first order with respect to weight. Second, the degree of polymerisation remains constant throughout decomposition.

FIGURE 9

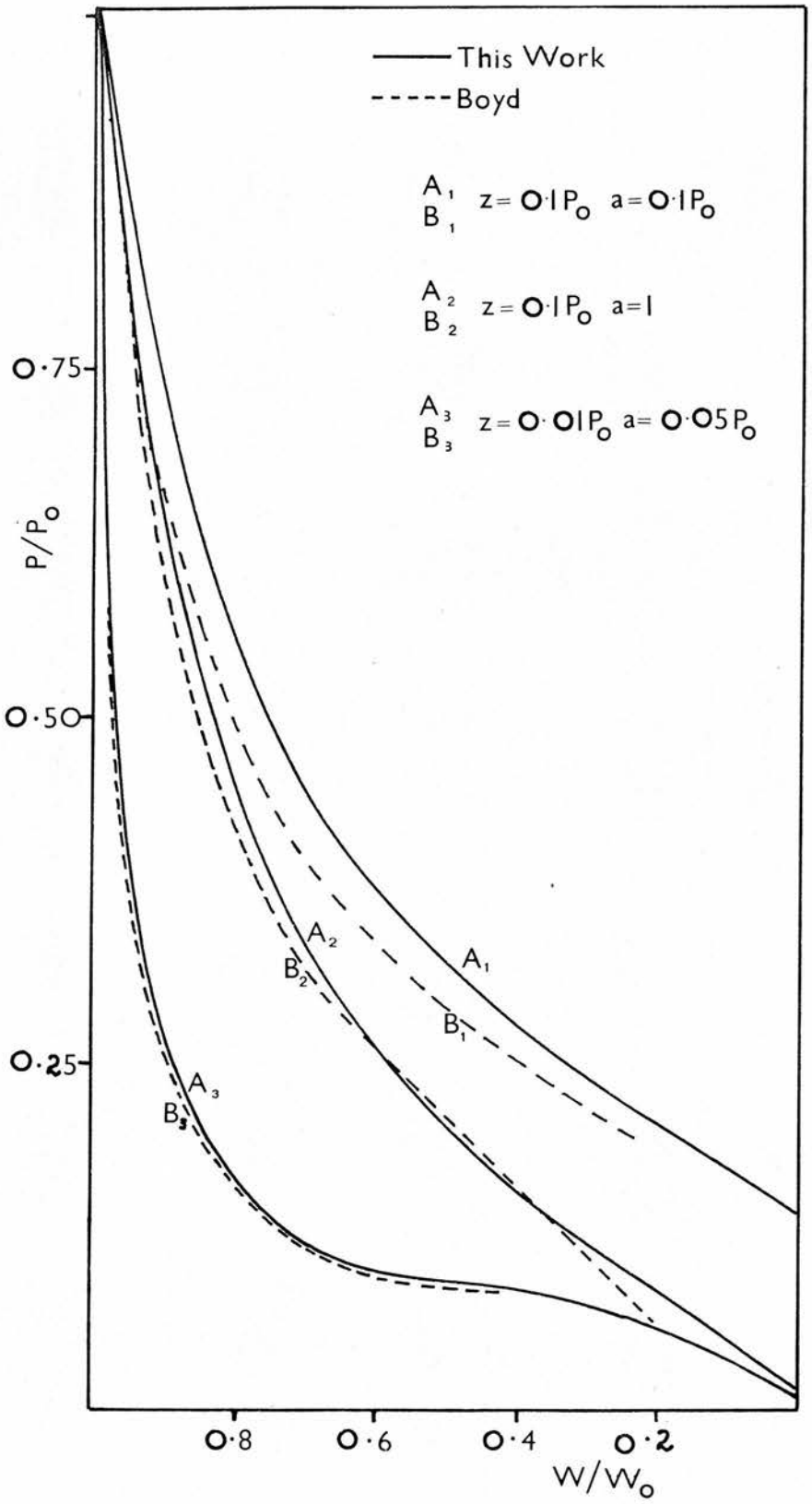
This Work
Boyd
A1 B1 z = 0·1P0 a = 0·1P0
A2 B2 z = 0·1P0 a = 1
A3 B3 z = 0·01P0 a = 0·05P0
0·75
0·50
0·25
P/P0
0·8
0·6
0·4
0·2
W/W0
A1
A2
A3
B1
B2
B3

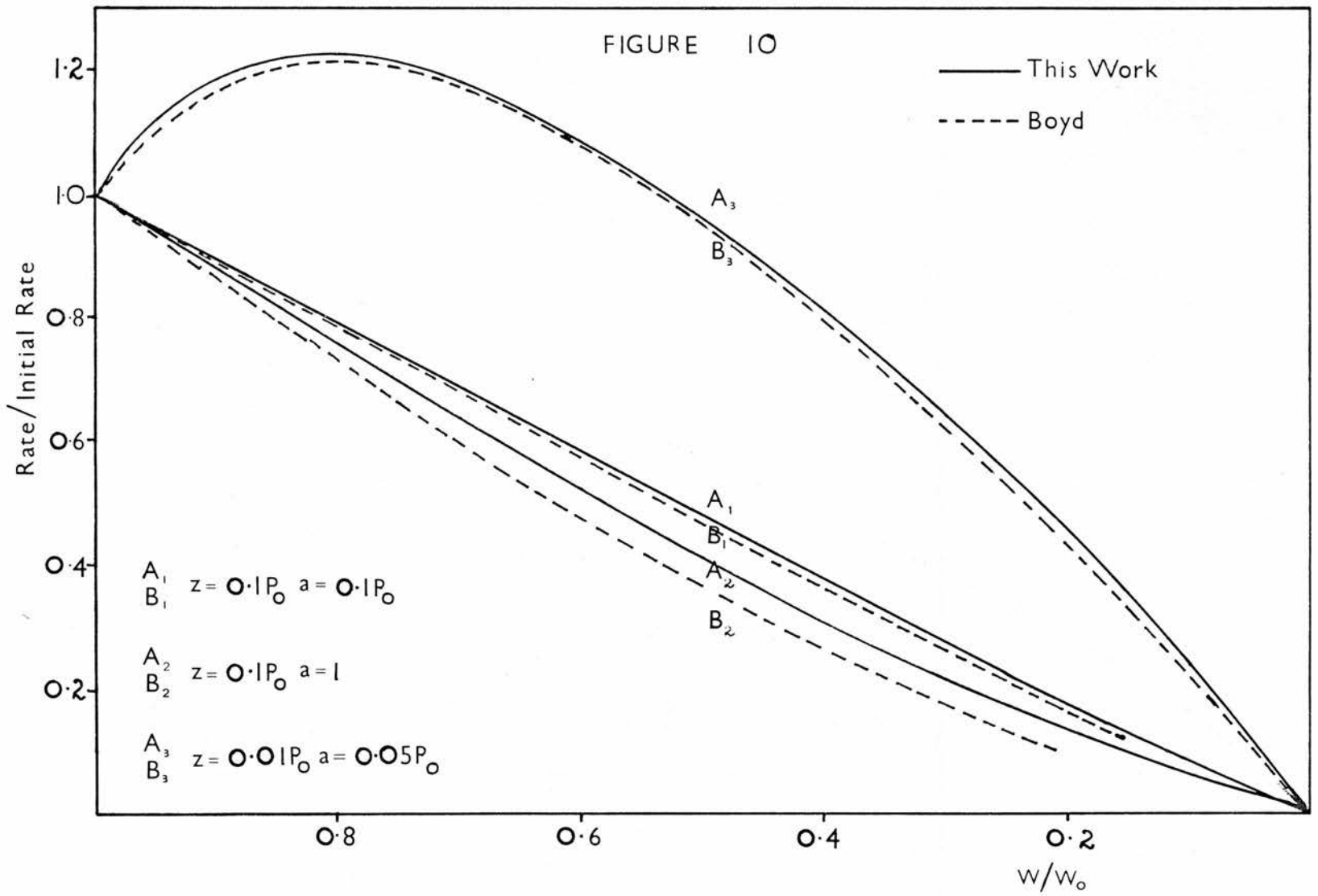
FIGURE 10
This Work
Boyd
Rate/Initial Rate
1·2
1·0
0·8
0·6
0·4
0·2
0·8
0·6
0·4
0·2
W/W₀
A₃
B₃
A₁
B₁
A₂
B₂
A₁ B₁ z = 0·1P₀ a = 0·1P₀
A₂ B₂ z = 0·1P₀ a = 1
A₃ B₃ z = 0·01P₀ a = 0·05P₀

PART TWO - BIBLIOGRAPHY

(1) Simha, R., J. Applied Physics, 12, 569 (1941)

(2) Sillen, L.G., Svensk. Kem. Tid., 55, 221 (1943)

(3) Tucket, R.F., Trans. Faraday Soc., 41, 351 (1945)

(4) Simha, R., Wall, L.A. and Blatz, P.J., J. Polymer Sci., 5, 615 (1950)

(5) Simha, R. and Wall, L.A., J. Phys. Chem., 56, 707 (1952)

(6) Boyd, R.H., J. Chem. Phys., 31, 321 (1959)

(7) Boyd, R.H. and Lin, T.P., J. Chem. Phys., 31, 773 (1959)

(8) Boyd, R.H., J. Polymer Sci., A1, 5, 1573 (1967)

(9) MacCallum, J.R., Eur. Polymer J., In Press

(10) Fairweather, G., C.A.C.M.,324, June (1969)

(11) Wall, L.A., Flynn, J.H. and Straus, S., J. Phys. Chem., 74, 3237 (1970)

CONCLUSIONS

1. The Polymers Investigated

In addition to the findings of Richards and co-workers[17], the following points have arisen from this work. Firstly, the n = 1 copolymer probably contains more than one tacticity (or configuration) within the molecular chain. This is based on evidence from the U.V. spectrum of the polymer which contains very little fine structure in the 240 - 270 nm region. This lack of fine structure is also found in the U.V. spectra of head to head, and of head to tail poly-α-methyl styrene, both of which have been shown to contain different tacticities. The U.V. spectrum of 1, 2 diphenyl ethane which has two carbons between the phenyl groups gives a U.V. spectrum (in cyclohexane) very similar to that of the monoalkyl benzenes. Similarly, the dimer of molecular weight, 238,

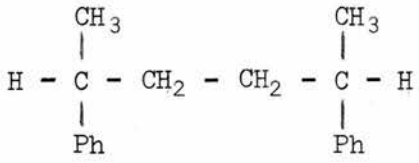

also gives rise to a U.V. spectrum containing the fine structure. This same type of fine structure is also found in all of the other copolymers. In the ^{1}H N.M.R. spectra of the n = 3 - 10 copolymers, only one methyl peak is found and this would suggest none of these species contains more than one tacticity. Hence for the case of the head to head homopolymer, it is not unreasonable to suggest that the lack of fine structure in the U.V. spectrum is due to the presence of the different tacticities. The U.V. spectra of toluene, ethyl benzene, 1, 2 diphenyl ethane and the saturated dimer (shown above) all give rise to

slightly different fine structures in their U.V. spectra. Hence, the benzene rings in two different environments in the head to head homopolymer are also likely to give rise to different fine structures which could interfere with each other. This is probably the explanation for the lack of fine structure found in the U.V. spectrum of this polymer.

The lack of fine structure in the U.V. spectra of the n = 1 copolymer can also be attributed to the same cause. Furthermore, the ^{1}H N.M.R. spectrum of this polymer is rather vague in the 9-10τ region in comparison with the spectra of the other copolymers. This may also be attributed to the presence of more than one tacticity.

Second, it would appear that the copolymers might contain a small number of head to head linkages within the molecular chains. This fact is based on evidence from the kinetics of breakdown where at low percentage decomposition, low activation energies were found for all the copolymers. This could well be due to the presence of a weak bond and as the incorporation of a head to head linkage was shown to be possible, it was concluded that the presence of a small number of these linkages within the polymer was not unlikely.

2. The Polymer Degradations

From the changes in molecular weight during degradation, it is clear that the chain breaking process was random scission. The products arising from the breakdown of the head to head homopolymer at all temperatures of decomposition, consisted of low molecular weight fragments together with α-methyl styrene. The residue and low molecular weight fraction both contained carbon-carbon double bonds which appeared to exist as the Ph - $\overset{|}{C}$ = CH_2 group.

The products arising from the copolymer degradations at 350°C consisted largely of low molecular weight species. Only in the case of the n = 1 copolymer was the quantity of α-methyl styrene greater than 10% of the total product. All of the low molecular weight fractions contain at least three types of carbon-carbon double bond, the most prevalent being the isolated - CH = CH_2 group. The other two are the Ph - $\overset{|}{C}$ = CH_2 group and the trans - CH = CH - function. The volatile liquid products contain a number of components which are common to each copolymer. The quantity of these components is always greater than 70% of the total volatile liquid fraction. Apart from these 'common' products, each copolymer gives rise to a number of other volatile liquid components, the nature of which varies from copolymer to copolymer. In fact, the copolymers could be characterised by the pattern of these 'non-common' products. The gaseous products from all the copolymers consisted primarily of methane and ethylene. However, other low molecular weight alkanes and alkenes were found in all cases. The residues of degradation were virtually unchanged polymer, the only detectable difference being the presence of a small amount of unsaturation. This is mainly present as the isolated - CH = CH_2 group.

3. Analysis of Kinetics

Because of the variation of the activation energies with extent of degradation, the kinetic results were used primarily to show the occurrence of more than one type of scission reaction and the possible presence of weak bonds within the polymer molecule.

4. Mechanistic Schemes

For the case of head to head poly-α-methyl styrene, the production of α-methyl styrene and the presence of the Ph - $\overset{|}{C}$ = CH_2 group have been

fully explained. However, for the case of the copolymers, it was impossible to postulate mechanisms for all the decomposition products. Mechanisms are proposed which show how various of the functional groups and some of the identified compounds can arise.

5. Theorectical Calculations

Using the "most probable" distribution of molecular sizes and a totally different treatment from previous workers, kinetic equations were deduced for three separate types of mechanism of degradation. The results from the calculations were found to be in good agreement with those of other workers who had used the same "most probable" distribution. The differences which do arise may well be due to the somewhat doubtful use of the stationary state hypothesis by previous workers.